AD_____

Award Number: DAMD17-99-1-9065

TITLE: Magnetic Resonance Studies of Photosensitizers and Their Effect in Tumors

PRINCIPAL INVESTIGATOR: Subbaraya Ramaprasad, Ph.D.

CONTRACTING ORGANIZATION: University of Nebraska Medical Center
Omaha, NE 68198-5100

REPORT DATE: October 2004

TYPE OF REPORT: Final

PREPARED FOR: U.S. Army Medical Research and Materiel Command
Fort Detrick, Maryland 21702-5012

REPORT DOCUMENTATION PAGE

Form Approved
OMB No. 0704-0188

1. REPORT DATE *(DD-MM-YYYY)*	2. REPORT TYPE	3. DATES COVERED *(From - To)*
01-10-2004	Final	15 Jul 2003 – 14 Jul 2004

4. TITLE AND SUBTITLE
Magnetic Resonance Studies of Photosensitizers and Their Effect in Tumors

5a. CONTRACT NUMBER

5b. GRANT NUMBER
DAMD17-99-1-9065

5c. PROGRAM ELEMENT NUMBER

6. AUTHOR(S)
Subbaraya Ramaprasad, Ph.D.

E-mail: SRAMAPRASAD@UNMC.EDU

5d. PROJECT NUMBER

5e. TASK NUMBER

5f. WORK UNIT NUMBER

7. PERFORMING ORGANIZATION NAME(S) AND ADDRESS(ES)
University of Nebraska Medical Center
Omaha, NE 68198-5100

8. PERFORMING ORGANIZATION REPORT NUMBER

9. SPONSORING / MONITORING AGENCY NAME(S) AND ADDRESS(ES)
U.S. Army Medical Research and Materiel Command
Fort Detrick, Maryland 21702-5012

10. SPONSOR/MONITOR'S ACRONYM(S)

11. SPONSOR/MONITOR'S REPORT NUMBER(S)

12. DISTRIBUTION / AVAILABILITY STATEMENT
Approved for Public Release; Distribution Unlimited

13. SUPPLEMENTARY NOTES

14. ABSTRACT
In this project we used
specifically fluorine labeled photosensitizers which will be of utility in the treatment of breast cancer via photodynamic therapy(PDT). The accumulation of the photosensitizer in the tumor and the muscle were evaluated using noninvasive 19F spectroscopic modality in mice bearing RIF tumor. By determining the relative disposition of the sensitizer we can determine the best time to irradiate the tumor causing minimal damage to nearby healthy cells around the tumor. The absorption, distribution and elimination of the labeled sensitizer were determined using 19F spectroscopy of tumor models after administering a single dose of the sensitizer. The tumor regression was achieved by irradiating the tumor with an appropriate wavelength laser light. The process of tumor regression and the accompanying changes in the high energy phosphates and diffusion process were monitored by 31P and 1H MR studies. The 31P MR studies performed before and after the use of 19F labeled PS(DOD2,DOD6) showed changes in the spectra and tumor regression was observed after PDT studies under fractionated laser doses. The corresponding nonlabeled compounds showed less significant 31P spectral changes and lower tumor response following PDT.

15. SUBJECT TERMS
^{19}F NMR, ^{31}P MR, Relaxation Times, Diffusion, Photodynamic Therapy, Dark Cytotoxicity, Tumor Regression, RF Coils

16. SECURITY CLASSIFICATION OF:			17. LIMITATION OF ABSTRACT	18. NUMBER OF PAGES	19a. NAME OF RESPONSIBLE PERSON
					USAMRMC
a. REPORT	b. ABSTRACT	c. THIS PAGE			19b. TELEPHONE NUMBER *(include area code)*
U	U	U	UU	94	

Table of Contents

INTRODUCTION

Initiation and management of the project

The P.I was awarded the grant titled "Magnetic Resonance Studies of Photosensitizers and their effects in tumors" in the latter half of 1999 while he was Associate professor of Radiology at the University of Arkansas for Medical sciences. Subsequently he moved to the University of Nebraska for Medical Center as Associate Professor and University MR physicist. This led to the availability of modern high field MR instrument there by adding significant advantage for the success of the project. The grant was reworked to meet the DOD-Army requirements and the project received formal approval and activated in October of year 2001.

Soon there after an undergraduate level technician was hired and a year later a graduate level technician was hired to perform higher level data analysis involved in the project. The project did have ups and downs and the initial hurdle was that the 7T magnet could not be charged to the required field strength and hence was maintained at 4.7T while the manufacturer would provide a replacement magnet. The true 7T magnet was operational by end of April 2002 leaving 2 years 5 months to finish the three year project. The transition from the 4.7T to 7.0T also necessitated retooling of the many radiofrequency coils built for 4.7T instrument. This also led to some slow down in the progress of the project and consumed a substantial part of the project period. The first technician had to leave the job to take care of her new born baby in mid 2004. A quick replacement was found although the new person had to be trained for 5-6 months before the required preliminary work could be performed towards the grant. As such, a request for an additional year of no cost extension was sought.

We provide here a detailed progress report of the entire work done on this grant. The papers published and results presented in scientific meetings are also provided as a part of this report (please see Appendix B1 and B2). .

Introduction to Scientific project and Progress

The diagnosis and treatment of cancer is an important healthcare issue. This project is concerned with the development and monitoring of fluorine labeled photosensitizer (PS) for the treatment of breast cancer by a relatively new and evolving cancer treatment modality. The photosensitizers are new and hence can not be administered to humans directly. This necessitates the use of a suitable tumor model. Using a mouse foot tumor model, the fluorine labeled photosensitizers (called DOD-2 and DOD-6) were monitored over time in single subjects. The information obtained from in vivo MR studies on the rate of rate of absorption, the time period during which the PS concentration peaked , and the rate of elimination were used to choose the time to irradiate the tumor with laser light at appropriate wavelength. The response to photodynamic therapy (PDT) was measured by ^{31}P MR spectroscopy. These studies will provide information of significant value to breast cancer research and treatment via photodynamic therapy.

Body (Research accomplishments and details of the work)

Task-1

As a significant part of the study we have been able to obtain sufficient amount of fluorinated photosensitizer with 12 equivalent fluorine atoms in the porphyrin photosensitizer. This sensitizer has an absorption peak at 626nm and is effective at 10 μM/kg concentration in the animal model (months1-36). However the last of the four compounds arrived only in Nov. 2005 and we needed time to perform the stated MR studies.

As suggested in our original statement of work we developed two water soluble photosensitizers. The two photosensitizers and their nonfluorinated analogs were synthesized(Dr Ravi Pandey and Roswell park cancer Institute). Details of the synthesis of fluorinated chlorin PS are given here.

Preparation of Fluorinated Chlorin

Methyl pheophorbide-a **1** was converted into chlorin e_6 trimethyl ester **2** by following the literature procedure and was isolated in >75% yield. The intermediate unstable bromoderivative obtained by reacting **2** with 30% HBr/acetic acid was dried under vacuum and immediately reacted with 3,5-bis-(trifluoromethyl)benzyl alcohol. The resulting product obtained after the

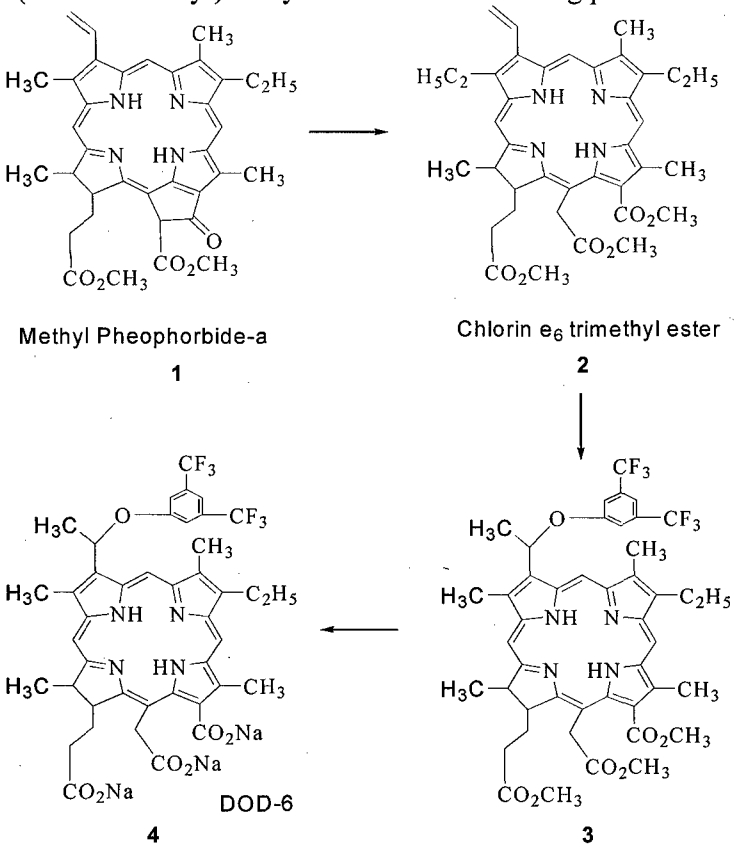

Scheme 1

Figure 1

standard work-up was purified by Alumina (Gr III) column chromatography, eluting with dichloromethane. The appropriate fractions were combined. Evaporation of the solvent gave **3** in 72% yield. The methyl ester functionalities were then hydrolyzed with aqueous sodium hydroxide/THF/methanol and the reaction was monitored by HPLC analysis. After the completion of the reaction the solvents were evaporated under high vacuum. The reaction product was redissolved in phosphate buffer and the pH of the solution was adjusted to 7.4.
The structures of the intermediates (see Figure 1) and the final product were confirmed by NMR and mass spectrometry analyses. The list of compounds received from the collaborator is shown in Appendix-A as a table which provides the year (with appox date, month and years) the compounds were received in our laboratory.

Task -2A

Grow tumors on mouse foot, inject photosensitizers and analyze effects using in vivo MR technique, and measure tumor volumes at 3, 24, and 48 hours.

Details of research work

The RIF tumors used in the study were produced following the protocol of Twentyman et al (1). We studied C_3H/HeJ mice tumors during the entire project period.

Effect of Photosensitizer alone

Photodynamic therapy is a novel cancer treatment modality in which the drug action is locally controlled by light (2). Development of new photosensitizers (PS) for clinical applications needs to minimize dark cytotoxicity while maximizing the PDT effects in the tumor. Photofrin with a long incubation time in human ovarian carcinoma cells has shown dark toxicity effects (3). Other photosensitizers such as Nile Blue A (NBA) have shown dark toxicity on human tumor cells in vitro (4). The dark toxicity of NBA was not due to apoptosis. The cytotoxicity of photosensitizers in an in vitro situation is often measured using a suitable cell system. For example the cytotoxicity in dark or in the presence of laser light is generally monitored by counting the number of cells in the untreated and PS treated cultures (5). Other methods such as MTT cell proliferation assay (6) is based on the ability of mitochondrial dehydrogenase enzyme from viable cells to cleave the tetrazolium rings of MTT and form a dark blue formazan crystal which is largely impermeable to cell membranes. The number of surviving cells is directly proportional of the formazan product created. The latter method has been used to detect a portion of dark toxicity manifested by Photofrin II (7).

In the above in vitro models the effect is only seen in the number of cells that die and the number of healthy cells that remain after a treatment. The results depend upon the concentration of PS which remain constant during the time of incubation. However,in practice, build up of the PS in the tumor and its subsequent cytotoxicity is a dynamic process involving different absorption and elimination rates. Thus, a true and realistic model when used to determine the cytotoxicity should take into account the dynamics of PS in the model. Additionally, the presence of vasculature in tumors is not represented in cellular systems thereby making it a less effective representation of a tumors present in humans. Thus, a tumor model in

a mammalian system should be of great preclinical value in obtaining more information on the effects of PS on the tumor either in the dark or in the presence of laser light. For these studies we use the murine tumor model where the tumor is grown on the foot dorsum.

Effect of new photosensitizers alone on tumor growth profiles

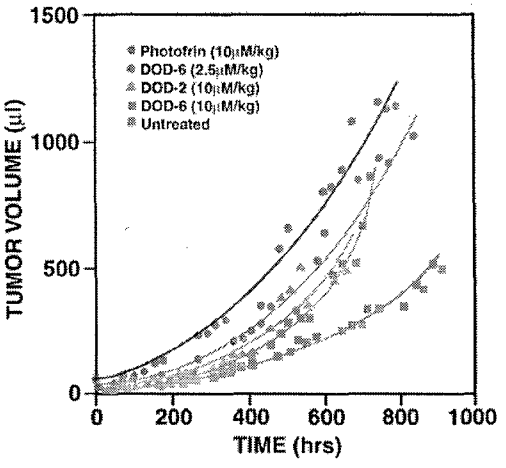

Figure 2. Growth profiles of mouse tumors treated with PFII and fluorinated photosensitizers such as DOD-2, DOD-6 along with untreated controls.

The effect of photosenitizers such as photofrin or the newly synthesized compounds at similar concentrations did not show visible effects on the growth profiles(see Figure 2). However the effect on the tumor bioenergetics were observed as demonstrated by the changes in high energy phosphates. Representative figures are provided in Appendix-A for a quick reference.

Effect of PDT on tumor volumes

The growth of tumors before PDT and regression following PDT were monitored by making tumor volume measurements 4 to 5 times a week. The volumes were measured by measuring the three diameters and the volume computed using the ellipsoid approximation. The studies were performed on the fluorine labeled photosensitizer, the non labeled analog and the FDA approved photofrin. The drug was administered at a dose of 10μM/kg. **A detailed presentation of the synthesis along with mass spectroscopic and high resolution MR data was presented at the ERA of Hope meeting at Florida (2002 August).** A copy of the abstract is attached in the appendix. The doubling times of tumor growth before PDT were found to be 125 mm^3 (n=9). A complete analysis of several tumor doubling times before and after therapy are documented in Table 1 (see Appendix A). The tumor regression with one PDT treatment with a single or fractioned dose was observed for a few days post therapy. No complete tumor regression was seen in a single treatment alone (Table 2, in Appendix A). Tumor regression with DOD-2 was as large as 30-40% and tumor regrowth started after a few days of regression.

MR Studies of PS and PDT treated tumors (^1H, ^{19}F, ^{31}P nuclei)

Magnetic resonance studies allow PDT effects to be detected and monitored by ^{31}P spectroscopic measurements and also by making measurements of parameters accessible by imaging techniques. Additionally, the Fluorine-19 labeled compounds used here will allow the quantitation of the photosensitizer in the tissue by using ^{19}F MR methods. These methods are noninvasive and hence are appealing as they can be translated to humans undergoing therapy with new photosensitizers labeled appropriately as described here.

RF coil construction for MR imaging and spectroscopy

The construction of radiofrequency coils were a significant requirement for the project. The coils that were require for this project were built at different stages of the grant period and only four representative coils are discussed in a little detail. The project required a number of RF coils of different shape, size and volume and operated at ^{19}F, ^{1}H, ^{31}P frequencies at 4.7T and subsequently 7.0T Bruker instrument.

The initial magnet that was charged could not hold steady at the required high field strength of 7Tesla and as such it was left operating at 4.7T. The machine was kept operational till April of 2002 when the switch to 7T was made. The 7T instrument has been operating with little interruptions.

The initial coils made for 4.7T were non opearational at 7T and they have to be refabrictaed. The coils were tested on phantoms and then on mice bearing tumors and treated with the new photosensitizers. In addition to the above we also had access to a larger ^{31}P-^{1}H coil (not shown) made by Bruker (the manufacturer of the instrument)

Below we display the two surface coils of 1.5 and 3.0 cm diameter (see Figs 1& 2) and saddle coils for ^{1}H and ^{31}P nuclei (Figs 3 & 4). These were used to detect and quantitate the fluorine in the tumor and the muscle.

Figure 3.
A 1.5 cm ^{19}F surface coil.

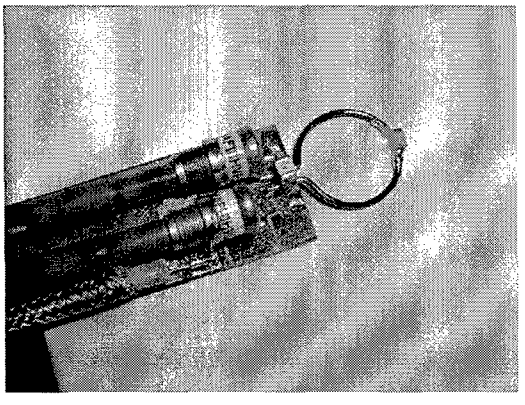

Figure 4.
A 3.0cm ^{19}F surface coil

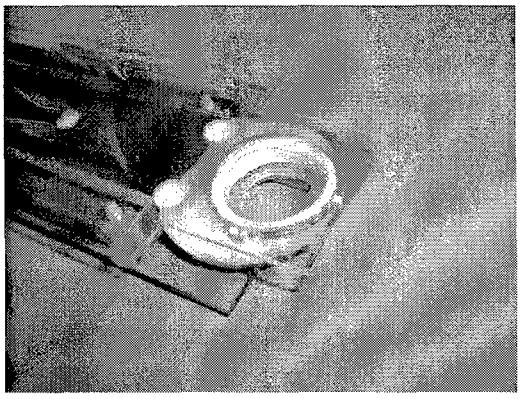

Figure 5.
1.5 cm diameter saddle coil for ^{1}H

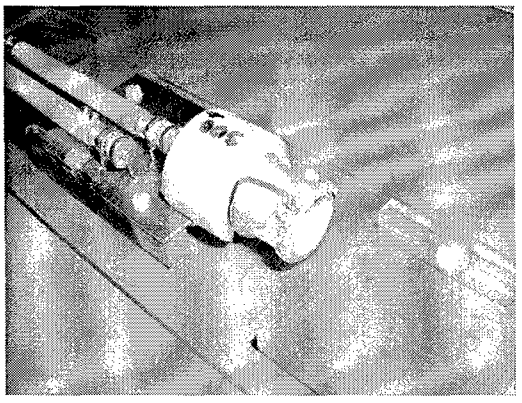

Figure 6.
1.5 cm diameter saddle coil for ^{31}P

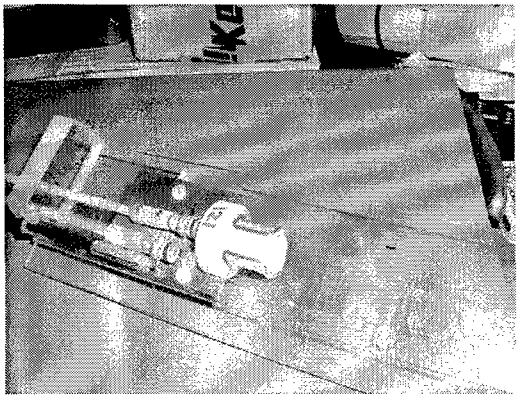

Task- 2B

PDT studies both the fluorine labeled nonlabeled Sensitizers

Our studies have shown that PDT performed with this drug administered IP at 10 μM/kg lead to tumor regression. Representative ^{31}P MR studies were performed on tumors both before and after the initiation of PDT. The effect of PDT on tumor volumes with each of the three photosensitizers (fluorine labeled, non labeled and photofrin) is shown in Figure7. The growth pattern of untreated tumors and those treated with PS alone or laser alone are shown in Figure 8 An examination of growth pattern clearly indicates the effect of PDT in tumor volume reduction which are substantial in the case of DOD-6 and are much smaller for DOD-2.

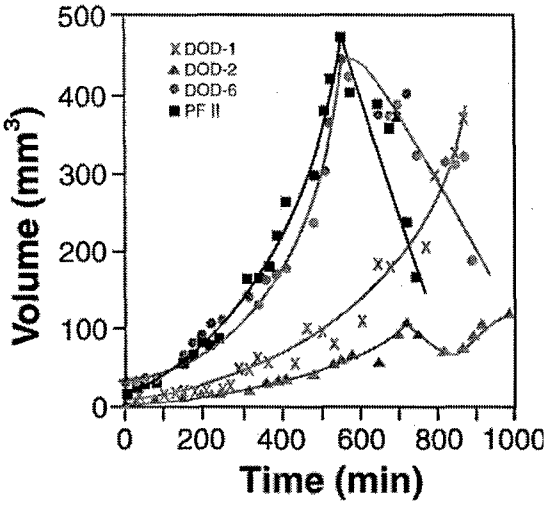

Figure 7. Growth profiles under PDT

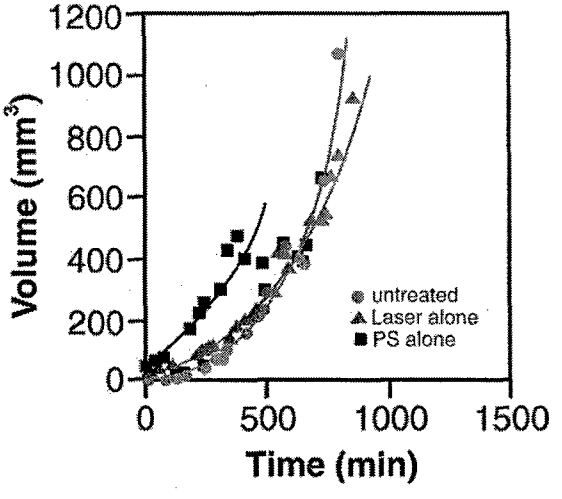

Figure 8.Growth profiles of controls

Task-3

A chlorine type photosensitizer which we refer to as DOD-6 (with 6 equivalent fluorines) was developed (with Co-I, Dr. Ravindra Pandey, Roswell Park Cancer Institute). A brief description of the synthesis of this compound has been provided earlier. Similarly the corresponding non labeled analog was also synthesized based on the principles shown in Figure 1 and this was also studied for its PS activity like fluorinated counterpart.

The above tasks included the studies required to observe changes in diffusion coefficients upon PDT treatments, relaxation measurements and detailed analysis from select regions of interest. In order to obtain optimum time for laser irradiation and to quantitate the photosensitizer in the tumor noninvasively, we used ^{19}F spectroscopic technique to follow the labeled photosensitizer. As a first approximation we assume that the rate of absorption, retention and elimination are independent on the drug dose. At present we are able to perform these ^{19}F MR studies at a drug dose of 100 μM/kg. A home built surface coil was used to perform these studies on the 7Tesla animal imager. A knowledge of the relaxation times T_1 and T_2 are necessary for optimization of the spectral data. The mean values of relaxation times in the solution were 924±38 ms for T_1 and 150±2 ms for T_2 and were used to optimize of tumor spectra. By comparing the intensities from the tumor volume with a phantom containing a known concentration of PS, the amount of PS in the tumor could be calculated. The entire Pharmacokinetic profile of PS in tumor model was constructed using three tumors (Figure 9). Based on this profile PDT was performed at time points 2hr, 4hr and 24 hrs post drug administration. The various parameters used in PDT studies are listed in Table 3.

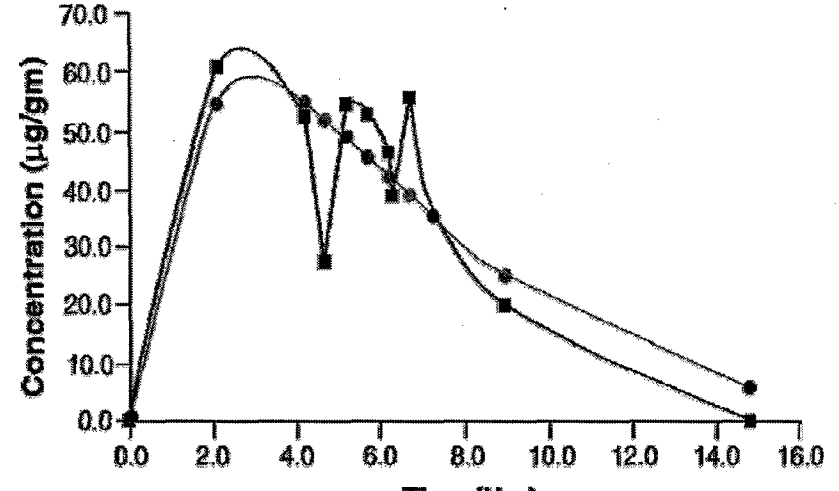

Figure 9: Pharmacokinetic profile for DOD-2 in RIF tumor model. The black line connects the experimental points while the red line is the fit to the data. The data were obtained using coil shown in Fig.3.

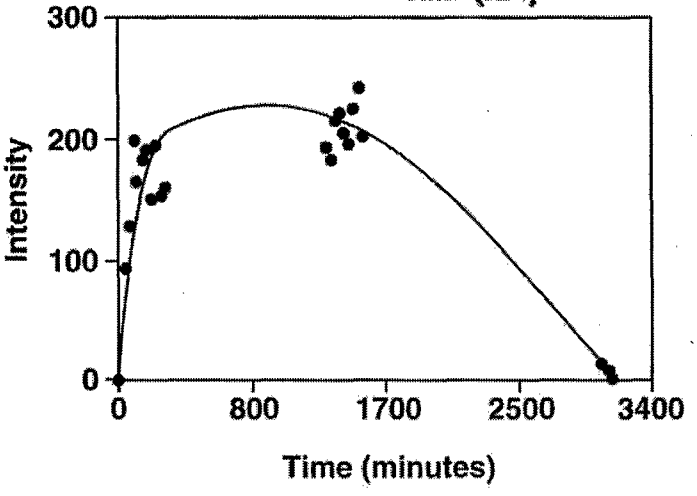

Figure 10: Pharmacokinetic profile for DOD-6 in RIF tumor model. The circles are experimental points while the solid blue line is pharmacokinetic profile that fits the data.

Using this information from in vivo ^{19}F MR studies, several mice tumors were studied for PDT effects using the fluorine labeled and nonlabeled analog. Representative graph indicating the PDT effects on the tumor volumes upon using DOD-1, DOD-2, DOD-6, and photofrin are shown in Figure 7. Under similar doses of photofrin and DOD-2 , the tumors showed similar regression pattern . The data shown in Figure 7 clearly demonstrates this (see the data shown in green and sea blue colors for photofrin and DOD-2). DOD-1 did not exhibit any tumor regression in the studies performed so far (data in green). Thus, under the assumption that the pharmacokinetics for the labeled compound is similar to that of the labeled compound, it appears that the PDT efficacy for the non labeled compound is comparatively low. This certainly demonstrates that the properties of fluorine labeled photosensitizer has significantly different efficacy in this case.

The results show that this photosensitizer has fast elimination constant. The drug is eliminated completely in about 16 hours. The peak value was reached around 2 hrs. The absorption, distribution and elimination were obtained using equation

$$C = Ae^{-\alpha t} + D\,e^{-\beta t} + E\,e^{-\gamma t}$$

Where α ,β and γ are the three rate constants for absorption, distribution and elimination phases. The analysis was done using the PK solutions software (8).

The laser energies used in the study were optimized at 10μM/kg dose of the PS. The laser power was at 75 or 150 mw/cm^2 at the surface of the tumor and the irradiation time was 30 minutes. In some cases, at the higher power of 150 mW/cm^2, laser irradiation was performed for two 30 minutes duration separated by a time interval of 2 hours. The results are summarized in Table 1(see appendix). It may be noted that tumor regression was more pronounced with the administration of fractionated doses of laser.

Our results so far show that both DOD-2 and photofrin show very similar response (see Figure 7). However the non labeled PS did not show any tumor regression at any of the above mentioned laser powers.

^{31}P MR studies

Phosphorus -31 MR studies were performed using a home built ^{31}P coil (diameter 1.5 cm, see Figure. 6) operating at 121.6 MHz.

The ^{31}P MR spectra were recorded for untreated, PS alone administered, and PDT treated tumors and were used as reference spectra. For each tumor that was subject to PDT using one of the photosensitizers, a control ^{31}P MR spectrum was recorded followed by ^{31}P spectra after PDT. Our results show that the ^{31}P spectra recorded post PDT using either DOD-1 or DOD-2 do not show any measurable changes in the first few hours. DOD-6 showed significant decrease in ATP and increase in Pi peaks. DOD-8 the nonfluorinated analog also showed decrease in ATP but was considerably less compared with DOD-6. Photofrin, on the other hand has shown measurable decreases in ATP peaks and a concomitant increase in Pi (inorganic phosphate

peaks) (9-13). The spectral analyses were done using the JMRUI software (14) and a typical spectral deconvolution is shown below.

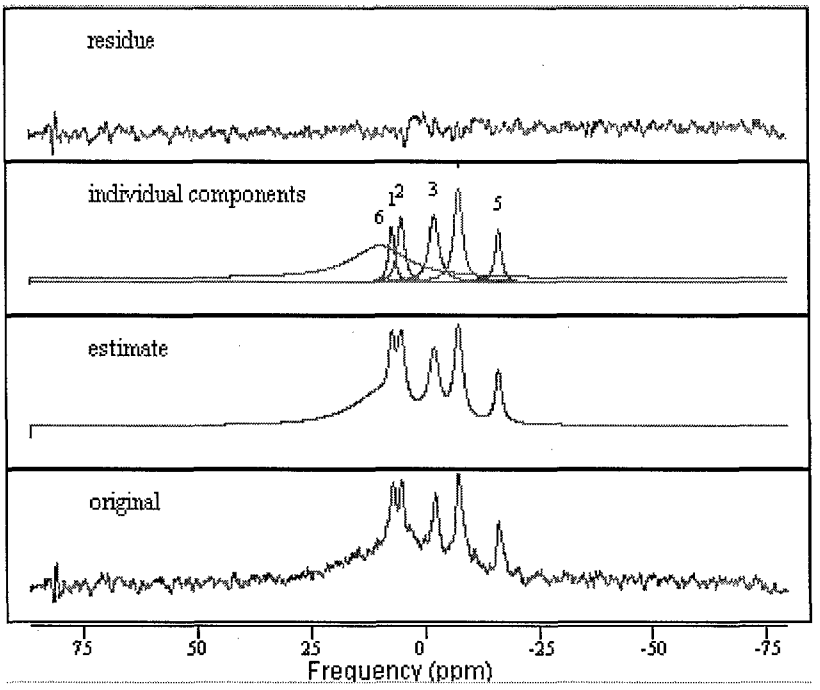

Figure 11: Typical fit to a tumor ^{31}P spectrum performed using the MRUI program. The peak assignments are: 1. PME, 2. Pi, 3. γATP, 4. αATP 5. βATP and 6. A hump arising mostly from immobile phosphorus such as bone.

Although both DOD-1 and DOD-2 did not show any changes in ^{31}P spectra, tumor administered with DOD-2 showed tumor regression. We extended our studies to ~ 4-6 hours. These results can provide more information about the function of the photosensitizer and aid in the construction of more potent and efficient photosensitizer.

MR studies of DOD-6 (newly synthesized 2nd photosensitizer)

This photosensitizer has a strong absorption maximum at 650 nm. Because of the higher wavelength we can expect better penetration in the tissue. We have performed relaxivity measurements using the in vivo MR imager at 7T. The T_1 measurements were performed using the saturation recovery method and the T_2 measurements were done using the Hahn spin echo technique. The mean T_1 and T_2 values are ~250 and ~ 25 ms respectively.

The preliminary PDT studies have been performed using laser power of 150 mW/cm^2 and photsenitizer dose of 10 mg/kg. Interestingly the tumor regression was observed approximately two days after the initiation of the therapy.

In our laboratory here at Nebraska, we have tested the efficacy of new photosensitizers (DOD-6 and DOD-8) in the mouse tumor model. Examples of this is shown below where the variation of tumor volume with time under PDT treatments are shown (Figures 12, 13)

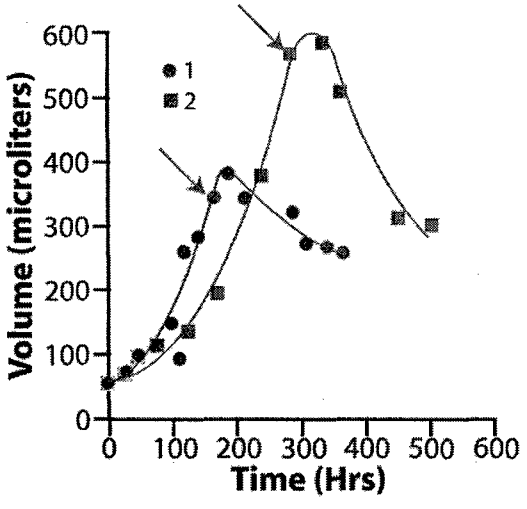

Figure 12 : Tumor volumes under PDT using DOD-6

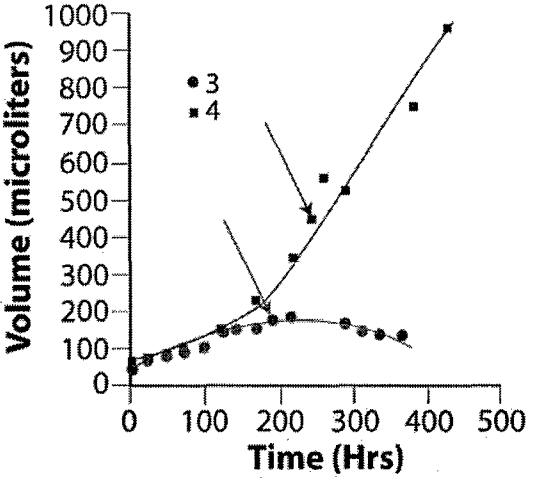

Figure 13: Tumor volumes under PDT using DOD-8

Task-4

Perform detailed image analyses using the standard software on the P.C. The images are transferred to a P.C with image analysis software. Average apparent diffusion coefficient will be measured following PDT and several hours after. Attempts will be made to find correlation between the tumor photosensitizer levels with the PDT effects that will be demonstrated via significant changes in tumor volumes.

Relaxivity Values

The tumors were investigated for the changes in T_1 and T_2 values following the therapy. The measurements were made in four different regions on the central slice of 2 mm thick similar to that shown in Figure 14. The mean T_2 values before and within 1hr after therapy were 64.5 ±2.9 ms and 63.8±2.3 ms respectively. Thus no changes were seen for the T_2 values after the therapy. The mean T_1 values before and after the therapy were 1828±235 ms and 2553 ± 63 ms respectively indicating an increase of 40 %(P=0.004). The increase in T_1 values were significant in all regions of the tumor area chosen in this study. These results are also consistent with our earlier studies on whole tumors studied on a 4.7T instrument (15).

The detailed image analysis included the evaluation of apparent diffusion coefficients (ADC) from several regions of interest from a given image of a slice. An example of the image and the regions of interest chosen is provided below (see publication 16 by the P.I and associates under list of references).

Apparent Diffusion Coefficients

From the diffusion weighted images the ADC's in four different regions of interest (ROIs) were obtained. The different ROIs chosen from 1mm thick mid slice of the tumor are shown in Figure 14. The signal intensities were extracted for each ROI and ADCs measured using the Bruker Paravision software for diffusion analysis. The standard deviations were recorded for the selected regions of interest shown in Figure 14. The ADC values measured before therapy were in the expected range for the tumor type studied here.

Figure 14: A diffusion weighted axial image from a central slice of the tumor recorded immediately following PDT. The four regions of interest that were considered in the study are also show

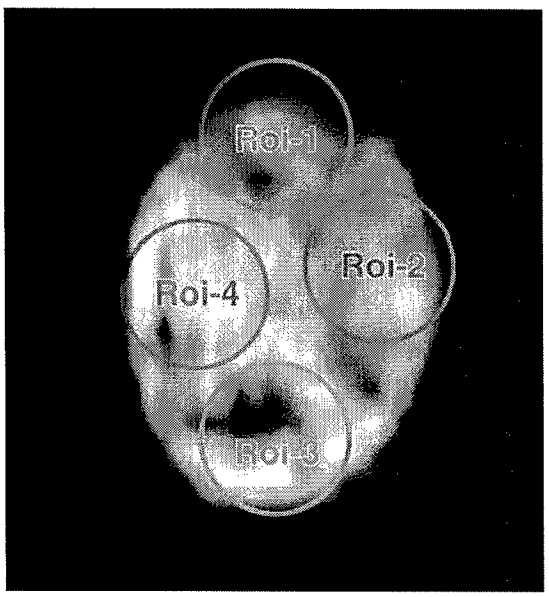

The control ADC values were measured before the induction of PDT in 4 different regions in a 1mm axial image that corresponds to the central slice of the tumor. The volumes of the regions of interest were typically of the order of 6-7 mm^3. Significant changes in the ADC values for both Photofrin® and DOD-6 sensitizers were observed in the first two hours post PDT. These changes were more concentrated in region 4 (see Figure 14). An increase in ADC was more evident with DOD-6 than with Photofrin®. In some regions a decrease in ADC was also observed. The four regions of

interest in a given slice that were chosen for ADC measurements along the x, y, and z directions led to a total of twelve measurements of ADCs per slice. From the set of 12 measured values, we observed increases in 7 values and decreases in 5 for the case of Photofrin® and 10 increases and 2 decreases for the case of DOD-6. The maximum increase in ADC was ~54% with Photofrin® and 165% with DOD-6. Together our studies demonstrate that in the time frame where ^{31}P studies indicate build up of inorganic phosphate, the different regions of the tumor also undergo changes in the diffusion values which are indicative of a substantial increase in water diffusivity that may be attributable to major cell loss, reduced cell density, and widening of extracellular space leading to high water mobility (17). A decrease in ADCs has been attributed to possible cell membrane break down that block active ion and water transport that lead to decline in ADC. Detailed bar graphs indicating changes in ADC after PDT treatment are provided in Appendix-A.

Key Research Accomplishments

- Using ^{19}F MR spectroscopic method, the entire pharmacokinetic profile of two fluorine labeled photosensitizers were generated (copy of the abstracts, poster presented at the Era of Hope meeting at Philadelphia are enclosed in the Appendix B2 and see publication # 18 for more details)).

- ^{31}P MR spectra of tumors were studied before and after the initiation of PDT (see publication #19).

- PDT studies were performed using laser light at 630 nm, 270 joules/cm energy. The time point was chosen to represent maximum concentration of the photosensitizer as obtained from the pharmacokinetics data.

- The photosensitizer DOD-2 showed tumor regression while the nonlabeled (DOD-1) did not show any tumor regression. The incorporation of fluorine in the PS appears to have a positive effect on the function of the photosensitizer. Similarly the nonlabeled photosensitizer (DOD-8) showed less tumor regression than the fluorine labeled counter part DOD-6. The results demonstrate the effect of fluorine on the PS activity which appears to enhance the PS activity.

Reportable Outcomes

1. Abstract of the presentation made at the ERA of HOPE meeting held at Orlando, Florida during September 25-28, 2002.
2. Abstract of the Talk to be presented at the ESMRMB meeting to be held at Rotterdam, Netherlands, during September 18-21, 2003.
3. Abstract of the talk presented at the SPIE international symposium held in San Diego, Feb15-17, 2004.
4. Abstract of the talk presented at the ESMRMB meeting held at Denmark, September 9-12, 2004

5. Abstract of the talk presented at the SPIE international symposium held in San Diego, Feb13-15, 2005.
6. Abstract of the talk that will be presented (upon acceptance) at the SPIE international symposium held in San Diego, Feb13-15, 2006.
7. Abstract of the presentation made at the ERA of HOPE meeting held at Pittsburgh, Pennsylvania, June 8-11, 2005.
8. Poster copy of the presentation made at the ERA of HOPE meeting held at Pittsburgh, Pennsylvania, June 8-11, 2005.
9. A full paper related to synthesis and in vivo fluorine MR studies was published in Tetrahedron, a well recognized scientific journal.
10. A full paper in the proceedings of SPIE (Medical imaging), Volume 5369, pp 380-386, 2004.
11. A full paper in the Proceedings of SPIE (Medical Imaging), Volume 5746, 16-22, 2005.

Funding applied for during the past two years in this or related area

1. DOD undergraduate research grant- submitted in year 2002. The proposal was not funded. A resubmission was not done as this category of research was not open for consideration in the year 2003 by DOD.

2. A grant application to Nebraska state was made in the early 2003 but was not funded.

3. A revised application was resubmitted in early 2004. This was not funded but the reviewers suggested that the work be done on a breast tumor model. This pilot grant will be will be submitted with more data in the year 2006.

4. A grant proposal to NIH/NCI is also being planned and will be submitted in early 2006.

Conclusions:

Our studies demonstrate the fluorine labeled compound can be noninvasively monitored in the tumor and muscle by ^{19}F magnetic resonance spectroscopy. The ^{31}P spectroscopic data on tumors show that even though the ^{31}P spectra after PDT do not undergo significant changes the tumor shows regression (for studies on DOD-1 and DOD-2 that were only sparingly soluble in water). The changes in ^{31}P spectra were indeed seen in both DOD-6 and DOD-8 that is a nonfluorine analog of DOD-6. The changes in ATP and Pi peaks were more

significant for DOD-6 and less so in the case of DOD-8. The tumor growth charts showed that DOD-6 leads to rapid tumor regression while DOD-8 shows much lower rate of regression. Occasionally we also saw no regression at all in the case of DOD-8. Together, it appears that the nonfluorinated analogs of the two fluorine labeled photosensitizers are considerably less active compared to their fluorinated analogs. The role of fluorine in enhancing the PS activity will be a different area of research.

It is possible to produce larger amounts of the labeled compounds for further detailed studies on the distribution in the animal and also in the tumor. The ability to monitor the fluorine labeled PS in the animal model will provide useful data before PDT is performed. In vivo MR will be a useful method in the development of new photosensitizers

Future Studies and Funding

The future studies will consider work on both RIF and subsequently breast tumor models. The distribution of PS in the entire mouse and further studies on its distribution in the tumor and muscle will be studied by ^{19}F MR. New MR methods will be developed and further improvements done to study small volumes of tissue and tumor. Relaxation, diffusion and imaging will be performed both before and after the PDT studies. The techniques will revolve around ^{1}H, ^{19}F, ^{31}P nuclei. Incorporation of nuclear overhauser methods to further improve the signal to noise will be considered for future projects and grant proposals in the coming years.

References

1. Twentyman PR, Brown JM, Gray JW, frank AJ, Scoles MA, Kallman RF. A new mouse tumor model system (RIF-1) for comparison of end point studies. J. Natl. cancer Inst., 1980, 64, 595-604.

2. T.J. Dougherty, C.J. Gomer CJ, B.W.Henderson , G. Jori , D. Kessel , M. Korbelik , J. Moan and Q. Peng . Photodynamic therapy, J.Natl. Cancer. Inst. 90:889-905, 1998.

3. J. Morgan , W.R. Potter , A.R.Oseroff . Comparison of photodynamic targets in a carcinoma cell line and its mitochondrial DNA-deficient derivative. Photochem. Photobiol. 71: 747-757, 2000

4. Z. Tong , G. Singh, A.J. Rainbow . Extreme dark cytotoxicity of Nile Blue A in normal human fibroblasts. Photochem. Photobiol. 74:707-711, 2001.

5 K. Urbanska , B. Romankowa-Dixon , Z. Matuszak , J. Oszajca , P.Nowak-Sliwinska , G. Stochel. Indocyanine green as a prospective sensitizer for photodynamic therapy of melanomas. Acta Biochimica Polonica. 49, 387- 391, 2002.

6. T. Mosmann . Rapid colorimetric assay for cellular growth and survival: application to proliferation and cytotoxicity assays. J. Immunol Methods. 16:55-63,1983.

7. D.A. Musser, A.R. Oseroff. The use of tetrazolium salts to determine sites of damage to the mitochondroial electron transport chain in intact cells following in vitro photodynamic therapy with Photofrin II. Photochem. Photobiol. 59:621-626,1994.

8. PK Solutions Software (version 2.0), Summit Research Services, Colorado, 2001

9. T L Ceckler, R.G. Bryant, D P Penney, S L Gibson and Hilf R, ^{31}P NMR spectroscopy demonstrates decreased ATP levels in vivo as an early response to photodynamic therapy, Biochem. Biophys. Res. Commun., 140, 273-279, 1986.

10. S Naruse, Y Horikawa, C Tanaka, T Higuchi, H Sekimoto, S Ueda, and K. Hirakawa, Evaluation of the effects of photoradiation therapy on brain tumors with in vivo ^{31}P MR spectroscopy, Radiology., 160, 827-830, 1986.

11. M. Chopp, H. Farmer, F.Hetzel and A P Schaap. In vivo ^{31}P NMR spectroscopy of mammary carcinoma subjected to subcurative photodynamic therapy, Photochem. Photobiol. 46, 819- 822, 1987.

12. R Hilf, S L Gibson, D P Penney, T.L. Ceckler, R G Bryant, Early biochemical responses to photodynamic therapy monitored by NMR spectroscopy. Photochem. Photobiol. 46,

809-817. 1987.

13. S.Ramaprasad, R K Pandey, R.M. Hawk, Y.H. Liu. Responses to Photodynamic therapy in a murine tumor model-- ^{31}P NMR and water proton relaxation studies, J. Environ. Sci. Health. A28, 2345-2357. 1993.

14. A. Naressi, C. Couturier, J.M. Devos, M. Janssen, C. Mangeat, R. deBeer, D. Graveron-Demilly, "Java-based graphical user interface for the MRUI quantitation package," *MAGMA,* 12, pp. 141-152, 2001.

15. Y.H. Liu, R.M. Hawk, S. Ramaprasad, "In vivo relaxation time measurements on a murine tumor model- Prolongation of T_1 after photodynamic therapy," *Magn Reson Imaging,* 13, pp. 251-258, 199.

16. S. Ramaprasad, E. Rzepka, J. Pi, SS. Joshi, M. Dobhal, J. Missert, R.K. Pandey Monitoring PDT Effects in Murine Tumors by Spectroscopic and Imaging Techniques. SPIE Proceedings vol 5369, 380-386. 2004.

17. R.A. Kauppinen, "Monitoring cytotoxic tumor treatment response by diffusion magnetic resonance imaging and proton spectroscopy," *NMR Biomed*, 15, pp. 6-17, 2002.

18. S.K .Pandey , A.L Gryshuk, A Graham, K Ohkubo, S. Fukuzumi, M.P Dobhal, G. Zheng, Z. Ou, R, Zahn, K.M.Kadish, A. Oseroff, S. Ramaprasad, R.K. Pandey, "Fluorinated photosensitizers: Synthesis, Photophysical, Electrochemical, Intracellular Localization, In vitro photosensitizing efficacy and determination of tumor-uptake by ^{19}F in-vivo MR spectroscopy," *Tetrahedron*, 59:10059-10073, 2003.

19. S. Ramaprasad, S, E.Ripp, J.Pi, SS. Joshi, S.K.Pandey, J.Missert, R.K. Pandey ."*In Vivo* Magnetic Resonance Measures of Dark Cytotoxicity of Photosensitizers in a Murine Tumor Model" Proceedings of SPIE (Medical Imaging), 2005, *5746*, 16-22.

Appendix-A

Research results Relevant to material reported here (Tables, Graphs etc)

Compounds Received from Roswell Park Institute

Material sent to UNMC from RPCI as of 10/19/04

Compound label	Date	Amount	
DOD 1	July 2002 as solution and solid: (methyl, 2(COOH))	solution 9 ml at 0. 356 mM solid 50 mg	
DOD 2	July 2002 as solution and solid: (trifluoromethyl, (2(COOH))	solution 9 ml at 0. 275 mM solid: 50 mg	
DOD 4 *	Oct 2002 (first batch)	40	*Also labeled DOD JM- 4 Trifluoromethyl (4(COOH))
DOD 4	Mar 2004 (second batch)	28	Sent May 2004
DOD 6	Apr. 2003	solution 3.73 mM (3.1 mg/ml) Ce6 derivative(fluorinated) Volume approx 9 ml Approx 27mg in solution	
DOD 6	June 2004	solution 3.73 mM (3.1 mg/ml) Ce6 derivative(fluorinated) Volume approx 9 ml Approx 27mg in solution	
DOD-8	November 2004	Appox 6mg in solution	

Results related to dark toxicity of compounds studied in this project

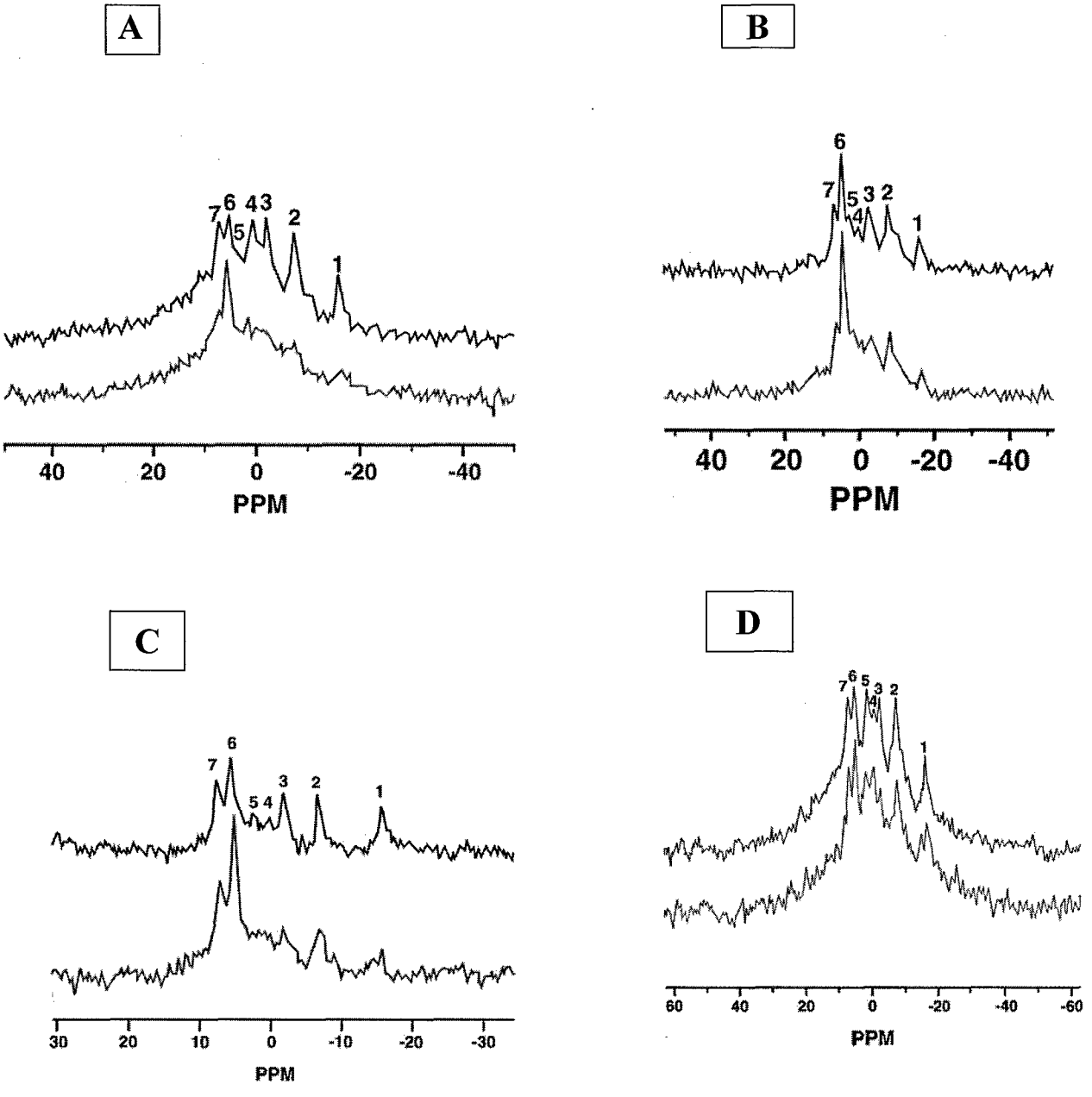

Figure 2: ^{31}P spectra of mouse foot tumor recorded before (upper trace) and after (lower trace) administration of Photosensitizers : A) DOD-6 administered at a dose of 10 μM/kg B) DOD-6 administered at a dose of 2.5 μM/kg C) DOD-2 administered at a dose of 10 μM/kg and D) Photofrin administered at a dose of 10 μM/kg respectively. The various peak assignments are: 1) β-ATP 2) α–ATP 3) γ- ATP 4) PCr 5) PDE 6) Pi and 7) PME.

Table 1
Tumor doubling times* for various PDT treated and untreated tumors.

Cage & Mouse	Drug used	Tumor treatment	Tumor Doubling Time (Hr)
C5M1	DOD1	PDT treated	173.3
C5M2	DOD1	PDT treated	115.5
C5M3	DOD1	PDT treated	115.5
C10M1	DOD2	PDT treated	173.3, 693.1
C10M3	DOD2	PDT treated	115.5, 231.0 693.1
C10M5	DOD2	PDT treated	173.3 231.0 173.3
C7M3	None	untreated	77.0
C7M4	None	untreated	69.3
C8M4	None	untreated	115.5
C8M1	Photofrin	PDT treated	173.3 693.1
C12M2	Photofrin	PDT treated	173 231

Note: In doubling time calculation is based on following segs.
C10M1: seg1 (ascending, March 24-April 17, 03), seg3 (descending, April 25-May 5, 03).
C10M3: seg1 (ascending, March 24-April 17, 03), seg2 (descending, April 17-21, 03), seg3 (ascending, April 23-May 5, 03).
C10M5: seg1 (ascending, March 24-April 24, 03), seg2(descending, April 24-30, 03), seg3 (ascending, April 30-May 19, 03).

C8M1: seg1 (ascending, Dec. 23, 02 – Jan. 17, 03), seg2(descending, Jan. 20-29, 03), no seg3.
C12M2: seg1 (ascending, May 23-June 19, 03), doubling time is 173.3. If taking all points after peak (June 19-July 11, 03), including peak, the doubling time (DT) is 693.1. After taking peak point and five points following it (June 19-June 27, 03), DT is 231.

* The term "doubling times" is used to define the increase or decrease in tumor volumes. The values corresponding to ascending or descending phases of the tumor growth refers to increasing or decreasing volumes of the tumor.

Table 2

Tumor regression after PDT with DOD1 and DOD2 photosensitizers

Cage & Mouse #	Drug used and Dose	Tumor vol (day of PDT)	Laser 1 Power	Laser 2 Power	Remarks
C5 M1	DOD1 0.35ml	458.76	135 Joules	---------	No real tumor regression seen
C5 M2	DOD1 0.33ml	148.82	135 Joules	---------	No real tumor regression seen
C5 M3	DOD1 0.33ml	487.03	135 Joules	---------	No real tumor regression seen
C12 M5	DOD1 0.7ml	131.78	270 Joules	---------	No real tumor regression seen
C13 M2	DOD1 0.565ml	65.54	270 Joules	270 Joules	A little tumor regression seen
C13 M4	DOD1 0.649ml	107.86	270 Joules	270 Joules	No real tumor regression seen
C4 M3	DOD2 0.43ml	271.73	135 Joules	---------	No real tumor regression seen
C4 M4	DOD 2 0.42ml	245.2	135 Joules	---------	No real tumor regression seen
C10 M1	DOD2 0.96ml	179.22	270 Joules	--------	A very slight tumor regression 4 days after irradiation
C10 M3	DOD2 10uM	391.18	270 Joules	---------	Some Tumor regression on days 1-4 after irradiation
C01 M4	DOD2 0.6ml	150.37	135 Joules	--------	No real tumor regression seen
C10 M5	DOD2 0.92ml	106.32	270 Joules	270 Joules	Tumor regression seen for 8 days after irradiation
C11 M1	DOD2 0.84ml	83.18	270 Joules	----------	A slight tumor regression 3 days after irradiation
C11 M2	DOD2 0.81ml	63.38	270 Joules	----------	No real tumor regression seen
C11 M3	DOD2 0.60ml	70.78	270 Joules	270 Joules	Regression seen the day after irradiation

Table 3

The laser power, duration of irradiation used in our PDT studies

Univ. #	Mice # (Cage #, ear notch #)	P.S. Admin.	Date of irradiation	Duration Of irradiation	Irradiation time post PS injections	Power used	Total incident energy (joules)
18	C4 M3	DOD 2 .43 ml	10/10/02	30 minutes	24 hours	75mW	135
19	C4 M4	DOD 2 .42 ml	10/10/02	30 minutes	24 hours	75mW	135
21	C5 M1	DOD 1 .35 ml	10/10/02	30 minutes	24 hours	75mW	135
22	C5 M2	DOD 1 .33 ml	10/10/02	30 minutes	24 hours	75mW	135
23	C5 M3	DOD 1 .33 ml	10/10/02	30 minutes	24 hours	75mW	135
26	C6 M1	Photofrin .245 ml	10/4/02	10 minutes	24 hours	225-230 mW	135
27	C6 M2	Photofrin .235 ml	10/4/02	10 minutes	24 hours	225-230 mW	135
28	C6 M3	Photofrin .240 ml	10/4/02	10 minutes	24 hours	225-230 mW	135
29	C6 M4	Photofrin .265 ml	10/4/02	10 minutes	24 hours	225-230 mW	135
30	C6 M5	Photofrin .260 ml	10/4/02	10 minutes	24 hours	225-230 mW	135
36	C8 M1	Photofrin 25mg/kg	1/15/03	30 minutes	24 hours	75mW	135
41	C9 M1	DoD2 3mg	3/20/03	30 minutes	24 hours	150mW	135
44	C9 M4	Photofrin .24 ml	3/12/03	30 minutes	24 hours	75 mW	135

Diffusion Coefficients for various slices using PFII and DOD-6 photosensitizers in a mouse tumor model

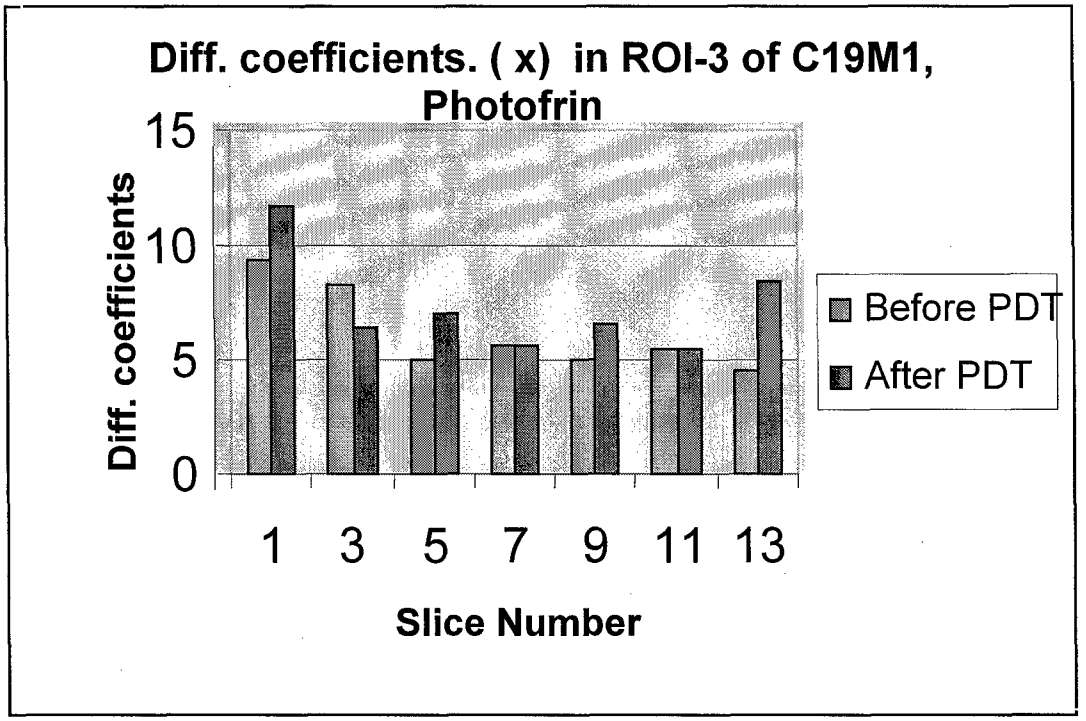

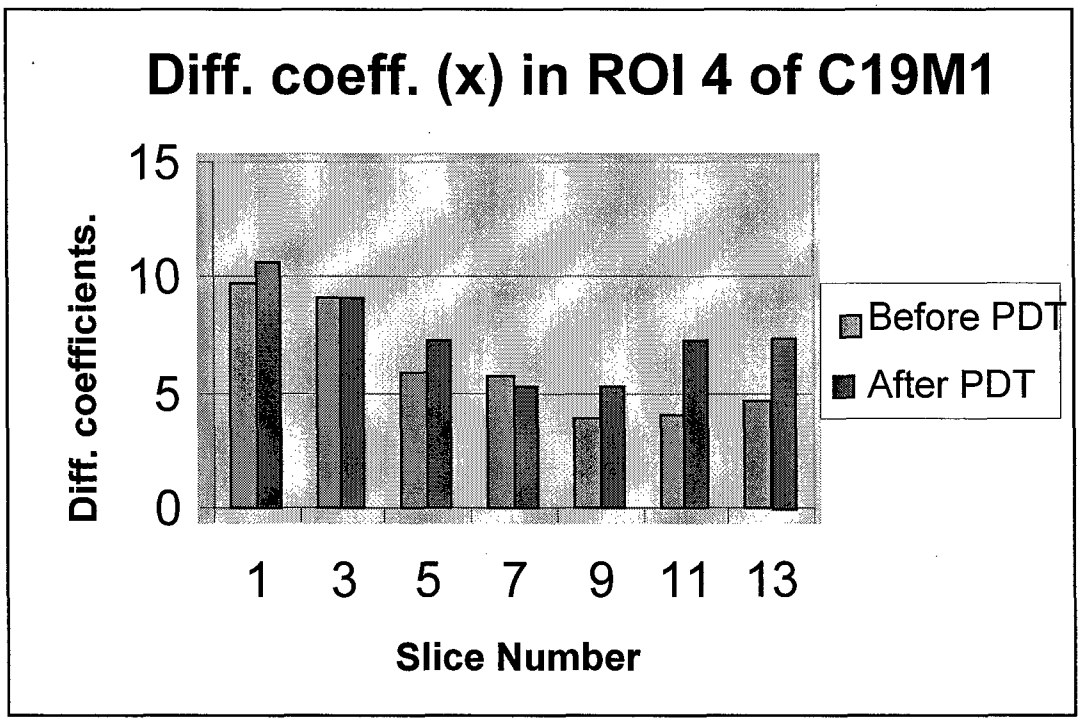

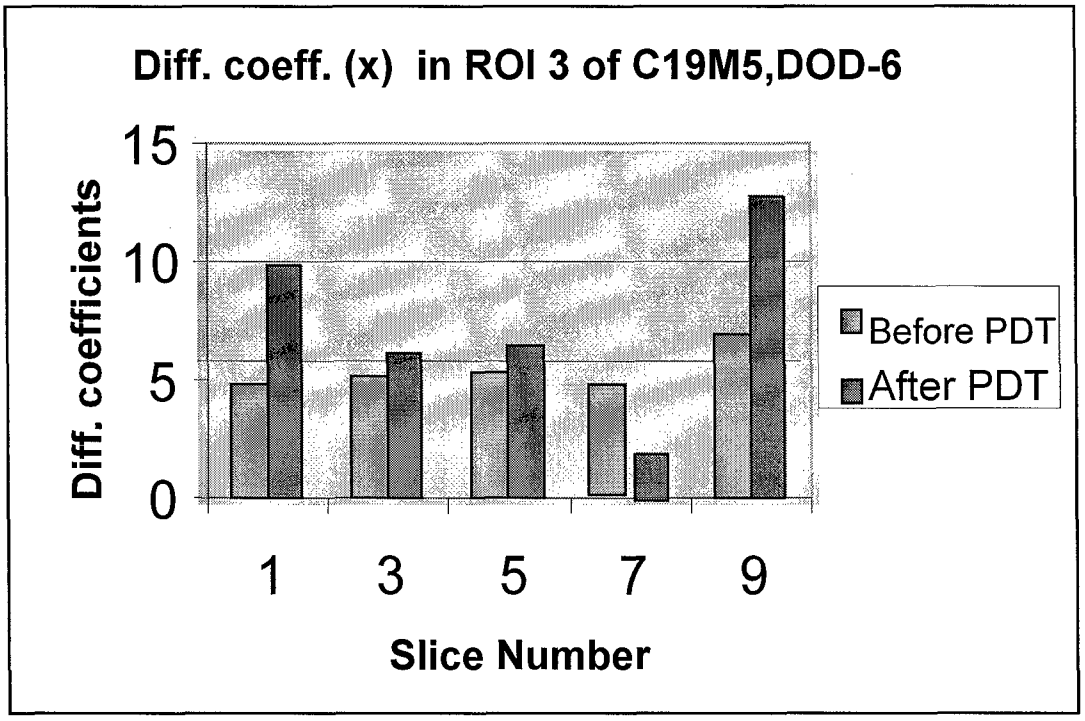
Diff. coeff. (x) in ROI 3 of C19M5,DOD-6
Diff. coefficients
15
10
5
0
1
3
5
7
9
Slice Number
Before PDT
After PDT

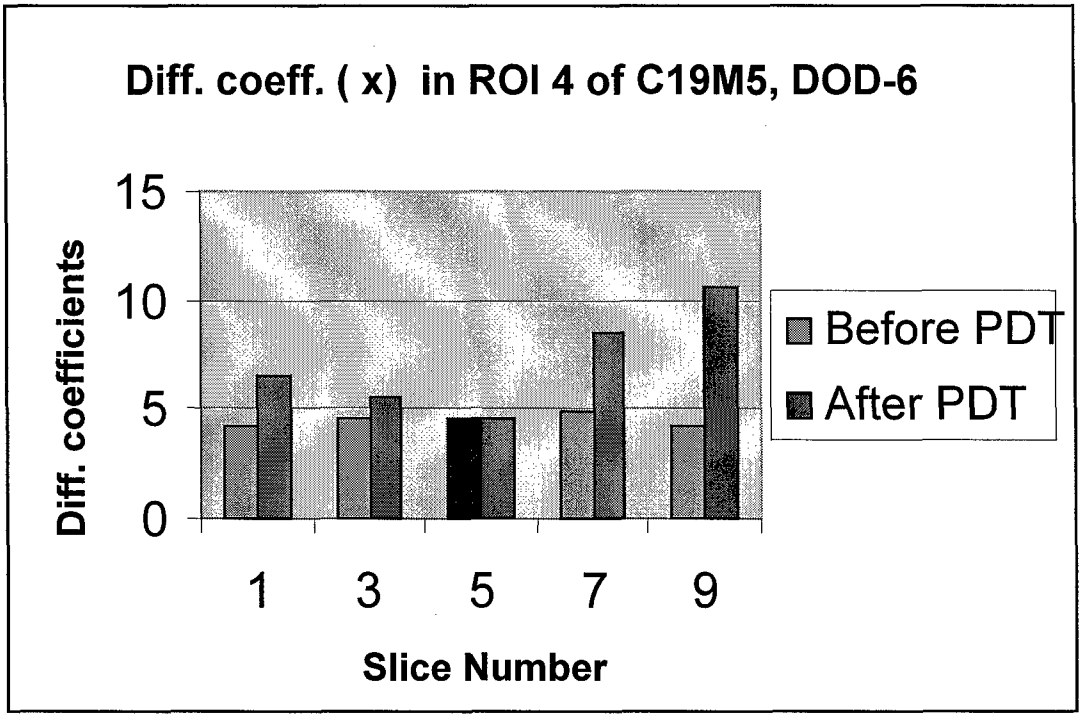
Diff. coeff. (x) in ROI 4 of C19M5, DOD-6
Diff. coefficients
15
10
5
0
1
3
5
7
9
Slice Number
Before PDT
After PDT

Appendix-B1

Copy of the Abstracts resulting from this grant

Abstract of the Presentation made at the ERA of HOPE Meeting, held at Orlando, Florida, September 25-28, 2002.

SYNTHESIS AND IN VITRO PHOTOSENSITIZING EFFICACY OF FLUORINATED PORPHYRIN-BASED PHOTOSENSITIZERS FOR IN VIVO MR STUDIES

Suresh K. Pandey, Amy L. Gryshuk, Andrew Graham, Allan Oseroff, S. Ramaprasad,[1] and Ravindra K. Pandey

Photodynamic Therapy Center, Roswell Park Cancer Institute, Buffalo, NY 14263 and [1]Department of Radiology, Nebraska Medical Center, Omaha, NE 68198

ravindra.pandey@roswellpark.org and sramaprasad@unmc.edu

In vivo MR spectroscopy has been used increasingly to monitor metabolism and disease states in humans. Both magnetic resonance imaging and spectroscopy have evolved into sophisticated diagnostic techniques. In addition to the proton, nuclei such as fluorine can be studied by in vivo spectroscopy and imaging. Fluorine-19 NMR is a technique with significant potential because of the relatively high sensitivity and low endogenous background. Fluorine-19 MR has been used to study metabolism, tumor growth, and blood flow. MR of fluorinated compound is particularly attractive for in vivo studies of human and animal models. The F-19 isotope has a 100% natural abundance, a spin of 1/2, and an MR sensitivity that is 83% that of hydrogen.

To date, most of the fluorinated porphyrin-based analogs synthesized for in-vivo F-19 NMR studies have been unsymmetrical, and thus lead to signal dispersion. In order to have strong fluorine signal at a low concentration of the drug in tumor, it is necessary to have photosensitizers containing multiple fluorine units. It would be advantageous to have a center of symmetry in the fluorinated photosensitizer that will render the fluorine nuclei to be equivalent and provide signal addition of all equivalent nuclei. We have succeeded in synthesizing porphyrins containing six to 12 symmetrical fluorines. These compounds were prepared in multi-step syntheses. The structures were confirmed by NMR, mass spectrometry and elemental analyses. The symmetry of the fluorines was confirmed by F-19 NMR studies. Compared to the non-fluorinated analogs, the fluorinated porphyrins showed enhanced singlet oxygen producing efficiency.

The in-vitro photosensitizing efficacy of the fluorinated porphyrins was investigated in RIF tumors at various doses and showed promising activity. The synthesis, photophysical characteristics and in-vitro photosensitizing results of the newly synthesized fluorinated porphyin-based compounds will be discussed.

The U.S. Army Medical Research and Materiel Command under DAMD17-99-1-9065 supported this work.

Oral Presentation at the European Society of Magnetic Resonance in Medicine in Rotterdam, Netherlands, September 2003.

In Vivo ^{19}F MR Studies of Fluorine Labeled Photosensitizer in Murine Tumor Model

S. Ramaprasad[1], E.Rzepka[1], S.S. Joshi[2], M. P. Dobhal [3], J. Missert [3], R.K. Pandey[3]
[1] Department of Radiology, University of Nebraska Medical Center, Omaha, NE, U.S.A
[2] Departments of Genetics, Cell Biology, and Anatomy, University of Nebraska Medical Center, Omaha, Nebraska, U.S.A. [3] Photodynamic Therapy Center, Roswell Park Cancer Institute, Buffalo N.Y, U.S.A.

Introduction

Photodynamic therapy (PDT) is a cancer treatment modality that combines light sensitive drug and lasers [1]. Monitoring the photosensitizer (PS) in the tumor and in normal tissue is helpful in the development of new photosensitizers. Syntheses of labeled photosensitizer that can be monitored by MR studies offer the advantage of noninvasive assessment of the photosensitizer in a single subject [2]. The assessment of the same in the skin and underlying muscle may provide information about the cutaneous toxicity of PS. In this work we present the construction of pharmacokinetic profile of a new photosensitizer in a tumor model and its utility in PDT studies.

Methods

The Radiation induced fibrosarcoma (RIF) cells were maintained according to the protocol of Twentyman et al [3]. Tumors were grown on mouse foot dorsum by inoculating $2x10^5$ cells. The photosensitizer was administered IP (~100μM). ^{19}F MR spectra were collected on a Bruker 7T instrument using a home built surface coil. The ^{19}F MR spectral parameters included a 90° pulse of 16μs, a spectral width of 20 KHz, 8K data points, and a 2s repetition time for a total accumulation time of 30 minutes. PDT measurements were performed at 630 nm with an argon ion (Spectra physics model 2045) pumped dye laser (Spectra Physics, 375B). Laser irradiation was done for 30 minutes at a power of 150 mW cm^{-2} leading to a total light dose of 270 J cm^{-2}.

Results

In this presentation we report the results obtained using a newly synthesized water soluble form of fluorine labled photosensitizer which was monitored in mouse tumor model over time. The measured relaxation times in the solution were 924±38 ms for T_1 and 150±2 ms for T_2 and were used to optimize of tumor spectra. The Pharmaco- kinetic profile of PS in tumor model was constructed using three tumors (Figure 1). Based on this

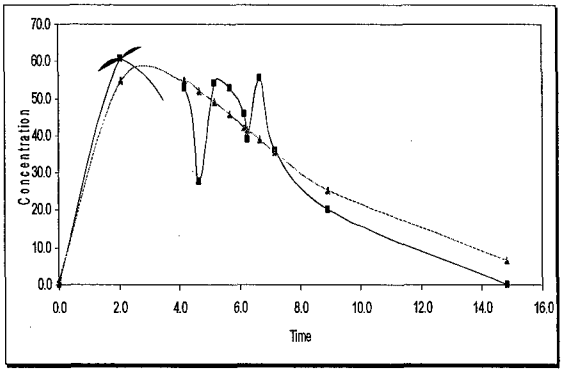

profile PDT was performed at time points 2hr, 4hr and 24 hrs post drug administration.

Conclusions:
MR studies can provide quantitative data on photosensitizer in tumor and a rational basis for PDT initiation. PDT studies done at 2hrs post PS administration led to tumor regression between days 2-4.

References

1. Dougherty, TJ, et al. [1998] J.Natl. Cancer. Inst. 41:351-359.
2. Ramaprasad et al [1994] Proc. Soc.Magn. Reson Med. 3: 1348.
3. Twentyman et al [1980] J.Natl. Cancer. Inst.64: 595-604.

Acknowledgement

This research was funded by the Department of Defense (DAMD 17-99-1-9065).

Presented at the SPIE meeting (Medical Imaging) held at Sandiego, Feb, 2004.

ABSTRACT

Monitoring PDT Effects in Murine Tumors by Spectroscopic and Imaging Techniques

S. Ramaprasad[a*], E. Rzepka[a], J. Pi[a], SS. Joshi[b], M Dobhal[c], J. Missert[c], RK. Pandey[c]
[a]Department of Radiology, University of Nebraska Medical Center, Omaha, NE, USA, 68198-1045; [b]Department Genetics and Cell Biology, University of Nebraska Medical Center, Omaha, NE, USA, 68198-6395, [c]PDT Center, Roswell Park Cancer Institute, Buffalo, NY-14263,USA.

The changes in the tumor that occur following photodynamic therapy (PDT), a cancer treatment modality, were studied using a small animal MR imager operating at 7Tesla. The animal model used in these studies was mice implanted with radiation -induced fibrosarcoma (RIF). The tumor bearing mice were injected with 10μM/kg of one of the three photosensitizers: 1) Photofrin 2) Fluorine labeled photosensitizer and 3) Non-labeled analog of the fluorine labeled sensitizer. Laser light at 630 nm (150 mW/cm^2, 270 joules/ cm^2) was delivered to the tumor at 2-24 hours of photosensitizer administration. The MR spectroscopic and imaging examination of the tumors involved both the ^{1}H and ^{31}P nuclei. The tumor bioenergetics was measured by ^{31}P spectroscopy. The water proton relaxivity and diffusion measurements are used to obtain local changes in different regions of the tumor.

Significant changes in ^{31}P MR spectra were observed using photofrin while no statistically significant changes were observed when the fluorine labeled or its non labeled analogs were used. The PDT induced changes in tumor volumes (as measured by calipers) showed significant tumor regression with photofrin followed by moderate regression with the fluorine labeled PS and no regression with the non labeled PS. The growth pattern of tumors using nonlabeled photosensitizers followed the general pattern of unperturbed tumors. The possible relationship between the function of these sensitizers and the various MR derived parameters that characterize the tumor status will be discussed.

In Vivo ^{19}F MR Studies of Fluorine Labeled Photosensitizer in Murine Tumor Model

S. Ramaprasad[1], E.Rzepka[1], J. Pi[1], S.S. Joshi[2], J. Missert [3], M. P. Dobhal [3], R.K. Pandey[3] [1] Department of Radiology, University of Nebraska Medical Center, Omaha, NE, U.S.A. [2] Departments of Genetics, Cell Biology, and Anatomy, University of Nebraska Medical Center, Omaha, Nebraska, U.S.A. [3] Photodynamic Therapy Center, Roswell Park Cancer Institute, Buffalo N.Y, U.S.A.

Introduction

Photodynamic therapy (PDT) is a cancer treatment modality that combines light sensitive drug and lasers [1]. PDT is most beneficial when laser light is delivered at a time when the photosensitizer is greater in the tumor than the surrounding normal tissue. Monitoring the photosensitizer (PS) in the tumor and in normal tissue is helpful in the development of new photosensitizers. The assessment of the PS in the skin and underlying muscle has the potential to provide information about the cutaneous toxicity. Syntheses of photosensitizers labeled with an NMR observable nucleus, such as Fluorine-19, offer the advantage of noninvasive assessment of the photosensitizer concentration in a living subject [2]. In this work we present the construction of pharmacokinetic profiles of two new photosensitizers in the tumor and muscle and their utility in PDT studies. The structures of the two photosensitizers are shown in Figure 1. The details of the synthesis and subsequent confirmation of the structures have been recently published [3]. Here we report the in vivo results obtained using new fluorine labeled photosensitizers that were monitored in tumor bearing mice.

Figure 1

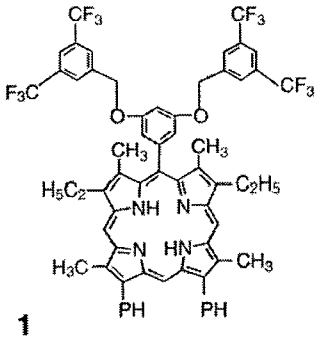

1

PH = -$CH_2CH_2CO_2H$

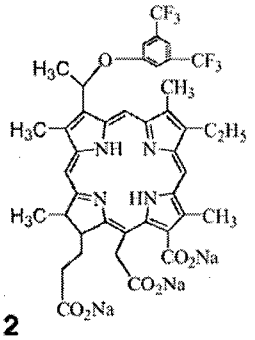

2

Methods

Tumor model: The Radiation induced fibrosarcoma (RIF) cells were maintained according to the protocol of Twentyman et al [4]. Tumors were grown on mouse foot dorsum by inoculating $2x10^5$ fresh cells. A total of 12 animals were studied here.

Laser and Delivery system: An argon ion (Spectra physics model 2017) pumped dye laser (Spectra Physics, 375B) was used. PDT measurements were performed at 630 nm for sensitizer **1** and at 650 nm for sensitizer **2**. Laser irradiation was done for 30 minutes at a power of 150 mW cm^{-2} leading to a total light dose of 270 J cm^{-2}. Fractionated laser irradiation was also employed in some studies.

In vivo MR and PDT studies: In vivo MR and PDT measurements were performed under mild anesthesia maintained by 1% isoflurane mixed with Nitrous oxide and Oxygen in 70:30 ratio. The photosensitizer was administered IP (~100μM). ^{19}F MR spectra were collected on a Bruker 7T instrument using a home built surface coil. The ^{19}F MR spectral parameters included an RF pulse of 16μs, a spectral width of 20 KHz, 8K data points, and a 2s repetition time for a total accumulation time of 30 minutes. The magnetic field homogeneity was optimized for each tumor by shimming on the water proton signal. The in vivo ^{19}F signal was compared with the signal from a phantom of known concentration to quantify the photosensitizer in the tumor. These values were used to construct the profiles for the tumor and the muscle. Figure 2 shows the data for compound **1**. The data for compound could be obtained on the muscle but not on foot tumors indicating compound **2** is less sensitive to detection in the tumor due to less number of fluorines in the molecule and small size of the tumors studied. Alternatively the accumulation of the PS in the tumor may be significantly low compared to that in the muscle.

Figure 2

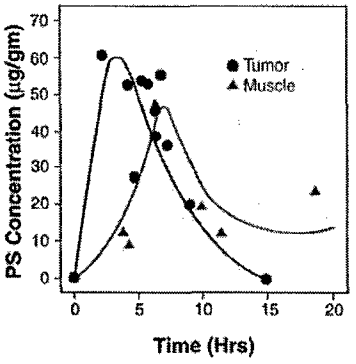

Results

The mean values of relaxation times for compound **1** in the solution were 924±38 ms for T_1 and 150±2 ms for T_2. Similarly for compound **2** the mean values were 250and 25 ms respectively. These values were used in the optimization of tumor ^{19}F spectra. The signals from the labeled sensitizers were found to be broad with mean line widths at 404±176 and 481±150 Hz for **1** and **2** respectively. The Pharmacokinetic profile of PS **1** in tumor model was constructed using three tumors (Figure 2). Based on this profile, PDT was performed at 2, 4 or 24 hrs post drug administration. The PDT studies performed at 2 and 4 hours led to tumor regression while that done at 24 hrs did not show any tumor regression. These data are in accordance with the pharmacokinetics of compound **1** shown in Figure 2. While using compound **2**, laser irradiation was done at 24 hrs post drug administration and there was significant tumor regression following PDT.

Conclusions

MR studies can provide quantitative data on photosensitizer in tumor and a rational basis for PDT initiation. PDT studies designed using the pharmacokinetic data showed significant tumor regression.

References

1. Dougherty, TJ, et al. *J. Natl. Cancer. Inst.* 41:351, 1998.
2. Ramaprasad et al. *Proc. Soc.Magn. Reson. Med.* 3: 1348, 1994.
3. Pandey SK et al, *Tetrahedron*, in press.
4. Twentyman et al. *J. Natl. Cancer. Inst.* 64: 595-604, 1980.

Acknowledgement

This research was funded by the Department of Defense (DAMD 17-99-1-9065).

Presented at the ESMRMB meeting held at Debmark, 2004

Dark Cytotoxicity Measures of Photosensitizers in a Murine Tumor Model by ^{31}P MR Studies

S. Ramaprasad[1], J. Pi, E.Rzepka[1], S.S. Joshi[2], J. Missert [3] ,M. P. Dobhal [3], R.K. Pandey[3]
[1] Department of Radiology, University of Nebraska Medical Center, Omaha, NE, U.S.A
[2] Departments of Genetics, Cell Biology, and Anatomy, University of Nebraska Medical Center, Omaha, Nebraska, U.S.A. [3] Photodynamic Therapy Center, Roswell Park Cancer Institute, Buffalo N.Y, U.S.A.

Introduction

Photodynamic therapy (PDT) is a novel cancer treatment modality in which the drug action is locally controlled by light (1). Development of new photosensitizers (PS) for clinical applications needs to minimize dark cytotoxicity while maximizing the PDT effects in the tumor. Here we report the observation of dark toxicity of PS by in vivo ^{31}P MR and discuss their utility in the development of new photosensitizers.

Methods

The Radiation induced Fibrosarcoma (RIF) cells were maintained according to the protocol of Twentyman et al (2). Tumors were grown on mouse foot dorsum by inoculating $2x10^5$ cells Male C3H/HeJ mice bearing foot tumors (N=9) in the volume range of 200-300μ were used in this study. Two new water soluble photosensitizers (3) were tested for dark toxicity and tumor growth monitored over 3-4 weeks. Of the two photosensitizers used in this study one was a porphyrin derivative (DOD-4) and the other was a chlorin derivative (DOD-6). The PS administered was in the dose range of 2.5-10μM/kg. ^{31}P spectra from the foot tumor were collected on Bruker 7 tesla animal imager and analyzed using the JMRUI software (4)

Results

Both DOD-4 and DOD-6 showed significant increase in inorganic phosphate (Pi) resonance in the first 2 hours post drug administration. Representative spectra for DOD-6 are shown in Figure 1. Studies performed between 5-24 hours

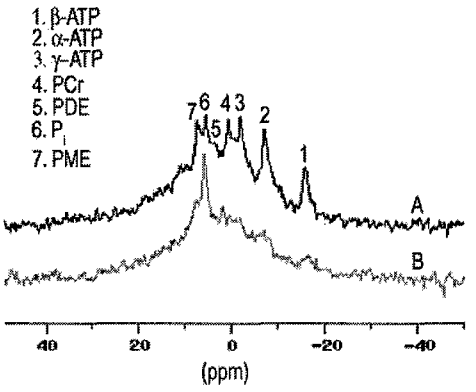

Figure 1: ^{31}P spectra of mouse foot tumor before(A) and after (B) administering DOD-6.

showed characteristics of control spectra recorded before drug injection. When photofrin was administered at similar doses, no significant changes were seen in ^{31}P MR spectra indicating minimal dark toxicity for Photofrin.

Discussion

The studies on tumors using the new Photosensitizers demonstrate that dark toxicity can be observed by ^{31}P MR. The tumor volumes monitored over several days did not show any tumor shrinkage as observed in PDT induced cytotoxicity. Although dark toxicity was shown by the two new PS, it was not strong enough to interfere with the normal tumor growth. Our study provides information on dark toxicity of a PS in an in vivo model and hence provides a complete picture than those on cell lines.

Acknowledgement

This research was funded by the Department of Defense (DAMD 17-99-1-9065).

References

1. Dougherty TJ, et al. [1998] J.Natl. Cancer. Inst. 90:889-905.
2. Twentyman PR, et al. [1980] J.Natl. Cancer. Inst. 64: 595-604.
3. Pandey SK, et al.[2003] Tetrahedron
4. Naressi A, et al. [2001] MAGMA, 12:141-152.

Presented at the SPIE meeting (Medical Imaging) held at Sandiego, Feb, 2005.

In Vivo Magnetic Resonance Measures of Dark Cytotoxicity of Photosensitizers in a Murine Tumor Model.

S. Ramaprasad[a*], E. Ripp[a], J. Pi[a], SS. Joshi[b], SK. Pandey[c], J. Missert[c], RK. Pandey[c]
[a]Department of Radiology, University of Nebraska Medical Center, Omaha, NE, 68198-1045, USA; [b]Department of Genetics and Cell Biology, University of Nebraska Medical Center, Omaha, NE, 68198-6395, USA; [c]PDT Center, Roswell Park Cancer Institute, Buffalo, NY, 14263, USA

SUMMARY

Photodynamic therapy (PDT) is a novel cancer treatment modality where the therapeutic action is controlled by light and the potency of the photosensitizer used. Development of new potent photosensitizers (PS) for clinical applications requires that the PDT effects are maximized while minimizing dark cytotoxicity. The dark toxicity of photosensitizers is generally confirmed using cell lines. Photososensitizers that appear promising from in vitro assays need further investigations under in vivo conditions. As in vivo MR methods have the potential to provide information on the tumor status, they can be very effective tools to study dark toxicity of tumors.

The tumor produced on the mouse foot dorsum was tested on two newly synthesized photosensitizers along with Photofrin as a control. The MR studies consisted of serial ^{31}P spectral measurements both before and after PS injection. The results show significant changes in the tumor metabolism with increased inorganic phosphate while using new photosensitizers. However these changes slowly approached control levels several hours later. The studies performed while using Photofrin did not show any significant changes indicating minimal or no dark cytotoxicity. Similar studies performed on normal tissue such as the muscle indicated that the energy metabolism was minimally compromised.

Our studies demonstrate that the effects of dark cytotoxicity can be observed by ^{31}P MR. The growth profiles of tumors treated with PS alone indicate that the metabolic changes are temporary and do not interfere with the tumor growth. The studies suggest that MR is a new method of monitoring the effect of PS administered toxicity in an in vivo model.

PRESENTED AT THE DOD SPONSORED ERA OF HOPE-2005 MEETING

MAGNETIC RESONANCE SPECTROSCOPIC QUANTITATION AND PDT EFFECTS OF FLUORINE LABELED PHOTOSENSITIZERS

S. Ramaprasad[1], J. Pi[1], S Singh[1], SS. Joshi[2], M. Dobhal[3], J. Missert[3], R.K. Pandey[3]

[1] Department of Radiology, University of Nebraska Medical Center, Omaha NE;
[2] Department of Genetics and Cell Biology, University of Nebraska Medical Center, Omaha NE; [3] Photodynamic Therapy Center, Roswell Park Cancer Institute, Buffalo, NY.

Background and Objective: The purpose of these studies was to investigate by magnetic resonance techniques the accumulation of fluorine labeled photosensitizers (PS) in tumor and normal tissue in mice bearing RIF tumors. Additionally we demonstrate that MR can be used to study the effects of PS alone as well as those from Photodynamic therapy.

Methods: RIF tumors were grown on mouse foot dorsum by inoculating $2x10^5$ fresh cells. An Argon ion (spectra physics model 2017) pumped dye laser (spectra physics 375B) was used to deliver laser light.

In vivo MR and PDT studies were performed under mild anesthesia by using 1% isoflurane mixed with N_2O and O_2 in 70:30 ratio.

Results: The T_1 and T_2 relaxation times of the two photosensitizers were measured in solution. For porphyrin PS the values were 924±38 and 150±2 ms (n=3), while for the chlorin based PS the values wee 250 and 25 ms respectively (n=1). The line widths of ^{19}F signals in the tumor were in the neighborhood of 400Hz.

The results from ^{31}P studies monitored over several hours (0-26) suggested that dark toxicity was present for both the photosensitizers when administered at or above 5μM concentration. A decrease in ATP and an increase in inorganic phosphate were observed for several hours after PS administration. These effects were very little or none at 8-24 hrs post PS administration.

The PDT studies were initiated at several time points post PS administration. The ^{19}F pharmacokinetic data was used as a guide in the design of PDT studies. The PDT results showed significantly higher decease in ATP and increase in Pi peaks. The tumor volumes measured before and after the PDT clearly showed significant tumor regression.

Conclusions: The multinuclear MR methods provide quantitative data on PS in the tumor and allow us to noninvasively follow the PS and their effects when administered alone or with laser to initiate PDT. This line of research has a high potential to treat and follow the patient noninvasively when labeled photosensitizers are used.

Original work supported by the U.S. Army Medical Research and Materiel Command under DAMD17-99-1-9065 and current work supported by the department of Radiology.

MAGNETIC RESONANCE SPECTROSCOPIC QUANTITATION AND PDT EFFECTS OF FLOURINE LABELLED PHOTOSENSITIZERS.

Ramaprasad[1], J. Pi[1], S.Singh[1], S.S. Joshi[2], M.Dobhal[3], J.Missert[3], R.K.Pandey[3].

1Department of Radiology, University of Nebraska Medical Center, Omaha NE; [2]Department of Genetics and Cell Biology, University of Nebraska Medical Center, Omaha NE; [3]Photodynamic therapy Center, Roswell Park Cancer Institute, Buffalo, NY.

Introduction

Photodynamic Therapy is a non invasive cancer treatment technique for killing cancer cells (Dougherty TJ, 1993) with the laser treatment after the pre- treatment with photoactive compounds known as photosensitizers. The drugs upon administration into the body (either IP or IV) enter the blood stream and collect in and around the tumor cells.

Photosensitizers are activated only when the light of certain wavelength is delivered on the cancer area. The most desirable wavelengths is the red end of the visible spectrum where the tissue penetration is greatest.

Photosensitizers absorb light energy and pass it onto molecular oxygen thereby producing an activated form of molecular oxygen known as singlet oxygen. It is a cytotoxic species that causes cellular damage in the localized area and prevents the cancer cells from receiving necessary nutrients thereby initiating tumor necrosis.

Magnetic resonance Imaging (MRI) and spectroscopy(MRS) are excellent non- invasive methods used to detect tumor response to PDT(Winsborrow BG, et al., 1997; Ramaprasad et al., 2004). Magnetic resonance techniques used are: a) MR Imaging – a technique based on the detection of hydrogen nuclei in water, displayed as anatomical images and b) MR spectroscopy, which is used to study the biochemistry of tissue from a variety of nuclei such as for example, 1 H, 31 P and 19 F.

Method

Radiation induced fibro sarcoma (RIF) cells were grown by following the standard cell culture procedure (Freshney RI, 1992). Cells were passaged at least two times a week and were harvested when they reached required density. Cell numbers were determined using a hemocytometer. The RIF cells (2x105 cells / ml) were inoculated on mouse foot dorsum.

The inoculation sites were observed two to three times a week for tumor growth. The tumor volumes were estimated using the formula V= ÉŒ (a x b x c)/6 where a, b, and c are the tumor dimensions measured using a caliper. PDT therapy: The photosensitizers were administered intra peritoneally (IP) 24 hours prior to laser treatment at a dose of 10 E M/Kg. The photo sensitizers used here were: Fluorinated photosensitizer (DOD-6) and non Fluorinated photosensitizer (DOD-8)

In vivo MR and PDT studies were performed under mild anesthesia by using 1 % isofluorane mixed with N20 and O2 in 70: 30 ratio. The 31P MR spectra were collected using a Bruker 1H – 31P dual coil. 19F spectra were collected using a home built surface coil.

Typical ^{31}P Parameters for mouse tumor study

- Acquisition Size : 8192
- Repetition time : 2.0 sec
- Pulse Angle : 45 degrees
- Excitation Pulse length : 70 usec
- Total. Expt. Time : 30min
- Number of Averages : 900

The photosensitizing drugs used were: Fluorinated photosensitizer (DOD-6) and non Fluorinated photosensitizer (DOD-8).The tumor was irradiated with laser light over 30 minutes for a total dose of 270 J cm-2. An Argon Ion (spectra physics model 2017) pumped dye laser (spectra physics 375B) was used to deliver laser light. Laser irradiation was done for ten minutes each on three dimensions leading to a total of 30 minutes of laser irradiation.

Results

The PDT studies were initiated at several time points post PS administration. The 19 F pharmacokinetic data (Fig.1) was used as a guide in the design of PDT studies. The tumor volumes measured before and after the PDT clearly showed significant tumor regression when Fluorine labeled DOD-6 was used as a photosensitizer (Fig. 2). However, there was no tumor regression when non fluorine labeled DOD-8 was used(Fig3). The MR studies consisted of serial 31 P spectral measurements both before and after PS injection(Fig.4). The results did not show any significant changes indicating no dark toxicity.

Pharmacokinetics of DOD-6, a fluorine labeled Photosensitizer, in the muscle tissue.

Figure 1

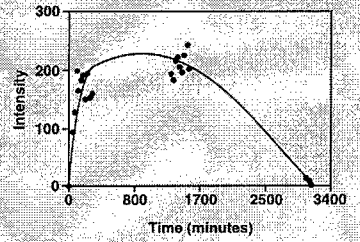

Altered Growth of RIF Tumors Under PDT (Arrows indicate PDT initiation).

Figure 2

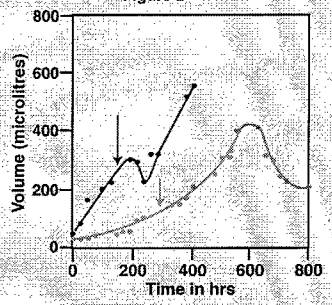

Serial ^{31}P Spectra of muscle recorded after PS administration

Figure 3

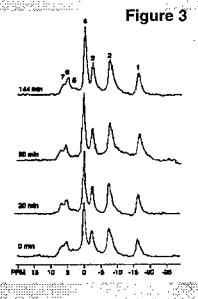

The peak assignments are as follows: 1) β–ATP 2) α-ATP 3) γ–ATP 4) PCr 5) PDE 6) Pi and 7) PME.

Figure 4

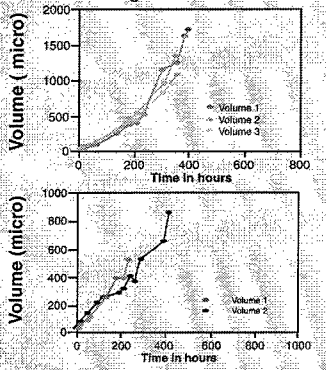

Conclusions

The multinuclear MR methods provide quantitative data on PS in the tumor and allow us to noninvasively follow the PS and their effects when administered alone or with laser to initiate PDT. This line of research has a high potential to treat and follow the patient noninvasively when labeled photosensitizers are used.

References

1. Dougherty TJ, (1993) Photodynamic Therapy. Photochem. Photobiol. 58: 895-900.
2. Freshney R. I., 1983. Culture of animal cells. A manual of basic technique, pp 43-45. Alan R. Liss, Inc., New York.
3. Ramaprasad S, Rzepka E., Pi J, Joshi SS, Dobhal M, Missert J, Pandey RK, (2004)Monitoring PDT effects in murine tumors by spectroscopic and imaging techniques. SPIE Proceedings 5369, 389-396.
4. Winsborrow B. G., Grondey H, Savoie H, Fyfe C.A,and Dolphin D.(1997) Magnetic Resonance Imaging Evaluation of photodynamic Therapy- Induced Hemorrhagic Necrosis in the Murine M1 Tumor Model. Photochem. Photobiol. 65(6): 847-852.

Acknowledgements

This research was funded by the Department of Defense (DAMD17-99-1-9065).

To be Presented at the SPIE meeting (Medical Imaging) to be held at Sandiego, Feb, 2006.

In Vivo Magnetic Resonance Measures of PDT Effects on the Tumor and Normal Tissue.

S. Ramaprasad[a*], S.Singh[a], J. Pi[a], SS. Joshi[b], SK. Pandey[c], J. Missert[c], RK. Pandey[c]
[a]Department of Radiology, University of Nebraska Medical Center, Omaha, NE, 68198-1045, USA; [b]Department of Genetics and Cell Biology, University of Nebraska Medical Center, Omaha, NE, 68198-6395, USA; [c]PDT Center, Roswell Park Cancer Institute, Buffalo, NY, 14263, USA

ABSTRACT

Photodynamic therapy (PDT) is a novel cancer treatment modality where the therapeutic action is controlled by light and the potency of the photosensitizer used. Development of new potent photosensitizers (PS) requires PDT effects are maximized for the tumor while minimizing its effects on the surrounding normal tissue. We are currently investigating effects of PDT on the tumor and normal tissue using photofrin and the newly developed fluorine labeled photosensitizers. As an initial part of the overall study we have used ^{31}P MR spectroscopy to gain insight into biochemical mechanisms that underlie cell death caused by PDT. Magnetic resonance experiments were performed on tumor bearing mice to evaluate photosensitizer effects in the absence and presence of laser irradiation at appropriate wavelength. The MR studies consisted of serial ^{31}P spectral measurements both before and after PS injection or PDT initiation as the case may be. Metabolic differences were seen in ^{31}P spectra following PDT treatment. These differences include reductions in phosphocreatine and changes in phosphodiester levels. These results will be further examined in the light of ^{1}H relaxation measurements and imaging studies.

Our studies demonstrate that the effects of PDT on normal tissue can be observed by ^{31}P MR. The studies suggest that MR is a noninvasive method of monitoring the effects of PDT on the normal tissue and subsequent recovery thereafter in an in vivo model.

Appendix-B2

Copies of Publications resulting from this grant

Pergamon

Tetrahedron 59 (2003) 10059–10073

TETRAHEDRON

Fluorinated photosensitizers: synthesis, photophysical, electrochemical, intracellular localization, in vitro photosensitizing efficacy and determination of tumor-uptake by ^{19}F in vivo NMR spectroscopy

Suresh K. Pandey,[a] Amy L. Gryshuk,[a] Andrew Graham,[b] Kei Ohkubo,[c] Shunichi Fukuzumi,[c,*] Mahabeer P. Dobhal,[a,†] Gang Zheng,[a] Zhongping Ou,[d] Riqiang Zhan,[d] Karl M. Kadish,[d,*] Allan Oseroff,[b] S. Ramaprasad[e,*] and Ravindra K. Pandey[a,f,*]

[a]*Photodynamic Therapy Center, Roswell Park Cancer Institute, Elm and Carlton Streets, Buffalo, NY 14263, USA*
[b]*Department of Dermatology, Roswell Park Cancer Institute, Buffalo, NY 14263, USA*
[c]*Department of Material and Life Science, Graduate School of Engineering, Osaka University, CREST, Japan Science and Technology Agency (JST), Yamada-oka, Suita, Osaka 565-0871, Japan*
[d]*Department of Chemistry, University of Houston, Houston, TX 77204-5003, USA*
[e]*Department of Radiology, University of Nebraska, Omaha, Nebraska, USA*
[f]*Department of Nuclear Medicine, Roswell Park Cancer Institute, Buffalo, NY 14263, USA*

Received 4 September 2003; revised 6 October 2003; accepted 6 October 2003

Abstract—For in vivo NMR studies, starting from pyrroles, a series of fluorinated porphyrins were synthesized by following the MacDonald reaction conditions. Upon reaction with osmium tetroxide, a fluorinated porphyrin containing four trifluoromethyl groups (12 fluorine units) was converted into the related chlorin and bacteriochlorin which exhibited long-wavelength absorptions at 652 and 720 nm, respectively. All compounds produced good singlet oxygen production efficiency. A comparative study of nine porphyrins with and without fluorine substituents indicated no adverse effects of the presence of fluorinated groups in the photophysical properties of the porphyrins, chlorins or bacteriochlorins. The first and second one-electron reduction potentials (vs SCE) of the investigated compounds range between −1.29 and −1.49 V and between −1.66 and −1.84 V in PhCN containing 0.1 M TBAP. UV–visible spectroelectrochemical data suggested the formation of π-anion and π-cation radicals upon the first reduction and first oxidation. The in vivo ^{19}F MR study of a representative fluorine labeled compound with twelve equivalent fluorines confirmed the presence of the fluorine labeled sensitizer in mouse (C3H/HeJ) implanted with RIF tumors on mouse foot dorsum by inoculating 2×10^5 cells (the studies were repeated on four tumored mice to confirm the feasibility and reproducibility). All fluorinated compounds were found to be quite effective in vitro. In a comparative intracellular localization study with Rhodamine-123 in RIF tumor cells, the most soluble porphyrin containing two propionic ester side chains was found to localize in mitochondria as well as the related chlorin and bacteriochlorin.

1. Introduction

Photodynamic therapy (PDT) is now a well recognized modality that has been used both independently and in conjunction with other cancer treatments.[1] Combining the use of a light-sensitive drug, lasers and fiber-optic probes, PDT has emerged as one of the promising strategies in cancer treatment. In this therapy, patients are given intravenous injections of a drug that accumulates in cancer cells in much higher concentrations than in normal cells. Laser light with an appropriate wavelength delivered by fiber optics to these tumor sites produces highly reactive oxygen species (e.g. $^1O_2$) that destroy the tumor cells.[2] Therefore, for a drug to be effective, it is necessary that the compound be in high concentration in tumor cells. PDT is most beneficial when laser light is delivered at a time point when the photosensitizer's concentration is greater in the tumor than in the surrounding tissue. Thus, a comprehensive knowledge of the extent of localization and the rate of accumulation is of immense value. While the photo sensitizer's concentration in tissue may be determined by chemical extraction techniques, these methods are

Keywords: photodynamic therapy; photosensitizers; porphyrins; chlorins; bacteriochlorins; mitochondria.
* Corresponding authors. Address: Photodynamic Therapy Center, Roswell Park Cancer Institute, Elm and Carlton Streets, Buffalo, NY 14263, USA. Tel.: +1-71684533203; fax: +1-7168458920; e-mail: ravindra.pandey@roswellpark.org; fukuzumi@ap.chem.eng.osaka-u.ac.jp; kkadish@uh.edu; sramaprasad@unmc.edu
† On leave from the Department of Chemistry, University of Rajasthan, Jaipur 302004, India.

0040–4020/$ - see front matter © 2003 Elsevier Ltd. All rights reserved.
doi:10.1016/j.tet.2003.10.016

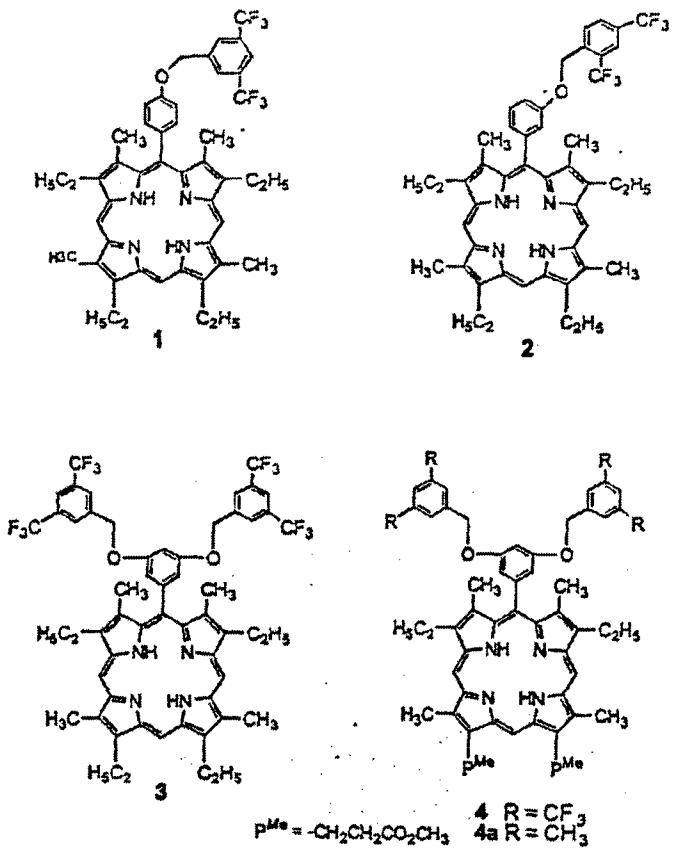

Chart 1.

invasive, time consuming, and clinically non-feasible. In contrast, in vivo NMR is minimally invasive, considered safe, and the therapy can be monitored over time in a single living system.[3]

In vivo MR spectroscopy has been used increasingly to monitor metabolism and disease states in humans. Both magnetic resonance imaging and spectroscopy have evolved into sophisticated diagnostic techniques. In addition to the proton, nuclei such as fluorine[4] can be studied by in vivo spectroscopy and imaging. Fluorine-19 (^{19}F) NMR is a technique with significant potential because of the relatively high sensitivity and low endogenous background. Due in part to its high MR sensitivity, fluorine has received considerable attention as an MR nucleus. Fluorine-19 MR has been used to study metabolism, tumor growth, and blood flow.[5] More recently, in vivo ^{19}F MR has been used to measure tumor integrity and vasculature in subcutaneously implanted tumors in rats.[6] MR of fluorinated compounds is particularly attractive for in vivo studies of human and animal models. The ^{19}F isotope has a 100% natural abundance, a spin of 1/2, and a MR sensitivity that is 83% then that of hydrogen.[7]

To date, most of the fluorinated porphyrin-based analogs synthesized for in vivo ^{19}F NMR studies have been unsymmetrical,[8] and thus lead to signal dispersion. In order to have a strong fluorine signal at a low concentration of the drug in tumors, it is necessary to have photosensitizers containing multiple fluorine units. It would be advantageous to have a photosensitizer with equivalent fluorine substituents that will render signal addition of all equivalent nuclei.

In this manuscript we report the synthesis of a series of fluorinated and the corresponding non-fluorinated porphyrin-based compounds, the effect of the substituents on their photophysical and electrochemical characteristics, their intracellular localization and their in vitro photosensitizing efficacy.

2. Results and discussion

2.1. Chemistry

For the synthesis of porphyrin-based fluorinated photosensitizers, our synthetic strategy was divided into two parts. These were the (a) synthesis of porphyrins 1 and 2 containing symmetrical trifluoromethyl groups (total fluorine: 6) introduced at the *meta*-or *para*-position(s) of the phenyl ring and (b) porphyrins 3 and 4 bearing symmetrical trifluoromethyl groups introduced at the 3 and 5-positions (total fluorine: 12) of the phenyl ring present at the *meso*-position of the porphyrin ring system (see Chart 1).

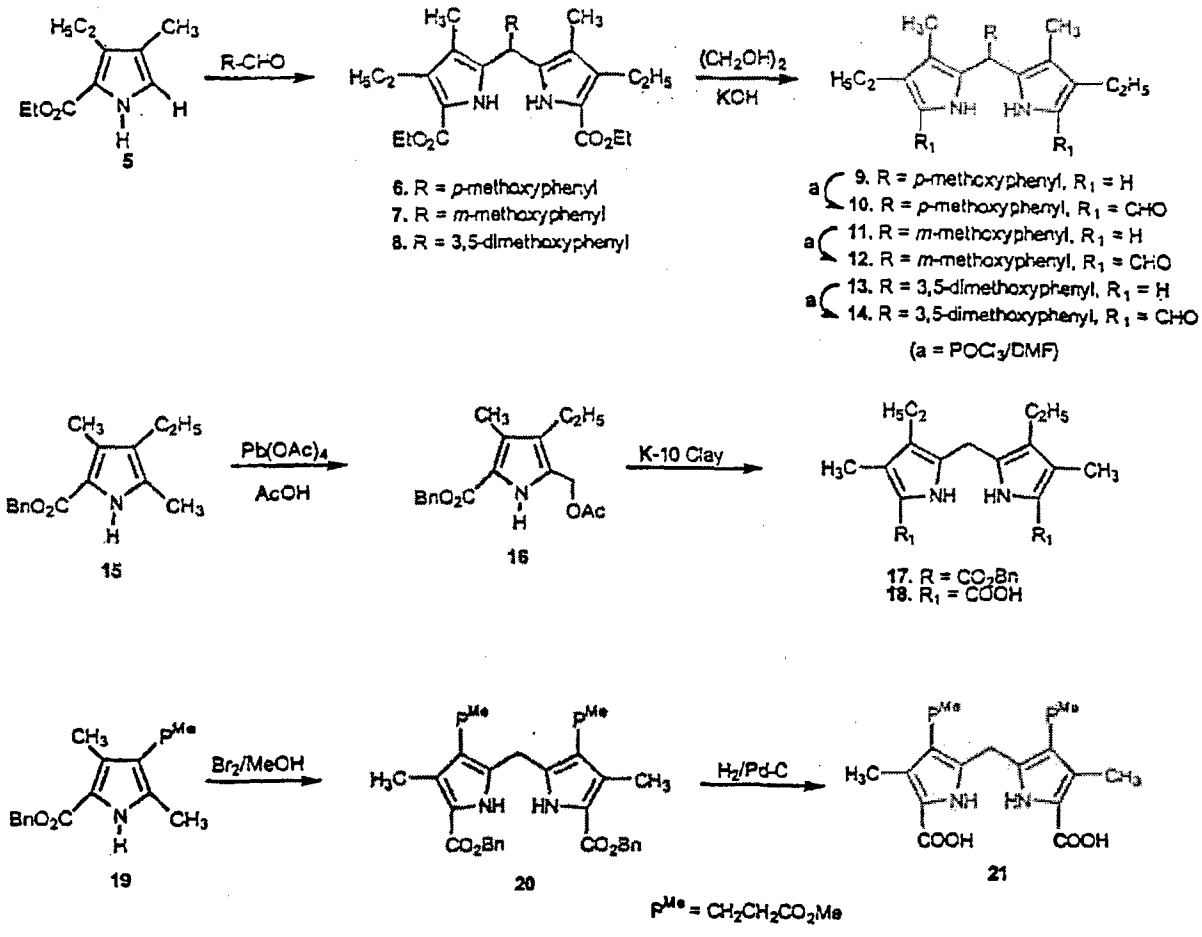

Scheme 1.

Porphyrins **1–4** were synthesized from pyrroles **5**,[9] **15**[10] or **19**[11] by following the well established '2+2' reaction approach[12] (see Scheme 1). In brief, reactions of pyrrole **5** with *p*-, *m*- or 3′,5′-dimethoxyphenyl aldehyde under acidic reaction conditions produced the corresponding dipyrromethanes **6**, **7** and **8** in 60–80% yield, which on refluxing with ethylene glycol/KOH gave the related α-free dipyrromethanes **9**, **11** and **13**, respectively in >85% yield. Further reaction of these dipyrromethanes with $POCl_3$/DMF under Vilsmeier's reaction conditions[13] produced the corresponding diformyl dipyrromethanes **10**, **12** and **14** in excellent yields (>75%). For the preparation of dipyrromethane **17**, pyrrole **15** was first converted into the acetoxy derivative **16**, which on treating with K-10 clay[14] in dichloromethane at room temperature gave the desired dipyrromethane in 70% overall yield. Reaction of pyrrole **19** with bromine/methanol[15] gave the corresponding dipyrromethane **20** in 72% yield. Hydrogenation of dipyrromethane **17** and **20** in presence of Pd/C at room temperature produced the corresponding carboxylic acids **18** and **21** in quantitative yields.

Diformyldipyrromethanes **10**, **12** and **14** were then individually reacted with dipyrromethane dicarboxylic acid **18** under McDonald reaction conditions.[12] After purification porphyrins **22–24** were isolated in modest yield. By following a similar approach, pyrromethane **14** was also reacted with pyrromethane dicarboxylic acid **21**, and porphyrin **25** was obtained in 38% yield. For the preparation of the fluorinated analogs, porphyrins **22–25** containing methoxy groups in the phenyl rings were reacted with boron tribromide and the related hydroxyphenyl porphyrins **26–29** were obtained in 70–77% yields. Further reaction of these porphyrins with 3,5-trifluoromethylbenzyl bromide produced the desired fluorinated porphyrins **1–4** in modest yield (Scheme 2). Reaction of **29** with 3,5-dimethylbenzyl bromide produced the non-fluorinated porphyrin **4a** in good yield. The structures of the intermediates and the final products were confirmed by ^1H, ^{19}F NMR, mass spectrometry and elemental analyses.

Among the fluorinated porphyrins **1–4**, compound **4**, containing two propionic ester functionalities at the bottom half of the molecule showed enhanced solubility compared to those containing alkyl groups in 1% Tween 80/water formulation as well as improved in vitro photosensitizing efficacy in comparison to the other analogues. Therefore, for investigating the photosensitizing effect(s) of fluorinated groups in long-wavelength absorbing compounds, porphyrin **4** was reacted with osmium tetroxide (OsO_4) and

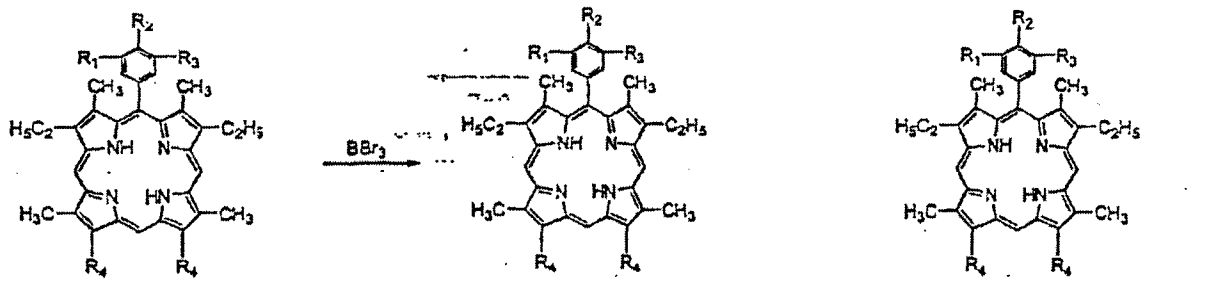

22. $R_1 = R_3 = H$, $R_2 = OCH_3$, $R_4 = C_2H_5$
23. $R_1 = R_2 = H$, $R_3 = OCH_3$, $R_4 = C_2H_5$
24. $R_1 = R_3 = OCH_3$, $R_2 = H$, $R_4 = C_2H_5$
25. $R_1 = R_3 = OCH_3$, $R_2 = H$, $R_4 = P^{Me}$

26. $R_1 = R_3 = H$, $R_2 = OH$, $R_4 = C_2H_5$
27. $R_1 = R_2 = H$, $R_3 = OH$, $R_4 = C_2H_5$
28. $R_1 = R_3 = OH$, $R_2 = H$, $R_4 = C_2H_5$
29. $R_1 = R_3 = OH$, $R_2 = H$, $R_4 = P^{Me}$

1. $R_1 = R_3 = H$, $R_2 = OX$, $R_4 = C_2H_5$
2. $R_1 = R_2 = H$, $R_3 = OX$, $R_4 = C_2H_5$
3. $R_1 = R_3 = OX$, $R_2 = H$, $R_4 = C_2H_5$
4. $R_1 = R_3 = OX$, $R_2 = H$, $R_4 = P^{Me}$
4a $R_1 = R_3 = OY$, $R_2 = H$, $R_4 = CH_2CH_2CO_2CH_3$

[X = 3,5-trifluoromethylbenzyl]
[Y = 3,5-dimethyl)-benzyl]

Scheme 2.

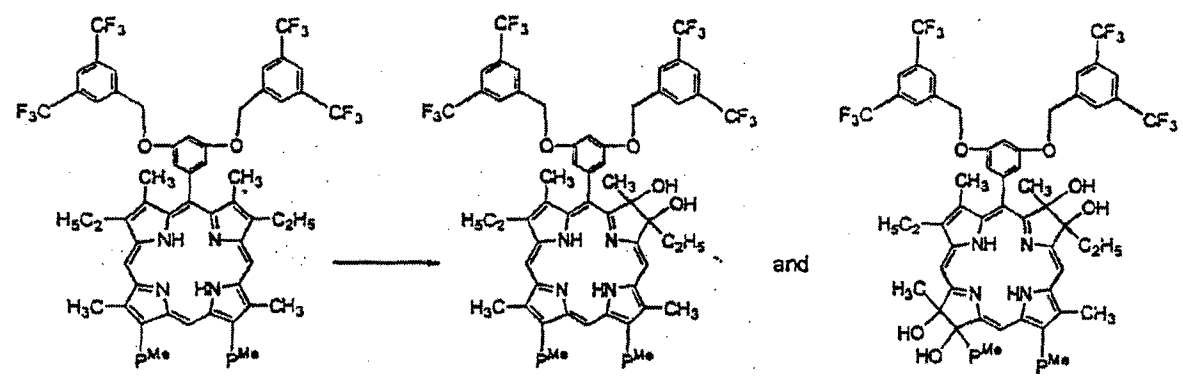

4 30 31

$P^{Me} = -CH_2CH_2CO_2CH_3$

Scheme 3.

the corresponding *vic*-dihydroxy chlorin **30** (λ_{max}: 648 nm) and tetra-hydroxy-bacteriochlorin **31** (as an isomeric mixture, λ_{max}: 716 nm) were synthesized. The relative yields of **31** and **32** were found to depend on the amount of OsO_4 used (Scheme 3).

As expected, the ^{19}F NMR spectra of all the fluorinated porphyrins **1–4** exhibited a single peak at δ 13.0 ppm, whereas chlorin **30** and bacteriochlorin **31** showed two peaks with equal intensity at 12.98 and 12.99 ppm, respectively.

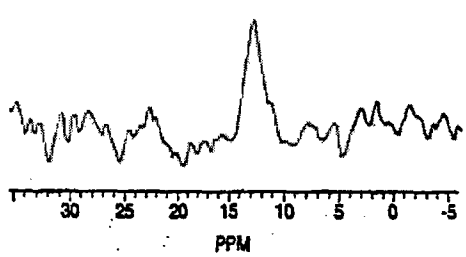

Figure 1. In vivo F-19 NMR spectrum of compound 4 obtained from a RIF tumor implanted in a C3H/HeJ mouse foot dorsum in one of the hind legs.

2.2. In vivo ^{19}F MR spectral characteristics

A typical ^{19}F MR spectrum of the fluorinated photosensitizer recorded on a 7T animal imager 8.0 h post IP administration of the compound (100 $\mu M\,kg^{-1}$) is shown in Figure 1. The tumor volume was 0.18 mL and spectra were recorded over 30 min. The ability to observe the photosensitizer by ^{19}F MR non-invasively is an important step towards understanding its pharmacokinetic characteristics and relating these to its in vivo photosensitizing efficacy. These details will be published elsewhere.

2.3. Photophysical properties

A typical fluorescence spectrum of fluorinated porphyrins in PhCN is shown in Figure 2. For the case of **3**, virtually the same fluorescence maxima at 628 and 693 nm was observed as for non-fluorinated porphyrins. The absorption and fluorescence maxima of investigated porphyrins **1–4**,

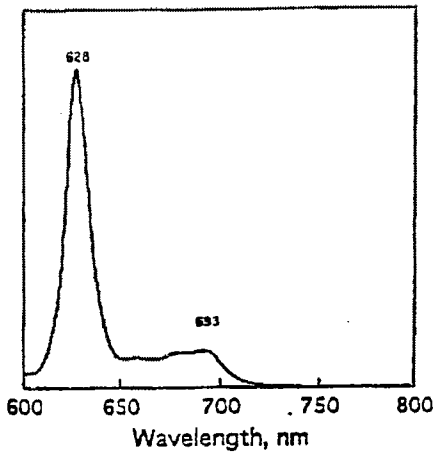

Figure 2. Fluorescence spectrum of 3 (7.3×10^{-5} M) in deaerated PhCN at 298 K by excitation at 535 nm.

26–29, chlorin 30 and bacteriochlorin 31 are listed in Table 1. The absorption and the fluorescence maxima are red-shifted in the order: porphyrin, chlorin and bacteriochlorin, but they are not affected by the fluorine substituents.

The fluorescence decay of 3 is well fitted by a single exponential line with lifetime of 18.5 ns as shown in Figure 3. The fluorescence lifetimes are also listed in Table 1. The fluorescence lifetimes (τ) are also unaffected by fluorinated substituents. The τ values of the nine porphyrins in this table are all similar in the range of 16.1–18.6 ns irrespective of substituents, but they are significantly longer than those of chlorin 30 (3.8 ns) and bacteriochlorin 31 (3.3 ns).

Phosphorescence spectra were observed in deaerated frozen 2-MeTHF at 77 K. The phosphorescence maxima are also summarized in Table 1. Again the phosphorescence maxima of porphyrins (822–823 nm) are not affected by the fluorinated substituents. The triplet excited states of the porphyrins were detected from the transient absorption spectra measured 4.0 ns after laser excitation at 355 nm. A typical example is shown in Figure 4 for the case of 3. The negative absorption at 410 nm in Figure 3 is due to bleaching of the ground-state absorption bands. The positive absorption at 450 nm in Figure 4 is due to the triplet–triplet (T–T) transition. The T–T absorption decay obeys first-

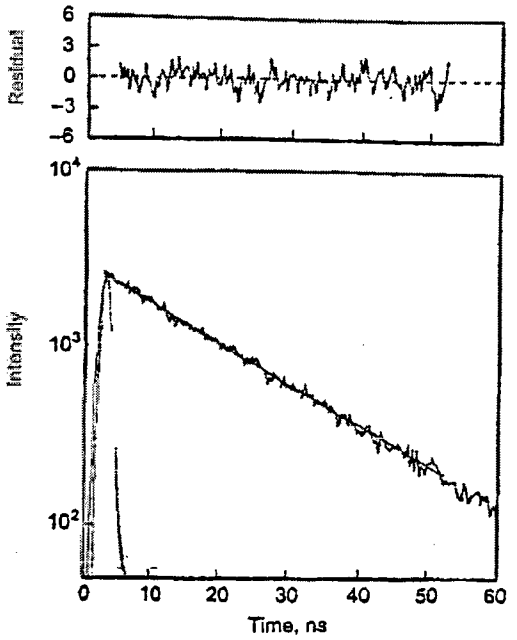

Figure 3. Fluorescence decay (λ_{em}=628 nm) of 3 (7.3×10^{-5} M) in deaerated PhCN at 298 K by excitation at 535 nm. The instrument response (gray line), decay data (solid line), and single-exponential fitted line are plotted in the bottom frame. The residuals of the fit for a lifetime of τ=18.5 ns are plotted in the top frame.

order kinetics as shown in Figure 5. This indicates that there is no contribution of the triplet–triplet annihilation under the present experimental conditions.

The T–T absorption maxima and the triplet lifetimes are summarized in Table 2. The triplet lifetimes of porphyrins are in the range of 8.3–25 μs, which are shorter than the lifetimes of chlorin 30 (185 μs) and the bacteriochlorin 31 (77 μs).

The decay of the T–T absorption in oxygen-saturated PhCN is enhanced significantly over that observed in deaerated PhCN. The decay rate obeys first-order kinetics and the decay rate constant increases with increasing oxygen concentration. Thus, an efficient energy transfer from the triplet excited state of 3 to oxygen occurs to produce singlet oxygen. The rate constants of the energy transfer (k_{EN}) were

Table 1. Fluorescence emission maxima and fluorescence lifetimes in deaerated PhCN at 298 K, and phosphorescence emission maxima in deaerated 2-MeTHF at 77 K

	λ_{max}(fluorescence) (nm)		τ (fluorescence)[a] (nm)	λ_{max}(phosphorescence) (nm)
26	628	693	18.5	822
27	627	693	17.9	822
28	628	693	17.3	822
29	628	692	17.6	823
1	628	693	18.6	823
2	627	692	16.1	823
3	628	693	18.5	822
4	628	691	17.7	822
4a	629	693	18.2	822
30	652	[b]	3.8	842
31	720	[b]	3.3	806

[a] The experimental errors are within ±5%.
[b] Shoulder peak.

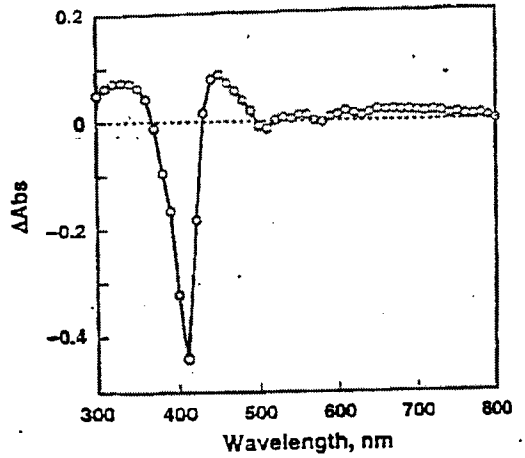

Figure 4. T–T absorption spectrum of 3 (7.3×10^{-6} M) obtained by the laser flash photolysis in deaerated PhCN at 4.0 μs after laser excitation (355 nm) at 298 K.

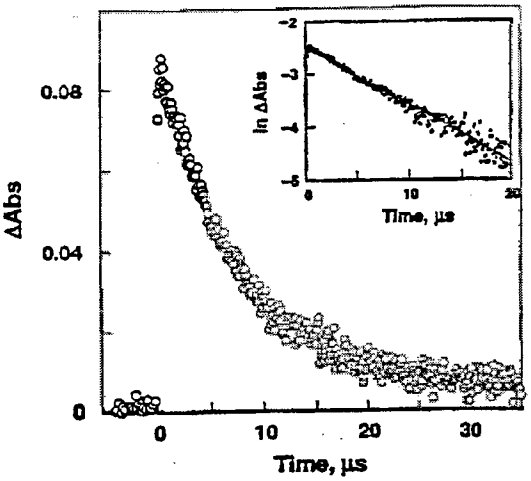

Figure 5. Kinetic trace for the T–T absorption of 3 (7.3×10^{-6} M) at 450 nm in deaerated PhCN after laser excitation (355 nm) at 298 K. Inset: First-order plot.

Table 2. T–T absorption maxima (λ_{max}(T–T)), triplet lifetimes (τ(T–T)) in the deaerated PhCN at 298 K, quenching rate constants of the triplet excited states by oxygen in PhCN, and quantum yields of singlet oxygen in C_6D_6

	λ_{max}(T–T) (nm)	τ(T–T) (s)[a]	k_{EN} (M^{-1} s^{-1})[a]	$\Phi(^1O_2)$[a]
26	450	1.0×10^{-5}		0.26
27	450	1.1×10^{-5}		0.57
28	450	1.1×10^{-5}		0.68
29	450	1.1×10^{-5}		0.33
1	450	8.3×10^{-6}		0.61
2	450	1.4×10^{-5}		0.75
3	450	1.9×10^{-5}		0.81
4	450	2.5×10^{-5}		0.36
4a	450	2.3×10^{-5}		0.27
30	440	1.9×10^{-4}		0.30
31	440	7.7×10^{-5}		0.31

[a] The experimental errors are within ±5%.

determined from the dependence of the decay rate constants on oxygen concentration as listed in Table 2. The k_{EN} values are in the range of 8.9×10^8–1.1×10^9 M^{-1} s^{-1}. There is no specific effects of the fluorinated substituents on the k_{EN} values which are smaller than the diffusion-limited value in PhCN (5.6×10^9 M^{-1} s^{-1}).[16]

Irradiation of an oxygen-saturated benzene solution of 3 results in formation of singlet oxygen which was detected by the $^1O_2$ emission at 1270 nm (see Section 3). Quantum yields (Φ) of $^1O_2$ generation were determined from the emission intensity which was compared to the intensity obtained using a C_{60} reference compound.[17] Relatively high Φ values are obtained for all investigated compounds as summarized in Table 2. The highest Φ value is obtained as 0.81 for the tetrafluorinated compound 3.

2.4. Electrochemical studies

The electrochemically investigated compounds can be divided into three groups based on the macrocycle and substitutents. The first group includes the four fluorinated porphyrins **1**, **2**, **3** and **4** (Chart 1, Scheme 2), the second, the four non-fluorinated porphyrins **26**, **27**, **28** and **29** (Scheme 2) and the third, the one fluorinated chlorin **30** and the one fluorinated bacteriochlorin **31** (Scheme 3). The electrochemistry of these ten complexes was carried out in PhCN containing 0.1 M TBAP as supporting electrolyte. The half-wave or peak potential for each reduction is listed in Table 3.

In all but one case (compound **29**), the first reduction was reversible and the second irreversible due to a chemical reaction following formation of the dianion. This led to cyclic voltammograms of the type illustrated in Figure 6. A chemical reaction also followed the first oxidation of each porphyrin and this led to irreversible or quasi-reversible oxidations as graphically shown in Figure 7 for the case of compounds **3** and **4**. The UV–visible spectral changes obtained upon the first reduction were recorded in PhCN containing 0.2 M TBAP. An example of the thin-layer spectral changes are shown in Figure 8 for compounds **3** and **30** and a summary of the spectral data for the eight singly reduced porphyrins is given in Table 3. The neutral compounds have a Soret band at 407–412 nm and four visible bands between 503 and 626 nm (see Table 4). Upon the first reduction, the Soret and visible bands decrease in intensity while a new broad visible band appears at 799–813 nm (see Table 3). These results are consistent with a one-electron addition to the porphyrin π-ring system and indicate the formation of a porphyrin π-anion radical.[18] The cyclic voltammograms illustrating the stepwise oxidation of compounds **3**, **4** and **30** are shown in Figure 7. The same spectral patterns are observed for the eight porphyrins in Table 3 and these data may be contrasted to what is observed for reduction of the chlorin **30** (Fig. 8(b)) and bacteriochlorin **31** whose π-anion radical absorption bands are also summarized in this table. The spectral changes obtained upon oxidation of the porphyrin **3** and the chlorin **30** are illustrated in Figure 8. The reaction of the porphyrin is quasi-reversible while that of the chlorin is reversible on the cyclic voltammetry timescale (see cyclic voltamogram Figure 7). Thus only the spectrum of the chlorin **30**

Table 3. Reduction potentials of investigated complexes and UV–visible spectral data of singly reduced compounds in PhCN containing 0.1 M TBAP

Group	Compound	Potential (V vs. SCE)		Singly reduced complexes			
		$E_{1/2}$	E_p	λ_{max}, nm ($\varepsilon\times10^{-4}$, M^{-1} cm^{-1})			
I	1		−1.78	409 (6.1)	432 (4.9)[sh]	–	806 (0.7)
	2		−1.80	408 (5.7)	435 (3.7)[sh]	–	813 (1.0)
	3		−1.80	407 (4.3)	–	–	801 (0.9)
	4		−1.66	412 (7.1)	–	–	801 (1.1)
II	26		−1.68	410 (6.8)	434 (6.3)	–	799 (1.8)
	27		−1.62	409 (5.1)	437 (4.1)	–	800 (1.9)
	28		−1.66	409 (5.7)	439 (2.8)	–	800 (1.0)
	29		−1.66	408 (5.2)	439 (2.5)[sh]	–	800 (1.2)
III	30		−1.74	402 (3.5)	–	535 (0.7)	735 (1.2)
	31		−1.84	406 (6.8)	–	750 (0.8)	827 (0.8)

[a] E_p at a scan rate of 0.1 V/s. Two small peaks at E_p=−0.52 and −0.94 V also can be seen on first scan.
[b] A peak at E_p=−1.29 V also can be seen. sh=shoulder peak.

corresponds to a true measurement of the first electrogenerated oxidation product which should be a π-cation radical. The oxidations of other compounds were not chemically or electrochemically reversible and thus no meaningful spectra could be obtained (Fig. 9).

2.5. In vitro photosensitizing efficacy

The in vitro photosensitizing activity of fluorinated photosensitizers 1–4 was determined in radiation induced fibrosarcoma (RIF) tumor cell lines.[19] For determining the drug dose, one of the fluorinated porphyins 4 was initially tested at two different concentrations (0.5 and 1.0 μM). The drug concentration at 1.0 μM, together with a light dose at

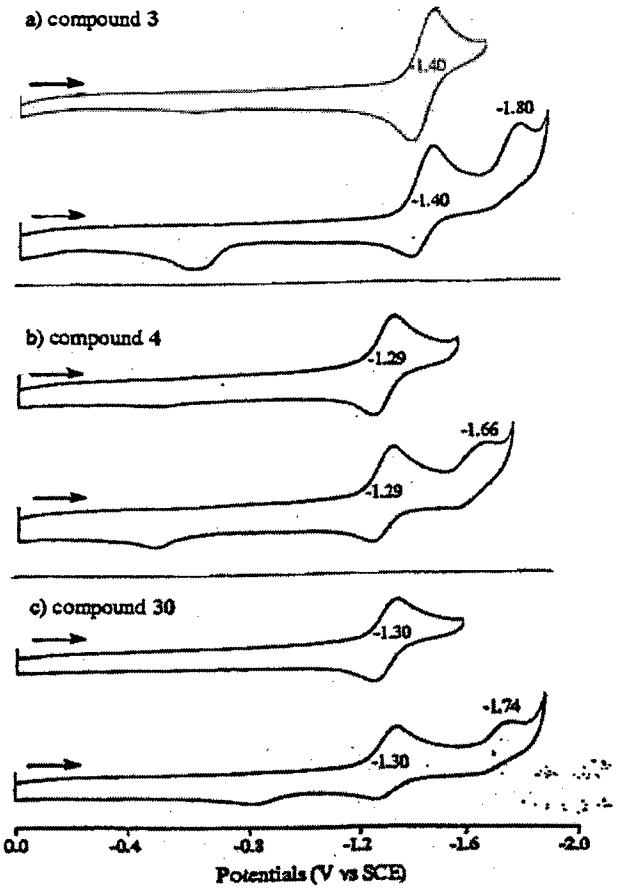

Figure 6. Cyclic voltammograms illustrating the stepwise reductions of compounds (a) 3, (b) 4 and (c) 30 in PhCN containing 0.1 M TBAP.

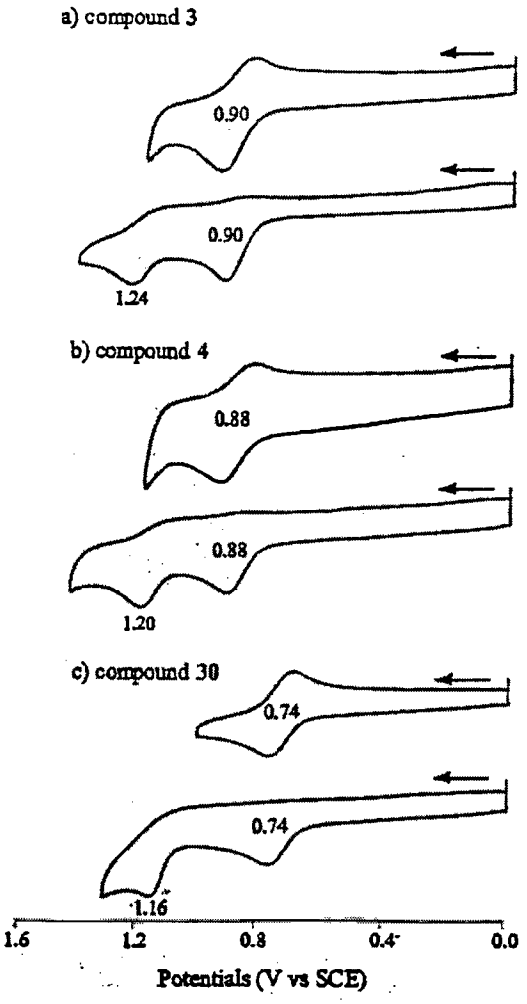

Figure 7. Cyclic voltammograms illustrating the stepwise oxidation of compounds (a) 3, (b) 4 and (c) 30 in PhCN containing 0.1 M TBAP.

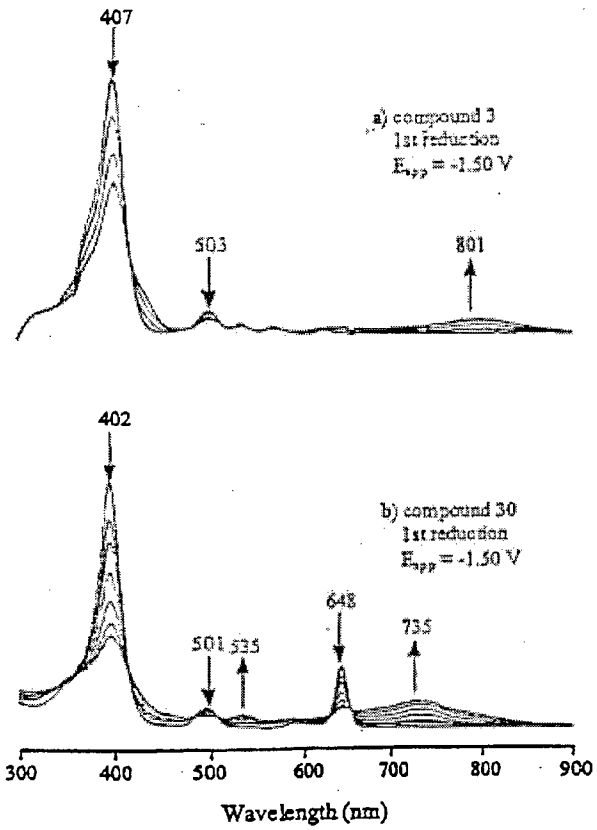

Figure 8. Thin-layer UV–visible spectral changes of (a) compound 3 and (b) compound 30 upon the first reduction at −1.50 V in PhCN containing 0.2 M TBAP.

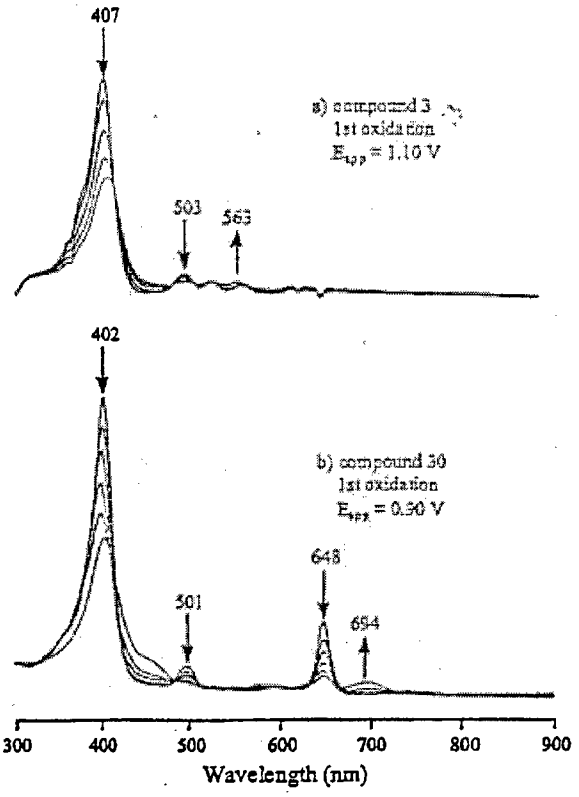

Figure 9. Thin-layer UV–visible spectral changes of (a) compound 3 and (b) compound 30 upon the first oxidation at 1.10 and 0.90 V in PhCN containing 0.2 M TBAP.

4.0 J/cm^2, produced a significant phototoxicity without any dark toxicity. Other photosensitizers were then evaluated under similar drug concentration. From the results summarized in Figure 10 it can be seen that all the fluorinated porphyrins, the chlorin and the bacteriochlorin produced significant in vitro efficacy. However, the compounds in the porphyrin series containing bis-trifluoromethyl groups were found to be less effective than those containing tetrakis-trifluoromethyl groups. The *vic*-dihydroxy chlorin **30** and the related tetrahydroxy bacteriochlorin **31** were quite effective with similar efficacy. In order to correlate the singlet oxygen efficiency with photosensitizing activity, these compounds were also evaluated for their photophysical characteristics. Although the presence and position of the fluorinated substituents in the porphyrin macrocycle produced a remarkable difference in singlet oxygen producing efficiency, no direct correlation was observed between singlet oxygen yield and in vitro photodynamic activity. For example, the singlet oxygen yields of porphyrins **1–3**, are quite similar (0.61–0.81) but these compounds showed a significant difference in photosensitizing activity. In contrast, similar photosensitizing results were obtained among the tetrakis-trifluorinated

Table 4. UV–visible data of investigated compounds in PhCN containing 0.2 M TBAP

Group	Compound	λ_{max}, nm (e×10^{-4}, M^{-1} cm^{-1})				
		Soret band	Visible bands			
I	**4**	408 (12.71)	503 (1.13)	536 (0.51)	572 (0.47)	626 (0.19)
	2	409 (11.23)	503 (0.74)	538 (0.60)	572 (0.74)	624 (0.29)
	3	407 (7.25)	503 (0.65)	535 (0.30)	571 (0.27)	625 (0.10)
	1	407 (13.12)	503 (1.29)	535 (0.62)	572 (0.58)	625 (0.28)
II	**26**	407 (16.20)	504 (1.24)	536 (0.27)	573 (0.23)	624 (0.09)
	27	407 (12.47)	503 (0.48)	535 (0.20)	572 (0.16)	624 (0.10)
	29	412 (12.70)	504 (0.57)	538 (0.74)	570 (0.95)	615 (0.21)
	28	407 (9.58)	503 (0.88)	535 (0.40)	572 (0.37)	624 (0.15)
III	**30**	402 (8.28)	501 (0.79)	548 (0.17)	593 (0.26)	648 (2.12)
	31	399 (8.90)	506 (1.28)	593 (0.35)	645 (2.02)	715 (1.70)

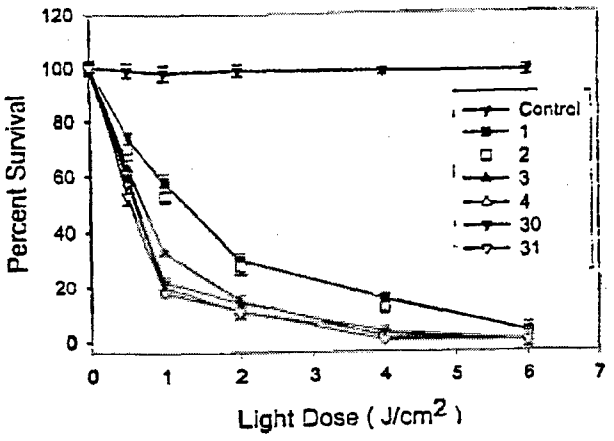

Figure 10. The in vitro photosensitizing activity of various fluorinated porphyrins 1–4, chlorin 30 and bacteriochlorin 31 (1.0 μM) in RIF tumor cells at 4 h incubation. Control: Cell exposed to light without photosensitizer and cells with photosensitizer but no light exposure.

analogs (3 and 4) in spite of a significant difference in singlet oxygen yields (0.81 and 0.36, respectively).

On the basis of in vitro results, it is difficult to predict the in vivo photosensitizing efficacy of these photosensitizers because the pharmacokinetic and pharmacodynamic profiles as well as photobleaching characteristics play important roles in drug localization and clearance. These properties could also be influenced by the overall lipophilicity of the molecule which has proven to be an important molecular descriptor that often is well correlated with the bioactivity of drugs. The lipophilicity is indicated by lipophilic indice such as the logarithm of a partition coefficient, log P, which reflects the equilibrium partitioning of a molecule between a non-polar and a polar phase, such as *n*-octanol/water system. Partition coefficients can be measured either experimentally by following a simple 'shake flask' approach or by using a currently available computer program (PALLAS system).[19c] We calculated the log *P* values of the fluorinated porphyrins 1–4, the chlorin 30 and the bacteriochlorin 31 and these were in the range of 12.76–19.75 [1 and 2: 15.58, 3: 19.75, 4: 18.43, 30:15.60 and 31:12.76]. For investigating a correlation between singlet oxygen yields and PDT efficacy, the in vivo studies of fluorinated photosensitizers at different drug/light doses are currently in progress. These results along with the in vivo ^{19}F tumor imaging data will be reported elsewhere.

2.6. Intracellular localization

In general, porphyrin-based compounds have shown very diverse patterns of localization, based on structure, lipophilicity and charge.[20] Localization in the lysosomes and mitochondria are reported to be predominant. However, in a QSAR study of certain photosensitizers the compounds that localize in mitochondria are generally found to be more effective. Therefore, the site of localization of the fluorinated porphyrin 4 and the related chlorin 30 and bacteriochlorin 31 were compared with Rhodamine-123, which is known to target mitochondria. Images of the

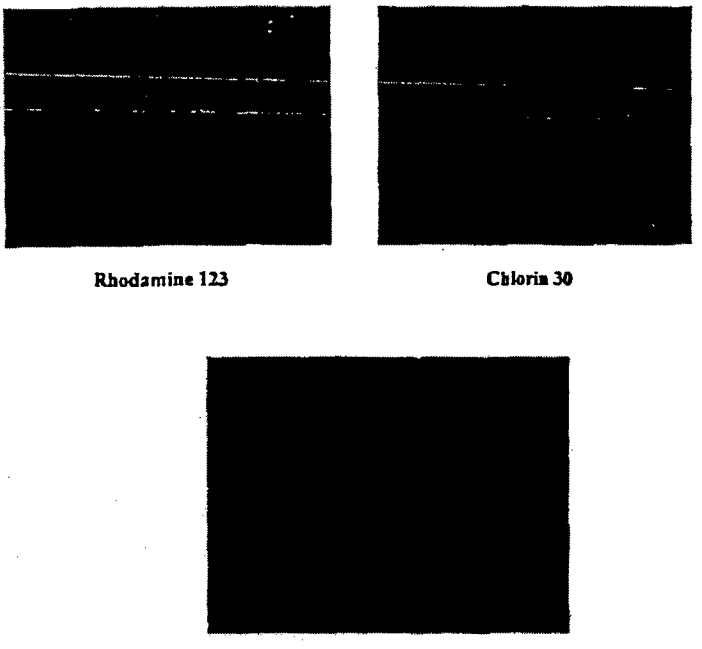

Figure 11. Comparative intracellular localization of Rhodamine-123 (mitochondrial probe) and fluorinated chlorin 30 in RIF cells at 24 h post-incubation. Similar patterns were observed from fluorinated porphyrin 4 and the corresponding bacteriochlorin 31 (only a representative example is shown). The overlay picture clearly indicates that both Rhodamine-123 and chlorin 30 localize in mitochondria.

photosensitizers and Rhodamine-123 were taken in rapid succession. The resulting images clearly indicate that these photosensitizers localize to the same cellular region as Rhodamine-123, suggesting that these compounds localize in mitochondria, a more sensitive site for cell damage by PDT (see Figure 11 for a representative example).

3. Experimental

3.1. Chemistry

All chemicals were of reagent grade and used as received. Solvents were dried using standard methods unless stated otherwise. Reactions were carried out under a N_2 atmosphere and were monitored by analytical precoated (0.20 mm) silica TLC plates (POLYGRAM® SIL N-HR). Melting points were determined on electrically heated melting point apparatus and are uncorrected. UV–vis spectra were recorded on a Varian (Cary-50 Bio) spectrophotometer. ^1H and ^{19}F NMR spectra were recorded on a Brucker AMX 400 and 376.5 MHz NMR spectrometer, respectively at 303°K in $CDCl_3$ containing tetramethylsilane (TMS) as an internal standard. Proton chemical shifts (δ) are reported in parts per million (ppm) relative to TMS (0.00 ppm) or $CDCl_3$ (7.26 ppm) while fluorine chemical shifts are reported in ppm relative to trifluoroacetic acid (0.00 ppm). Coupling constants (J) are reported in Hertz (Hz) and s, d, t, q, m, dd and br refer to singlet, doublet, triplet, quartet, multiplet, doublet of doublet and broad respectively. Mass spectral data (FAB) were obtained from the University of Michigan, East Lansing, MI (the matrix is usually nitrobenzyl alcohol) and from the Biopolymer Facility of Basic Studies Center, Roswell Park Cancer Institute, Buffalo, NY. Elemental analysis data were obtained from Midwest Microlab, LLC, Indianapolis, IN.

3.2. General method for the synthesis of dipyrromethane 6, 7 and 8

Pyrrole **5** (10.0 g, 0.055 mol) and *p*-methoxy benzaldehyde (3.74 g, 0.0275 mol) were dissolved in ethanol (70 mL) and *p*-toluenesulfonic acid (200 mg) was added. The reaction mixture was refluxed for 2 h under nitrogen. Analytical TLC at frequent intervals was used to monitor the completion of the reaction. It was then cooled, the solid was filtered, the product was washed with cold water and dried under vacuum at room temperature. The desired pyrromethane **6** [3,9-diethyl-6-(*p*-methoxyphenyl)-4,8-dimethyl-2,10-diethoxycarbonyl dipyrromethane] was isolated as a white powder in 80% (21.2 g) yield.

3.2.1. 3,9-Diethyl-6-(*p*-methoxyphenyl)-4,8-dimethyl-2,10-diethoxycarbonyl dipyrromethane (6). Mp 105–108°C; ^1H NMR: δ 8.20 (brs, 2H, 2×NH), 7.01 (d, J=8.9 Hz, 2H, ArH), 6.87 (d, J=8.9 Hz, 2H, ArH), 5.43 (s, 1H, CH), 4.26 (q, J=7.3 Hz, 4H, $2\times OCH_2CH_3$), 3.81 (s, 3H, OCH_3), 2.74 (q, J=7.5 Hz, 4H, $2\times CH_2CH_3$), 1.78 (s, 6H, $2\times CH_3$), 1.31 (t, J=7.1 Hz, 6H, $2\times OCH_2CH_3$), 1.12 (t, J=7.7 Hz, 6H, $2\times CH_2CH_3$). Anal. calcd for $C_{28}H_{36}N_2O_4$: C, 69.98; H, 7.55; N, 5.83. Found: C, 70.15; H, 7.37; N, 5.93. By following a similar approach, pyrrole **5** was reacted with *m*-methoxy or 3, 5-dimethoxy benzaldehyde and the corresponding dipyrromethane **7** and **8** were synthesized.

3.2.2. 3,9-Diethyl-6-(*m*-methoxyphenyl)-4,8-dimethyl-2,10-diethoxycarbonyl dipyrromethane (7). Yield 70%; mp 122–125°C; ^1H NMR: δ 8.25 (brs, 2H, 2×NH), 7.23–7.27 (m, 1H, ArH), 6.82 (dd, J=2.2, 7.8 Hz, 1H, ArH), 6.68 (d, J=7.4 Hz, 1H, ArH), 6.63 (s, 1H, ArH), 5.45 (s, 1H, CH), 4.25 (q, J=7.3 Hz, 4H, $2\times OCH_2CH_3$), 3.76 (s, 3H, OCH_3), 2.73 (q, J=7.6 Hz, 4H, $2\times CH_2CH_3$), 1.79 (s, 6H, $2\times CH_3$), 1.30 (t, J=7.1 Hz, 6H, $2\times OCH_2CH_3$), 1.11 (t, J=7.3 Hz, 6H, $2\times CH_2CH_3$). Anal. calcd for $C_{28}H_{36}N_2O_5$: C, 69.98; H, 7.55; N, 5.83. Found: C, 70.08; H, 7.60; N, 5.82.

3.2.3. 3,9-Diethyl-6-(3′,5′-dimethoxyphenyl)4,8-dimethyl-2,10-diethoxycarbonyldipyrromethane (8). Yield 60%; viscous oil; ^1H NMR: δ 8.25 (brs, 2H, 2×NH), 6.38 (s, 1H, ArH), 6.24 (s, 2H, ArH), 5.39 (s, 1H, CH), 4.26 (q, J=7.3 Hz, 4H, $2\times OCH_2CH_3$), 3.74 (s, 6H, $2\times OCH_3$), 2.70–2.78 (m, 4H, $2\times CH_2CH_3$), 1.79 (s, 6H, $2\times CH_3$), 1.32 (t, J=7.2 Hz, 6H, $2\times OCH_2CH_3$), 1.10–1.16 (m, 6H, $2\times CH_2CH_3$).

3.3. General method for the preparation of pyrromethanes 9, 11, 13

The diethoxycarbonyl dipyrromethanes **6**, **7** or **8** (for example 11.6 g of **6**) were individually dissolved in ethylene glycol (250 mL). Sodium hydroxide (12 g, crushed powder) was added, and the reaction mixture was refluxed for 1 h. It was then cooled, diluted with dichloromethane (250 mL) and washed with water (2×200 mL). The dichloromethane layer was dried over anhydrous sodium sulfate. The residue obtained after evaporating the solvent was chromatographed over silica column eluted with chloroform. The appropriate eluates were combined, the solvent was evaporated, and the desired dipyrromethane **9** was obtained in 95% yield.

3.3.1. 3,9-Diethyl-6-(*p*-methoxyphenyl)4,8-dimethyl-dipyrromethane (9). Mp 64–66°C; lit.[21] ^1H NMR: δ 7.30 (brs, 2H, 2×NH), 7.06 (d, J=8.8 Hz, 2H, ArH), 6.85 (d, J=8.8 Hz, 2H, ArH), 6.38 (s, 2H, 2×Pyrrolic CH), 5.45 (s, 1H, CH), 3.81 (s, 3H, OCH_3), 2.44 (q, J=7.2 Hz, 4H, $2\times CH_2CH_3$), 1.81 (s, 6H, $2\times CH_3$), 1.19 (t, J=7.9 Hz, 6H, $2\times CH_2CH_3$).

3.3.2. 3,9-Diethyl-6-(*m*-methoxyphenyl)-4,8-dimethyl-dipyrromethane (11). Yield 88%; mp 202–204°C: ^1H NMR: δ 9.49 (s, 2H, 2×CHO), 9.08 (brs, 2H, 2×NH), 7.23–7.27 (m, 1H, ArH), 6.83 (dd, J=2.5, 8.0 Hz, 1H, ArH), 6.66 (d, J=7.6 Hz, 1H, ArH), 6.62 (s, 1H, ArH), 5.53 (s, 1H, CH), 3.75 (s, 3H, OCH_3), 2.71 (q, J=7.6 Hz, 4H, $2\times CH_2CH_3$), 1.86 (s, 6H, $2\times CH_3$), 1.20 (t, J=7.8 Hz, 6H, $2\times CH_2CH_3$). Anal. calcd for $C_{22}H_{28}N_2O.2H_2O$: C, 70.94; H, 8.66; N, 7.52. Found: C, 71.29; H, 7.17; N, 7.24.

3.3.3. 3,9-Diethyl-6-(3′,5′-dimethoxyphenyl)-4,8-dimethyl-dipyrromethane (13). Yield 97%; mp 119–121°C; ^1H NMR: δ 7.34 (brs, 2H, 2×NH), 6.33–6.36 (m, 3H, ArH), 6.31 (s, 2H, 2×pyrrolic CH), 5.40 (s, 1H, CH), 3.74 (s, 6H, $2\times OCH_3$), 2.40–2.45 (m, 4H, $2\times CH_2CH_3$), 1.81 (s, 6H,

2×CH_3), 1.14–1.19 (m, 6H, 2×CH_2CH_3). Anal. calcd for $C_{23}H_{30}N_2O_2.5H_2O$: C, 60.50; H, 8.83; N, 6.40. Found: C, 60.00; H, 8.82; N, 5.91.

3.4. General method for the preparation of diformyldipyrromethanes 10, 12 and 14

The pyrromethane(s) [e.g. **9** (7.1 g)] was dissolved in Vilsmeier reagent, prepared by reaction $POCl_3$ (10.5 mL) and DMF (45 mL) was added and the reaction mixture was stirred at room temperature overnight. The reaction mixture was poured into ice cold water (250 mL) and aqueous sodium hydroxide (50%, 35 mL) was then added slowly; the pH was adjusted to 10–12 and stirred overnight before extracting with dichloromethane (3×200 mL). The organic layer was separated, washed with water (2×200 mL) until neutral and dried over anhydrous sodium sulfate. Evaporation of the solvent gave a residue which was chromatographed over a silica column, eluting with 1:1 ethyl acetate/cyclohexane. The major band was separated, and the product obtained after evaporating the solvent was crystallized with methanol and compound **10** was isolated in 80% (6.80 g) yield.

3.4.1. 3,9-Diethyl-2,10-diformyl-6-(*p*-methoxyphenyl)-4,8-dimethyldipyrromethane (10). Mp 168–169°C; ^{1}H NMR: δ 9.50 (s, 2H, 2×CHO), 8.70 (brs, 2H, 2×NH), 6.98 (d, J=8.7 Hz, 2H, ArH), 6.86 (d, J=8.7 Hz, 2H, ArH), 5.47 (s, 1H, CH), 3.80 (s, 3H, OCH_3), 2.70 (q, J=7.5 Hz, 4H, 2×CH_2CH_3), 1.81 (s, 6H, 2×CH_3), 1.20 (t, J=7.5 Hz, 6H, 2×CH_2CH_3). Anal. calcd for $C_{24}H_{28}N_2O_3.1/2H_2O$: C, 71.80; H, 7.28; N, 6.98. Found: C, 71.69; H, 6.74; N, 6.76.

3.4.2. 3,9-Diethyl-2,10-diformyl-6-(*m*-methoxyphenyl)-4,8-dimethyldipyrromethane (12). Yield 79%; mp 202–204°C; ^{1}H NMR: δ 9.49 (s, 2H, 2×CHO), 9.08 (brs, 2H, 2×NH), 7.23–7.27 (m, 1H, ArH), 6.83 (dd, J=2.5, 8.0 Hz, 1H, ArH), 6.66 (d, J=7.6 Hz, 1H, ArH), 6.62 (s, 1H, ArH), 5.53 (s, 1H, CH), 3.75 (s, 3H, OCH_3), 2.71 (q, J=7.6 Hz, 4H, 2×CH_2CH_3), 1.86 (s, 6H, 2×CH_3), 1.20 (t, J=7.8 Hz, 6H, 2×CH_2CH_3). Anal. calcd for $C_{24}H_{28}N_2O_3$: C, 73.44; H, 7.19; N, 7.14. Found: C, 73.65; H, 7.29; N, 7.06.

3.4.3. 3,9-Diethyl-2,10-diformyl-6-(3,5-di-methoxyphenyl)-4,8-dimethyldipyrromethane (14). Yield 78%; mp 202–204°C; ^{1}H NMR ($CDCl_3$, 400 MHz) δ 9.52 (s, 2H, 2×CHO), 8.56 (brs, 2H, 2×NH), 6.40 (s, 1H, ArH), 6.20 (s, 2H, ArH), 5.42 (s, 1H, CH), 3.74 (s, 6H, 2×OCH_3), 2.70 (q, J=7.7 Hz, 4H, 2×CH_2CH_3), 1.81 (s, 6H, 2×CH_3), 1.20 (t, J=7.8 Hz, 6H, 2×CH_2CH_3). Anal. calcd for $C_{25}H_{30}N_2O_4.1/2H_2O$: C, 69.58; H, 7.24; N, 6.49. Found: C, 69.52; H, 7.00; N, 6.16.

3.5. General method for the synthesis of porphyrins 22–25

The diformyl dipyrromethane (e.g. **10**, 2.52 g, 6.43 mmol), and dipyrromethane **18** (2.04 g, 6.42 mmol) were dissolved in dichloromethane (500 mL). *p*-Toluenesulfonic acid (6.0 g) dissolved in methanol (100 mL) was added, and the reaction mixture was stirred at room temperature overnight under nitrogen atmosphere. A saturated solution of zinc acetate/methanol (125 mL) was added, and the reaction was stirred for another 12 h. It was then diluted with dichloromethane, washed with water and the organic layer was dried over anhydrous sodium sulfate. Evaporation of the solvent gave a residue which was dissolved in trifluoroacetic acid (30 mL) and stirred at room temperature for 30 min. The Zn-free porphyrin thus obtained after standard work-up was chromatographed over a short Grade III Alumina column and eluted with dichloromethane. The major band was collected and the solvent evaporated. The residue was crystallized from dichloromethane/hexane and porphyrin **22** was isolated in 17% (640 mg) yield.

3.5.1. 2,8,13,17-Tetraethyl-5-(*p*-methoxyphenyl)-3,7,12,18-tetramethylporphyrin (22). Mp 280–282°C; UV–vis [CH_2Cl_2, nm (ε, M^{-1} cm^{-1})] 403 (3.82×10^5), 503 (3.15×10^4), 535 (1.39×10^4), 571 (1.35×10^4), 623 (4.82×10^3); ^{1}H NMR: δ 10.13 (s, 2H, 2×*meso*H), 9.92 (s, 1H, *meso*H), 7.86 (d, J=9.0 Hz, 2H, ArH), 7.16 (d, J=9.0 Hz, 2H, ArH), 4.00–4.06 (m, 8H, 4×CH_2CH_3), 3.99 (s, 3H, OCH_3), 3.62 (s, 6H, 2×CH_3), 2.47 (s, 6H, 2×CH_3), 1.87 (t, J=7.7 Hz, 6H, 2×CH_2CH_3), 1.75 (t, J=7.6 Hz, 6H, 2×CH_2CH_3), −3.19 (brs, 1H, NH), −3.27 (brs, 1H, NH). Anal. calcd for $C_{39}H_{44}N_4O$: C, 80.10; H, 7.58; N, 9.58. Found: C, 80.14; H, 7.54; N, 9.62.

3.5.2. 2,8,13,17-Tetraethyl-5-(*m*-methoxyphenyl)-3,7,12,18-tetramethylporphyrin (23). Yield 30%; mp 270–272°C; ^{1}H NMR: δ10.16 (s, 2H, 2×*meso*H), 9.96 (s, 1H, *meso* H), 7.67 (d, J=7.2 Hz, 2H, ArH), 7.59 (t, J=7.8 Hz, 1H, ArH), 7.50 (s, 1H, ArH), 4.02–10 (m, 8H, 4×CH_2CH_3), 4.00 (s, 3H, OCH_3), 3.65 (s, 6H, 2×CH_3), 2.60 (s, 6H, 2×CH_3), 1.90 (t, J=7.7 Hz, 6H, 2×CH_2CH_3), 1.78 (t, J= 7.94 Hz, 6H, 2×CH_2CH_3), −3.20 (brs, 1H, NH), −3.35 (brs, 1H, NH). Anal. calcd for $C_{39}H_{44}N_4O$: C, 80.10; H, 7.58; N, 9.58. Found: C, 80.76; H, 7.60; N, 9.54.

3.5.3. 2,8-Diethyl-5-(3′,5′-dimethoxyphenyl)-2, 8-diethyl-13,17-bis-(2-methoxycarbonylethyl)-3,7,12,18-tetramethylporphyrin (25). The title compound was prepared by reacting diformyldipyrromethane **14** with dipyrromethane dicarboxylic acid **21** by following the procedure reported by Chen et al.[22]

3.6. General method for the synthesis of porphyrins 26–29

Reaction of porphyrins **22–25** (100 mg each) with ethereal boron tribromide solution afforded porphyrin **26–29** in 70–77%.

3.6.1. 2,8,13,17-Tetraethyl-5-(*p*-hydroxyphenyl)-3,7,12,18-tetramethylporphyrin (26). Yield 77%; mp >300°C; UV–vis [CH_2Cl_2, nm (ε, M^{-1} cm^{-1})] 404 (3.79×10^5), 503 (2.91×10^4), 536 (1.19×10^4), 570 (1.14×10^4); ^{1}H NMR: δ 10.15 (s, 2H, 2×*meso* H), 9.94 (s, 1H, *meso* H), 7.89 (d, J=9.2 Hz, 2H, ArH), 7.18 (d, J=8.7 Hz, 2H, ArH), 4.00–4.08 (m, 8H, 4×CH_2CH_3), 3.64 (s, 6H, 2×CH_3), 2.53 (s, 6H, 2×CH_3), 1.88 (t, J=7.7 Hz, 6H, 2×CH_2CH_3), 1.76 (t, J= 7.5 Hz, 6H, 2×CH_2CH_3), −3.75 (brs, 2H, 2×NH). Anal. calcd for $C_{38}H_{42}N_4O$: C, 79.66; H, 7.42; N, 9.82. Found: C, 79.75; H, 7.45; N, 9.70.

3.6.2. 2,8,13,17-Tetraethyl-5-(*m*-hydroxyphenyl)-3,7,12,18-tetramethylporphyrin (27). Yield 72%; mp >300°C; UV–vis [CH_2Cl_2, nm (ε, M^{-1} cm^{-1})] 402 (5.00×10^5), 502 (4.03×10^4), 536 (1.76×10^4), 570 (1.61×10^4), 623 (4.60×10^3); ^1H NMR: δ 10.18 (s, 2H, 2×*meso* H), 9.98 (s, 1H, *meso*H), 7.69 (d, J=7.0 Hz, 2H, ArH), 7.61 (t, J=7.7 Hz, 1H, ArH), 7.51 (s, 1H, ArH), 4.04–4.12 (m, 8H, 4×CH_2CH_3), 3.66 (s, 6H, 2×CH_3), 2.58 (s, 6H, 2×CH_3), 1.91 (t, J=7.7 Hz, 6H, 2×CH_2CH_3), 1.79 (t, J=7.94 Hz, 6H, 2×CH_2CH_3), −3.85 to −3.75 (each brs, 1H, 2×NH). Anal. calcd for $C_{38}H_{42}N_4O$: C, 79.66; H, 7.42; N, 9.82. Found: C, 80.02; H, 7.37; N, 9.83.

3.6.3. 2,8,13,17-Tetraethyl-5-(3′,5′-di-hydroxyphenyl)-3,7,12,18-tetramethylporphyrin (28). Yield 75%; mp >300°C; UV–vis [CH_2Cl_2, nm (ε, M^{-1} cm^{-1})] 402 (4.16×10^5), 502 (3.45×10^4), 536 (1.62×10^4), 569 (1.49×10^4), 623 (6.50×10^3); ^1H NMR ($CDCl_3$, 400 MHz) δ 10.18 (s, 2H, 2×*meso*H), 9.98 (s, 1H, *meso* H), 7.05 (s, 2H, ArH), 6.69 (s, 1H, ArH), 4.04–4.12 (m, 8H, 4×CH_2CH_3), 3.66 (s, 6H, 2×CH_3), 2.67 (s, 6H, 2×CH_3), 1.90 (t, J=7.7 Hz, 6H, 2×CH_2CH_3), 1.80 (t, J=7.5 Hz, 6H, 2×CH_2CH_3). Anal. calcd for $C_{38}H_{42}N_4O_2.H_2O$: C, 75.47; H, 7.33; N, 9.26. Found: C, 75.31; H, 7.38; N, 9.14.

3.6.4. 2,8-Diethyl-5-(3′,5′-dimethoxyphenyl)-13,17-bis-(2-methoxycarbonylethyl)-3,7,12,18-tetramethylporphyrin (29). Yield 70%; mp >300°C; UV–vis [CH_2Cl_2, nm (ε, M^{-1} cm^{-1})] 403 (4.64×10^5), 502 (5.21×10^4), 536 (3.39×10^4), 571 (4.00×10^4); ^1H NMR: δ 10.18 (s, 2H, 2×*meso* H), 9.95 (s, 1H, *meso* H), 7.10 (s, 2H, ArH), 6.70 (s, 1H, ArH), 4.30–4.40 (m, 4H, 2×$CH_2CH_2CO_2CH_3$), 3.98–4.08 (m, 4H, 2×CH_2CH_3), 3.70 (s, 6H, 2×OCH_3), 3.65 (s, 6H, 2×CH_3), 3.30–3.40 (m, 4H, 2×$CH_2CH_2CO_2CH_3$), 2.66 (s, 6H, 2×CH_3), 1.80–1.90 (m, 6H, 2×CH_2CH_3). Anal. calcd for $C_{42}H_{46}N_4O_6.H_2O$: C, 63.69; H, 6.11; N, 7.08. Found: C, 63.32; H, 6.07; N, 6.41.

3.7. General method for the synthesis of porphyrins 1 to 4

3,5-Bis(trifluromethyl)benzylbromide (40 μL, 0.22 mmol) and anhydrous K_2CO_3 (250 mg) were added to a stirred solution of 5-(4-hydoxyphenyl)tetraethylporphyrin **26** (85 mg, 0.15 mmol) in dry acetonitrile (10 mL) and the reaction mixture was refluxed overnight under nitrogen. Solvent was evaporated under reduced pressure; water (20 mL) was poured and extracted with CH_2Cl_2 (2×20 mL). The combined organic extracts were washed with water (2×20 mL) and organic fraction was dried over Na_2SO_4. Removal of organic solvent in vacuo gave a crude solid residue, which was chromatographed over silica column using CH_2Cl_2 as an eluant to yield 77 mg (65%) of 5-[4-{3,5-Bis(trifluromethyl)benzyloxy}phenyl]tetraethylporphyrin **1** as purple plates.

3.7.1. 5-[4-{3,5-Bis(trifluromethyl)benzyloxy}phenyl]-2,8,13,17-tetraethyl-3,7,12,18-tetramethylporphyrin (1). Mp. 274–276°C; UV–vis [CH_2Cl_2, nm (ε, M^{-1} cm^{-1})] 403 (2.52×10^5), 502 (2.08×10^4), 535 (9.25×10^3), 570 (8.82×10^3), 624 (3.13×10^3); ^1H NMR: δ 10.21 (s, 2H, 2×*meso* C*H*), 10.00 (s, 1H, *meso* C*H*), 8.14 (s, 2H, Ar*H*), 7.98 (s, 1H, Ar*H*), 7.96 (d, J=4.5 Hz, 2H, Ar*H*), 7.31 (d, J=4.5 Hz, 2H, Ar*H*), 5.42 (s, 2H, OCH_2), 4.06–4.13 (m, 8H, 4×CH_2CH_3), 3.70 (s, 6H, 2×CH_3), 2.52 (s, 6H, 2×CH_3), 1.94 (t, J=7.7 Hz, 6H, 2×CH_2CH_3), 1.82 (t, J=7.5 Hz, 6H, 2×CH_2CH_3). ^{19}F NMR: δ 13.12 (s, 6F, 2×CF_3). Anal. calcd for $C_{47}H_{46}N_4F_6O.H_2O$: C, 69.27; H, 5.94; N, 6.87. Found: C, 69.37; H, 6.19; N, 6.33.

3.7.2. 5-[3-Bis{3,5-trifluromethyl)benzyloxy}phenyl]-2,8,13,17-tetraethyl-3,7,12,18-tetramethylporphyrin (2). Yield 96%; mp 109–110°C; UV–vis[CH_2Cl_2, nm (ε, M^{-1} cm^{-1})] 404 (9.49×10^4), 501 (6.83×10^3), 537 (4.27×10^3), 570 (4.98×10^3); ^1H NMR: δ 10.17 (s, 2H, 2×*meso* C*H*), 9.96 (s, 1H, *meso* C*H*), 7.94 (s, 2H, Ar*H*), 7.75–7.85 (m, 3H, Ar*H*), 7.62 (t, J=7.8 Hz, 1H, Ar*H*), 7.40 (dd, J=2.6, 7.8 Hz, 1H, Ar*H*), 5.32 (s, 2H, OCH_2), 4.00–4.10 (m, 8H, 4×CH_2CH_3), 3.65 (s, 6H, 2×CH_3), 2.53 (s, 6H, 2×CH_3), 1.89 (t, J=7.8 Hz, 6H, 2×CH_2CH_3), 1.77 (t, J=7.6 Hz, 6H, 2×CH_2CH_3), −3.10 and −3.30 (each brs, 1H, 2×NH). ^{19}F NMR: δ 13.00 (s, 6F, 2×CF_3). Mass (FAB) calcd for $C_{47}H_{46}N_4F_6O$: 796.35. Found: 797.36 (M+1).

3.7.3. 5-[3′,5′-Bis{3″,5″-trifluromethyl)benzyloxy}phenyl]-2,8,13,17-tetraethyl-3,7,12,18-tetra-methyl porphyrin (3). Yield 45%; mp 214–216°C; UV–vis[CH_2Cl_2, nm (ε, M^{-1} cm^{-1})] 403 (2.29×10^5), 502 (1.93×10^4), 536 (9.27×10^3), 570 (8.53×10^3), 623 (3.34×10^3); ^1H NMR: δ 10.20 (s, 2H, 2×*meso* C*H*), 9.98 (s, 1H, *meso* C*H*), 7.96 (s, 4H, Ar*H*), 7.87 (s, 2H, Ar*H*), 7.42 (d, J=2.9 Hz, 2H, Ar*H*), 7.12–7.16 (m, 1H, Ar*H*), 5.37 (s, 4H, 2×OCH_2), 4.03–4.10 (m, 8H, 4×CH_2CH_3), 3.66 (s, 6H, 2×CH_3), 2.60 (s, 6H, 2×CH_3), 1.91 (t, J=7.5 Hz, 6H, 2×CH_2CH_3), 1.78 (t, J=7.5 Hz, 6H, 2×CH_2CH_3). ^{19}F NMR: δ 12.98 (s, 12F, 4×CF_3). Anal. calcd for $C_{56}H_{50}N_4F_{12}O_2$: C, 64.74; H, 4.85; N, 5.39. Found: C, 64.20; H, 4.94; N, 5.00.

3.7.4. 5-[3′,5′-Bis{3″,5″-trifluromethyl)benzyloxy}phenyl]-2,8-diethyl-13,17-bis(2-methoxycarbonylethyl)-3,7-dimethylporphyrin (4). Yield 75%; mp 72–75°C; UV–vis [CH_2Cl_2, nm (ε, M^{-1} cm^{-1})] 404 (3.81×10^5), 502 (3.02×10^4), 536 (1.41×10^4), 570 (1.32×10^4), 624 (4.82×10^3), 653 (2.59×10^3); ^1H NMR: δ 10.16 (s, 2H, 2×*meso* C*H*), 9.97 (s, 1H, *meso* C*H*), 7.92 (s, 3H, Ar*H*), 7.81–7.84 (m, 3H, Ar*H*), 7.37 (d, J=2.0 Hz, 2H, Ar*H*), 7.11 (d, J=2.4 Hz, 1H, Ar*H*), 5.35 (s, 4H, 2×OCH_2), 4.40 (t, J=7.6 Hz, 4H, 2×$CH_2CH_2CO_2CH_3$), 4.00 (q, J=7.8 Hz, 4H, 2×CH_2CH_3), 3.67 (s, 6H, 2×OCH_3), 3.66 (s, 6H, 2×CH_3), 3.30 (t, J=7.6 Hz, 4H, 2×$CH_2CH_2CO_2CH_3$), 2.56 (s, 6H, 2×CH_3), 1.74 (t, J=7.4 Hz, 6H, 2×CH_2CH_3), −3.27 (brs, 1H, NH), −3.33 (brs, 1H, NH). ^{19}F NMR: δ 12.96 (s,12F, 4×CF_3). Anal. calcd for $C_{60}H_{54}N_4F_{12}O_6.H_2O$: C, 61.43; H, 4.81; N, 4.77. Found: C, 61.56; H, 4.71; N, 4.71.

3.7.5. 5-[3′,5′-Bis(3″,5″-dimethylbenzyloxy)]phenyl-2,8-diethyl-13,17-bis(2-methoxycarbonylethyl)-3,7-dimethylporphyrin (4a). Yield 30%; mp 158–160°C; UV–vis [CH_2Cl_2, nm (ε, M^{-1} cm^{-1})] 404 (3.81×10^5), 502 (3.43×10^4), 536 (1.56×10^4), 570 (1.50×10^4), 623 (5.19×10^3); ^1H NMR ($CDCl_3$, 400 MHz) δ 10.18 (s, 2H, 2×*meso* C*H*), 9.98 (s, 1H, *meso* C*H*), 7.31–7.32 (m, 2H, ArH), 7.11 (brs, 1H, Ar*H*), 7.08 (s, 3H, Ar*H*), 6.99 (s, 1H, Ar*H*), 6.96 (brs, 2H, Ar*H*), 5.17 (s, 4H, 2×OCH_2), 4.42 (t, J=7.6 Hz, 4H, 2×$CH_2CH_2CO_2CH_3$), 4.04 (q, J=7.0 Hz, 4H, 2×CH_2CH_3), 3.70 (s, 6H, 2×OCH_3), 3.69 (s, 6H, 2×CH_3), 3.32 (t, J=7.8 Hz, 4H, 2×$CH_2CH_2CO_2CH_3$), 2.58 (s, 6H, 2×CH_3), 2.30

(s, 12H, 4×PhCH_3), 1.78 (t, J=7.4 Hz, 6H, 2×CH_2CH_3), −3.25 (brs, 1H, NH), −3.28 (brs, 1H, NH). Mass (FAB) Calcd for $C_{60}H_{66}N_4O_6$: 938.22. Found: 939.20 (M+1).

3.8. Synthesis of chlorin 30 and bacteriochlorin 31 from porphyrin 4

OsO_4 (75 mg) dissolved in diethyl ether (5 mL) was added to a stirred solution of 4 (100 mg) in dry CH_2Cl_2 (20 mL) and pyridine (0.2 mL). The reaction mixture was stirred at room temperature for 6 h. UV–vis spectrum showed two peaks at 645 nm (chlorin 30, major, R_f=0.6 in 5% MeOH in CH_2Cl_2) and at 713 nm (bacteriochlorin 31, minor, R_f=0.4 in 5% MeOH in CH_2Cl_2). The reaction was worked up by passing a stream of H_2S gas for one minute, diluted with CH_2Cl_2 (50 mL) and then filtered through fluted filter paper. The residue was washed with CH_2Cl_2 (3×50 mL), dried over Na_2SO_4. The solvent was concentrated and the crude mixture so obtained was purified by preparative TLC using 5% MeOH in CH_2Cl_2 as an eluant. Three bands were isolated. The fast moving band (10 mg) was identified as unreacted starting material 4, the middle band (25 mg, 40%) was found to be chlorin 30 and the slowest moving band isolated in 13 mg (20%) was characterized as bacteriochlorin 31.

3.8.1. 5-[3,5-Bis{3,5-bis(trifluromethyl)benzyloxy}phenyl]-2,8-diethyl-7,8-dihydroxy-3,7,12,18-tetramethyl-13,17-bis(2-methoxycarbonylethyl)porphyrin (30). Mp 172–174°C; UV–vis [CH_2Cl_2, nm (ε, M^{-1} cm^{-1})] 397 (4.44×10^5), 500 (4.16×10^4), 648 (1.17×10^5); ^{1}H NMR: δ 9.88 (s, 1H, *meso* C*H*), 9.61 (s, 1H, *meso* C*H*), 9.21 (s, 1H, *meso* C*H*), 7.97 (s, 2H, ArH), 7.91 (s, 2H, ArH), 7.88 (s, 1H, ArH), 7.84 (s, 1H, Ar*H*), 7.35 (s, 1H, Ar*H*), 7.12 (s, 1H, Ar*H*), 7.06 (s, 1H, Ar*H*), 5.40 (s, 2H, OCH_2), 5.30 (s, 2H, OCH_2), 4.24 (t, J=7.2 Hz, 2H, $CH_2CH_2CO_2CH_3$), 4.15 (t, J=7.4 Hz, 2H, $CH_2CH_2CO_2CH_3$), 3.96 (q, J=7.4 Hz, 2H, CH_2CH_3), 3.69 (s, 3H, OCH_3), 3.67 (s, 3H, OCH_3), 3.47 (s, 3H, CH_3), 3.44 (s, 3H, CH_3), 3.17 (t, J=7.6 Hz, 4H, 2×$CH_2CH_2CO_2CH_3$), 2.26 (s, 3H, CH_3), 2.23–2.34 (m, 3H, CH_3), 1.70 (t, J=7.8 Hz, 3H, CH_3), 0.89–0.93 (m, 2H, CH_2CH_3), 0.44 (t, J=8.0 Hz, 3H, CH_2CH_3), −2.32 (brs, 1H, NH), ^{19}F NMR: δ 12.98 (s, 6F, 2×CF_3), 12.99 (s, 6F, 2×CF_3). Mass (FAB) calcd. for $C_{60}H_{56}N_4F_{12}O_8$: 1188.12. Found: 1189.50 (M+1).

3.8.2. 5-[3,5-Bis{3,5-bis(trifluromethyl)benzyloxy}phenyl]-2,8-diethyl-7,8,17,18-tetrahydroxy-3,7,12,18-tetramethyl-13,17-bis(2-methoxycarbonylethyl)porphyrin (31). Mp 100–103°C; UV–vis (CH_2Cl_2) 395 (1.69×10^5), 504 (2.22×10^4), 644 (3.81×10^4), 716 (2.67×10^4). Note: Due to mixture of isomers it was difficult to assign the resonances for each proton in the ^{1}H NMR spectrum. The ^{19}F NMR spectrum showed mainly two peaks at δ 12.97 and 12.96 ppm. Mass (FAB) calcd for $C_{60}H_{58}N_4F_{12}O_{10}$: 1223.13. Found: 1223.30 (M+1).

3.9. Method for in vitro biological studies

The in vitro photosensitizing activity of fluorinated photosensitizers 1–4, chlorin 30 and bacteriochlorin 31 was determined in the radiation induced fibrosarcoma (RIF) tumor cell line.[18] The RIF tumor cells were grown in α-MEM with 10% fetal calf serum, penicillin and streptomycin. Cells were maintained in 5% CO_2, 95% air and 100% humidity. For determining the PDT efficacy, these cells were plated in 96-well plates at a density of 1.25×10^4 cells well in complete media. After an overnight incubation at 37°C, the photosensitizers were added at the same concentration (1.0 μM), incubated at 37°C for 4 h in the dark. Cells were then illuminated with a 1000 W quartz halogen lamp with IR and band pass dichroic filters to allow light between 400 and 700 nm, at a dose rate of 16 mW/cm^2. After PDT, the cells were washed once and placed in complete media and incubated for 48 h. Then 10 μL of 5.0 mg/mL solution of 3-[4,5-dimethylthiazol-2-yl]-2,5-diphenyltetrazoliumbromide dissolved in PBS (Sigma, St. Louis, MO) was added to each well. After a 4 h incubation at 37°C the MTT and media were removed and 100 mL DMSO was added to solubilize the formazin crystals. The 96-well plate was read on a microtiter plate reader (Miles Inc. Titertek Multiscan Plus MK II) at 560 nm. The results were plotted as percent survival of the corresponding dark (drug no light) control for each compound tested. Each data point is the average of 5 replicate wells and the error bars are the standard deviation of a single experiment.

3.10. Intracellular localization

In order to determine the subcellular localization of the fluorinated porhyrin 4, chlorin 30 and bacteriochlorin 31, the RIF cells were seeded on poly-L-lysine coated glass cover slips at 1×10^5 in 6 well plates and cultered for 48 h to allow for attachment and spreading. The cells were incubated at 37°C in dark with the 1 μM concentration of photosensitizers for 1, 4 and 24 h and then co-incubated with the 0.25 μM concentration of the organelle-specific dyes Rhodamine-123 for mitochondria and Fluospheres for lysosomes. Immediately prior to microscopy (Zeiss Axiovert 35, Carl Zeiss, Inc. Germany), the cells were gently rinsed with PBS. Cells were illuminated with a mercury arc lamp with a filter cube containing 530–585 nm excitation filter, a 600 nm dichoric filter and a long pass emission filter to detect the photosensitizer. Fluorescent images were recorded and analyzed using a GenIISys intesifier coupled toa Dage MTI CCD72 camera and digitally processed with Metamorph software (Universal Imaging Corp., Downingtown, PA).

3.11. Photophysical measurements

Absorption spectra were recorded on a Hewlett Packard 8453A diode array spectrophotometer. Time-resolved fluorescence and phosphorescence spectra were measured by a Photon Technology International GL-3300 with a Photon Technology International GL-302, nitrogen laser/pumped dye laser system, equipped with a four channel digital delay/pulse generator (Stanford Research System Inc. DG535) and a motor driver (Photon Technology International MD-5020). Excitation wavelengths were from 535 to 551 nm using coumarin 540A (Photon Technology International, Canada) as a dye. Fluorescence lifetimes were determined by a two-exponential curve fit using a microcomputer. Nanosecond transient absorption measurements were carried out using a Nd:YAG laser (continuum, SLII-10, 4–6 ns fwhm) at 355 nm with the

power of 10 mJ as an excitation source. Photoinduced events were estimated by using a continuous Xe-lamp (150 W) and an InGaAs-PIN photodiode (Hamamatsu 2949) as a probe light and a detector, respectively. The output from the photodiodes and a photomultiplier tube was recorded with a digitizing oscilloscope (Tektronix, TDS3032, 300 MHz). The transient spectra were recorded using fresh solutions in each laser excitation. All experiments were performed at 298 K.

For the $^1O_2$ phosphorescence measurements, an O_2-saturated C_6D_6 solution containing the sample in a quartz cell (optical path length 10 mm) was excited at 532 nm using a Cosmo System LVU-200S spectrometer. A photomultiplier (Hamamatsu Photonics, R5509-72) was used to detect emission in the near infrared region (band path 1 mm).

3.12. Electrochemical and spectroelectrochemical measurements

Cyclic voltammetry (CV) measurements were performed at 298 K on an EG&G Model 173 potentiostat coupled with an EG&G Model 175 universal programmer in deaerated benzonitrile solution containing 0.1 M TBAP as a supporting electrolyte. A three-electrode system was utilized and consisted of a glassy carbon working electrode, a platinum wire counter electrode and a saturated calomel reference electrode (SCE). The reference electrode was separated from the bulk of the solution by a fritted-glass bridge filled with the solvent/supporting electrolyte mixture. Thin-layer spectroelectrochemical measurements of the one-electron oxidized and one-electron reduced bacteriochlorin derivatives were carried out using an optically transparent platinum thin-layer working electrode and a Hewlett–Packard model 8453 diode array spectrophotometer coupled with an EG&G Model 173 universal programmer.

3.13. In vivo ^{19}F measurements

The radiation induced fibrosarcoma (RIF) cells were maintained according to the protocol of Twentyman et al.[23] Tumors were grown on mouse foot dorsum by inoculating 2×10^5 cells. The photosensitizer was administered IP (~100 μM). ^{19}F MR spectra were collected on a Bruker 7T instrument using a home built surface coil. The ^{19}F MR spectral parameters included a 90° pulse of 16 μs, a spectral width of 20 KHz, 8 K data points, and a 2 s repetition time for a total accumulation time of 30 min.

Acknowledgements

This research was supported by grants from DOD (DMAD17-99-1-9065), NIH (CA 55792), the Robert A. Welch Foundation (Grant E-680 to KMK), from the Ministry of Education, Culture, Sports, Science and Technology, Japan (13440216 and 13031059 to SF) and the shared resources of the Roswell Park Cancer Center Support Grant (P30CA16056). We thank Beverly Chamberlin, Michigan State University, East Lansing for mass spectrometry results. The elemental analyses were performed at Midwest Micro lab, Indianapolis.

References

1. (a) Pandey, R. K.; Zheng, G. In *The Porphyrin Handbook*; Smith, K. M., Kadish, K. M., Guilard, R., Eds.; Academic: San Diego, 2000. (b) Dougherty, T. J.; Gomer, C.; Henderson, B. W.; Jori, G.; Kessel, D.; Kobrelik, M. J.; Peng, Q. *J. Natl. Cancer Inst.* 1998, *90*, 889. (c) Bonnett, R. *J. Heterocycl. Chem.* 2002, *39*, 455. (d) Boyle, R. W.; Rousseau, J.; Kudrevich, S. V.; Obochi, M. O. K.; van Lier, J. E. *Br. J. Cancer* 1996, *73*, 49.
2. Sherman, W. M.; Allen, C. M.; van Lier, J. E. *Methods Enzymol.* 2000, *319*, 376.
3. (a) Workman, P.; Maxwell, R. J.; Griffiths, J. R. *NMR Biomed.* 1992, *5*, 270. (b) Blackstock, A. W.; Lightfoot, H.; Case, L. D.; Tepper, J. E.; Mukherji, S. K.; Mitchell, B. S.; Swarts, S. G.; Hess, S. M. *Clin. Cancer Res.* 2001, *7*, 3263–3268. (c) Martino, R.; Malet-Martino, M.; Gilard, V. *Curr. Drug Metab.* 2000, *1*, 271–303. (d) Hunjan, S.; Zhao, D.; Constantinescu, A.; Hahn, E. W.; Antich, P. P.; Mason, R. P. *Int. J. Radiat. Oncol. Biol. Phys.* 2001, *49*, 1097–1108.
4. Bottomly, P. A. *Radiology* 1989, *170*, 1.
5. Mason, R. P.; Shukla, H.; Antich, P. P. *Magn. Reson. Med.* 1993, *29*, 296.
6. (a) Ceckler, T. L.; Gibson, S. L.; Hilf, R.; Bryant, R. G. *Magn. Reson. Med.* 1990, *13*, 416. (b) Thomas, C.; Counsell, C.; Wood, P.; Adams, G. *Bull. Cancer* 1993, *80*, 666.
7. Jameson, C. J. In *Fluorine*; Mason, J., Ed.; Plenum: New York, 1987; p 437 Chapter 16.
8. Omote, M.; Ando, A.; Takagi, T.; Koyama, M.; Kumadaki, I. *Tetrahedron* 1996, *52*, 13961.
9. Barton, D. H. R.; Zard, S. Z. *J. Chem. Soc. Chem. Commun.* 1985, 1098.
10. Caveleiro, J. A. S.; Gonsalves, J. A. S.; Kenner, A. M. d.'A. R.; Smith, G. W. K. M. *J. Chem. Soc. Perkin Trans.* 1973, 240.
11. Jackson, A. H.; Smith, K. M. *The Total Synthesis of Natural Products*; ApSimon, J., Ed.; Wiley: New York, 1973; Vol. 3, p 144 1984, Vol. 6, p 23.
12. Arsenault, G. P.; Bullock, E.; MacDonald, S. F. *J. Am. Chem. Soc.* 1960, *82*, 4384.
13. Clezy, P. S.; Fookes, C. J. R.; Liepa, A. J. *Aust. J. Chem.* 1977, *30*, 2017.
14. (a) Pandey, R. K.; Jackson, A. H.; Smith, K. M. *J. Chem. Soc. Perkin Trans. 1* 1991, 1211. (b) Smith, K. M.; Pandey, R. K. *Tetrahedron Lett.* 1986, *27*, 2717. (c) Jackson, A. H.; Pandey, R. K.; Rao, K. R. N.; Roberts, E. *Tetrahedron Lett.* 1985, 793.
15. Smith, K. M. In *The Porphyrins and Metalloporphyrins*; Smith, K. M., Ed.; Elesvier: Amsterdam, 1975.
16. Fukuzumi, S.; Suenobu, T.; Patz, M.; Hirasaka, T.; Itoh, S.; Fujitsuka, M.; Ito, O. *J. Am. Chem. Soc.* 1998, *120*, 8060.
17. Arbogast, J. W.; Darmanyan, A. P.; Chrostopher, P. D.; Foote, S.; Rubin, Y.; Diederich, F. N.; Alvarez, M. M.; Anz, S. J.; Whetten, R. L. *J. Phys. Chem.* 1991, *95*, 11.
18. Felton, R. H. *The Porphyrins*; Dolphin, D., Ed.; Academic: New York, 1978; Vol. 5, Chapter 3.
19. (a) Pandey, R. K.; Sumlin, A. B.; Potter, W. R.; Bellnier, D. A.; Henderson, B. W.; Constantine, S.; Aoudia, M.; Rodgers, M. A. J.; Smith, K. M.; Dougherty, T. J. *Photochem. Photobiol.* 1996, *63*, 194. (b) Henderson, B. W.; Bellnier, D. A.; Graco, W. R.; Sharma, A.; Pandey, R. K.; Vaughan, L.; Weishaupt, K. R.; Dougherty, T. *J. Cancer Res.* 1997, *57*, 4000. (c) Zheng, G.; Potter, W. R.; Camacho, S. H.; Missert, J. R. G.; Wang, G.; Bellnier, D. A.; Henderson, B. W.;

Rodgers, M. A. J.; Dougherty, T. J.; Pandey, R. K. *J. Med. Chem.* 2001, *44*, 1540. and references therein.
20. Pandey, R. K.; Potter, W. R.; Meunier, L; Sumlin, A. B.; Smith, K. M. *Photochem. Photobiol.* 1995, *62*, 764.
21. Li, G.; Graham, A.; Potter, W. R.; Grossman, Z. D.; Oseroff, A.; Dougherty, T. J.; Pandey, R. K. *J. Org. Chem.* 2001, *66*, 1316.
22. Chen, Y. C.; Medforth, C. J.; Smith. K. M.; Alderfer, J. L.; Dougherty, T. J.; Smith, K. M. *J. Org. Chem.* 2001, *66*, 3930.
23. Twentyman, P. R.; Brown, J. M.; Gray, J. W.; Franko, A. J.; Scoles, M. A.; Kallman, R. F. *J. Natl. Cancer Inst.* 1980, *64*, 595.

PROGRESS IN BIOMEDICAL OPTICS AND IMAGING

SPIE—The International Society for Optical Engineering

Monitoring PDT effects in murine tumors by spectroscopic and imaging techniques

S. Ramaprasad, E. Rzepka, J. Pi, S. S. Joshi,
M. Dobhal, J. Missert, R. K. Pandey

Reprinted from

Medical Imaging 2004

Physiology, Function, and Structure from Medical Images

15–17 February 2004
San Diego, California, USA

Volume 5369

SPIE paper # 5369-44

Monitoring PDT Effects in Murine Tumors by Spectroscopic and Imaging Techniques

S. Ramaprasad[a*], E. Rzepka[a], J. Pi[a], SS. Joshi[b], M. Dobhal[c], J. Missert[c], RK. Pandey[c]
[a]Department of Radiology, University of Nebraska Medical Center, Omaha, NE, 68198-1045, USA; [b]Department of Genetics and Cell Biology, University of Nebraska Medical Center Omaha, NE, 68198-6395, USA; [c]PDT Center, Roswell Park Cancer Institute, Buffalo, NY, 14263, USA.

SUMMARY

The changes in the tumor that occur following photodynamic therapy (PDT) were studied using a small animal MR imager operating at 7Tesla. The animal model used in these studies was mice bearing radiation induced fibrosarcoma (RIF) tumor on the foot dorsum. The mice were injected with 10μM/kg of one of the photosensitizers: 1) Photofrin® 2) Non-fluorinated porphyrin photosensitizer (DOD-1) 3) Fluorinated porphyrin photosensitizer (DOD-2) and, 4) Fluorinated chlorin photosensitizer (DOD-6). Laser light at 630 or 650 nm (150 mW/cm^2, 270 joules/ cm^2) was delivered to the tumor at 2-24 hours of photosensitizer administration. The MR spectroscopic and imaging examination of the tumors involved both the ^{1}H and ^{31}P nuclei. The tumor bioenergetics was measured by ^{31}P spectroscopy. The water proton relaxivity and diffusion measurements were used to obtain local changes in different regions of the tumor.

Changes in ^{31}P MR spectra were observed following PDT using Photofrin® and fluorinated chlorin sensitizer (DOD-6). However, no significant changes were observed when the fluorinated porphyrin and its nonfluorinated analog were used. The PDT induced changes in tumor volumes showed significant tumor regression with Photofrin®, fluorinated porphyrin and chlorin sensitizers. No tumor regression was observed with the non labeled porphyrin sensitizer and the growth profile followed the general pattern of unperturbed tumors. Serial noninvasive measurements of tumor response to PDT are measurable by both MRI and MRS. The MR derived parameters that are characteristic of the tumor status before and after the therapy are discussed here.

KEY WORDS: RIF tumor, Tumor regression, Photodynamic therapy, Magnetic Resonance Spectroscopy, ^{31}P MR, Relaxivity, Diffusion, Solenoid coil

1. INTRODUCTION

Photodynamic therapy is a cancer treatment modality that combines light sensitive drugs and lasers. Cytotoxic singlet oxygen and free radicals produced by photodynamic therapy can damage the cell and lysosomal membranes. One of the other major contributions to tumor destruction may be damage to tumor circulation following PDT initiation (1). Monitoring the photosensitizer (PS) effects in the tumor and in normal tissue is helpful in the development and function of new photosensitizers. MR studies offer the advantage of noninvasive assessment of the photosensitizer in a single subject. The assessment of the same in the skin and underlying muscle may provide information about the cutaneous toxicity of PS.

Magnetic resonance measurements being noninvasive in nature have been used on humans and animal models to study in situ biochemistry and metabolism of tumors in a single individual subject. Phosphorous-31 NMR spectroscopy has been used to detect the early metabolic response of tumors to PDT (2-6) which generally indicate a decrease in nucleoside triphosphate (NTP) and an increase in inorganic phosphate (P_i) within 1 hour of treatment and continuing for several hours thereafter. These data generally demonstrate that early changes in ^{31}P metabolism can be studied by

Correspondence: Email:SRamaprsad@unmc.edu; Phone 402-559-6990; Fax 402-559-1011

Medical Imaging 2004: Physiology, Function, and Structure from Medical Images, edited by Amir A. Amini, Armando Manduca, Proceedings of SPIE Vol. 5369 (SPIE, Bellingham, WA, 2004) · 1605-7422/04/$15 · doi: 10.1117/12.535657

MR and early changes are attributable to direct cellular damage as opposed to later changes that may be indicative of overall hypoxia caused by vascular damage (7). Phosphorous -31 MR studies has been used to follow the therapeutic effects and to assess whether the initiation of therapy is optimal or subcurative (4). However, if a proton based imaging technique can provide basic information about the initiation and progress of therapy, it would be more widely applicable as tissue water protons are present at much higher concentrations than phosphorous-31 nuclei. When the spectral changes seen in ^{31}P MR examinations correlate with tumor regression and the spectral measures can be clearly correlated to changes in one or more of the MR parameters such as perfusion, diffusion, or relaxivity, then it will provide a quick way of effectively monitoring the therapeutic effects. Here we discuss the tumor response to PDT therapy while using new photosensitizers as measured from ^{31}P MR and ^{1}H diffusion weighted imaging studies at 7Tesla animal imager. The structures of new photosensitizers, representative in vitro PDT studies and, MR observation of fluorine labeled photosenitizer in an in vivo RIF tumor model have been published by us recently (8). The molecular structures of three such photosensitizers studied in this project are shown in Figure 1.

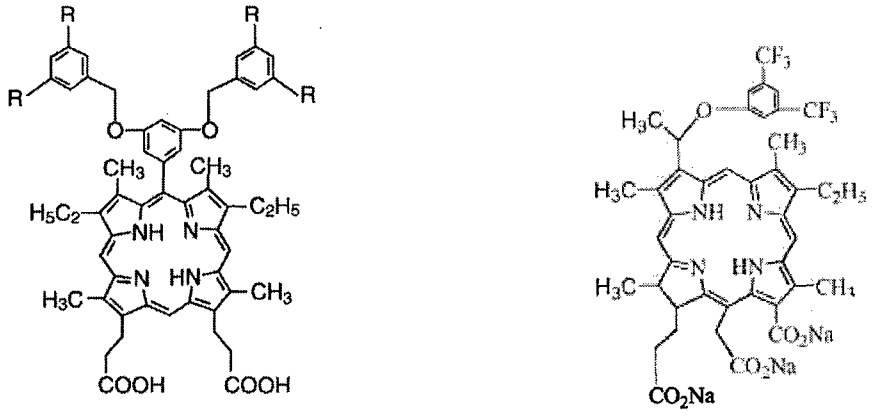

DOD -1: R=CH_3, DOD-2: R= CF_3 **DOD-6**

Figure The structures of photoensitizers used in the study.

An ideal tumor size for the studies involving PDT and MR is one which is not too large to be a physiological burden (9) to the animal but sufficient enough to provide signals of high signal to noise ratio from small tumor volumes. The tumor size we used in our studies was in the neighborhood of 1-2% of the body weight. The tumors grown on the foot dorsum with volumes in the range of 100-300 μl were found suitable for the studies using MR techniques.

2. METHODS

2.1Animal and tumor model

RIF tumor was implanted on the foot dorsum of male C3H/HeJ mice (Jackson laboratories, Bar harbor, ME). PDT and MRI studies were performed on foot tumors while the animal remained steady under 1% isoflurane anesthesia.

2.2 Tumor production

Male C3H/HeJ mice, three to four weeks of age, were used in our studies. The mice were housed at five per cage in humidity and temperature controlled animal facility with a 12 hour light/dark cycle. All mice were fed standard chow and provided with water ad libitum. Mice treated with photosensitizers were maintained in subdued light for the experiments.

Frozen RIF cells originally obtained from Roswell Park Cancer institute (Buffalo, NewYork) were maintained according to the general protocols of Twentyman et al (10) with appropriate changes of the growth media at least twice

a week. Tumors on the foot dorsum were produced by inoculating subcutaneously with $2x10^5$ fresh RIF cells on three week old male mice. The inoculation sites were observed two or three times a week for tumor growth until a tumor size of sufficient volume for NMR and in vivo experiments were obtained.

2.3 PDT

All PDT measurements were performed at 630nm using an argon ion (Spectra physics model 2045) pumped dye laser (Spectra Physics, 375B). A fractionated laser irradiation scheme was employed that consisted of two laser irradiations, separated by a dark interval of 2 hours. Laser irradiation was done for ten minutes each along each one of the three tumor directions leading to 30 minutes of laser irradiation and a light dose of 270 J cm^{-2}. This method provides nearly uniform light delivery to the entire tumor mass.

The photosensitizers were administered IP at a dose of ~10μM/kg. The photosensitizers considered in the study are: 1) Photofrin® 2) Non-fluorinated porphyrin photosensitizer (DOD-1) 3) Fluorinated porphyrin photosensitizer (DOD-2) and, 4) Fluorinated chlorin photosensitizer (DOD-6). After 2-24 hours post drug administration, the tumors were illuminated with laser light at the required wavelength.

2.4 Tumor growth before and after PDT

Tumor measurements were done every day both before and after the treatment. The tumor volumes were estimated using the formula $V= \pi$ (axbxc) /6 where a, b and c are the tumor dimensions in three directions measured using a caliper. Tumor bearing animals were divided into treated and control groups. The control study groups were those that remained untreated or those that were treated with photosensitizer alone or laser alone. The three tumor dimensions and the total tumor volume were recorded. The tumor volumes post PDT were used to measure the tumor regression and were used to evaluate the PDT effects using different photosensitizers on mice tumor model. Growth charts were produced for both the controls and treated tumors. The tumor doubling rates or tumor regression rates were computed from the charts so produced. To compare the PDT effects of different photosensitizers, the tumor doubling times from the day 0 to the day of laser irradiation and the tumor halving times post PDT were computed.

2.5 Magnetic resonance spectroscopy and imaging

The ^{31}P MR spectra were collected both before and after PDT using a Bruker 7T instrument and a home built saddle coil (see Figure 2). The MR spectral parameters included a 90° pulse of 20μs, a spectral width of 20 KHz, 8K data points and a 2s repetition time for a total accumulation time of 30 minutes. ^{31}P spectra were collected prior to injecting the drug, before PDT initiation, and up to 6 hrs after PDT initiation. The ratio of Pi to total phosphorus content is measured as a possible indicator of onset of PDT.

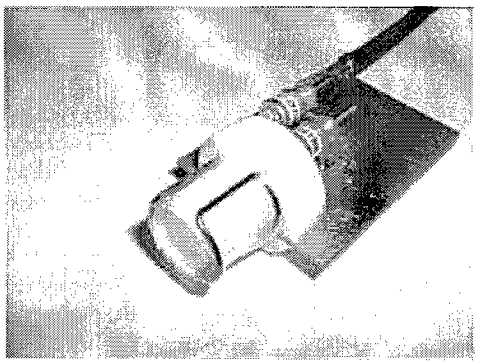

Figure 2: The ^{31}P saddle coil designed for 7T animal imager was constructed at our center. This coil with a diameter of 1.5 cm was used in foot tumor studies.

2.5.1 Relaxivity studies

The optimized imaging of tumors to visualize the contrast between the necrotic, viable and, edematous zones requires knowledge of both T_1 and T_2 relaxation times. We have performed multislice T_1 and T_2 relaxation time measurements on both control and PDT treated mice. The image based water T_1 relaxivity measurements were performed using variable repetition times (TRs). The T_2 measurements were done using a series of spin echo images with variable echo times. Both the studies were done in a multi-slice imaging mode.

2.5.2 Diffusion Imaging

Diffusion MRI studies were done using proton saddle coil of 1.5 cm diameter and 1.5 cm length. Diffusion weighted ^1H images were collected both before and after PDT on a 1 mm axial slice with 128x64 matrix with an FOV of 4cm. The data matrix was interpolated to obtain a 128x128 square matrix. Mice were covered with cotton blanket to keep them warm inside the magnet. Diffusion sensitizing gradient (0-120mT/M) pulse was applied in the three directions with durations (δ) of 10ms, a diffusion-gradient separation time (Δ) of 19.7 ms and 12 b values. The b values used in this study were: 57.125, 102.107, 162.083, 280.160, 431.974, 617.524, 836.811, 1001.744, 1181.672, 1376.593, 1586.508, and 1697.089 s/mm^2.

2.5.3 Image Processing

All MR data were analyzed using the Bruker Paravison software. Four regions of interest (ROI) were chosen for our measurements. The relaxation times (T_1 or T_2) and the apparent diffusion coefficients (ADC's) from different regions of interest (ROIs) were measured from the relaxivity and diffusion weighted images.

3. RESULTS

Representative tumor growth patterns of control tumors such as untreated, PS treated, and laser treated tumors are shown in Figure 3a. The growth profiles for the PDT treated tumors are shown in Figure 3b.

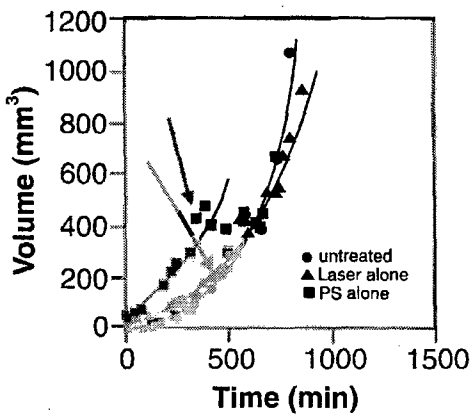

Figure 3a: Growth profiles for tumors for 1) unperturbed 2) laser irradiation alone and 3) drug alone. The arrows indicate time of drug or laser administration

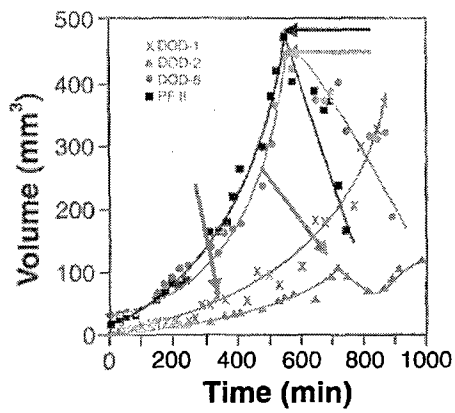

Figure 3b: Growth profiles for PDT treated tumors using DOD-1, DOD-2, DOD6, and Photofrin®. The arrows indicate the time at which PDT was started.

The slopes obtained from the growth phase alone and regression phase alone were used to compute the rates given in Table 1. The growth and regression rates correspond to increase or decrease in tumor volumes. As can be seen from the values in the last column, DOD-1 did not show any PDT response and there is only one rate which characterizes this growth profile. The growth is represented by the doubling time and the regression rates are represented by the time required for the tumor to regress to half its volume. The tumor volume measurements clearly demonstrate PDT effects with DOD-2, DOD-6, and Photofrin®. No such effects were seen on laser alone or drug alone controls.

Table 1

Mouse Number	Drug used	Treatment	Growth/ Regression Times
1	None	Untreated	110.3
2	Saline	Laser alone	178.9
4	DOD-6	Drug Alone	113.3
5	DOD-1	PDT treated	150.5
6	DOD-2	PDT treated	181.5 -177.0
7	DOD-6	PDT treated	138.6 -414.0
8	Photofrin®	PDT treated	122.9 -164.1

The changes that result following PDT studies were measured using ^{31}P MR spectroscopic technique. The fluorine labeled photosensitizer (DOD-2) did not show significant changes in ^{31}P spectra but the tumor volume measurements showed regression as shown in Table1. The studies involving Photofrin® and DOD-6 showed tumor regression and changes in ^{31}P spectra. The nonlabeled photosensitizer did not show tumor regression or changes in ^{31}P spectra.

The ^{31}P spectral data obtained for the case of Photofrin® were analyzed and percent inorganic phosphate and α-ATP with respect to total tumor phosphorous were measured. These values were obtained using the AMARES algorithm as included in jMRUI software package (11). An increase in the concentration of inorganic phosphate (Pi) and a corresponding decrease in ATP values over time after PDT initiation are shown in Figure 4. A similar set of results were also seen while using DOD6 sensitizer. There were greater effects on phosphate metabolism within in the first 2 hours of PDT when the sensitizer was Photofrin® or DOD-6. The effects of PDT on ^{31}P spectra were little or none when the sensitizers used were DOD-1or DOD-2. However all the photosensitizers except DOD-1 showed tumor regression as shown in Figure 3. The results presented in Figure 3 describing the growth profiles are for qualitative analysis only and further studies with DOD-1 and DOD-2 under similar treatment conditions as photofrin and DOD-6 are currently in progress.

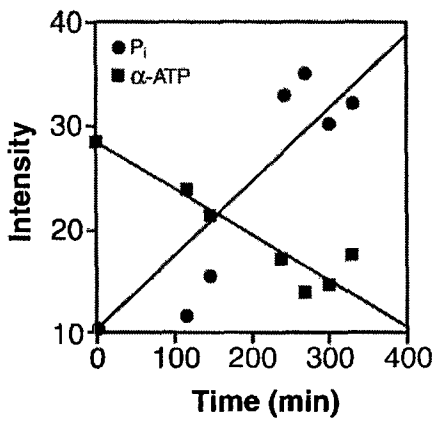

Figure 4: Intensities of P_i and α-ATP peaks measured at various times post PDT

3.1 Relaxivity Values

The tumors were investigated for the changes in T_1 and T_2 values following the therapy. The measurements were made in four different regions on the central slice of 2 mm thick similar to that shown in Figure 5. The mean T_2 values before and within 1hr after therapy were 64.5 ±2.9 ms and 63.8±2.3 ms respectively. Thus no changes were seen for the T_2 values after the therapy. The mean T_1 values before and after the therapy were 1828±235 ms and 2553 ± 163 ms respectively indicating an increase of 40 %(P=0.004). The increase in T_1 values were significant in all regions of the tumor area chosen in this study. These results are also consistent with our earlier studies on whole tumors studied on a 4.7T instrument (12).

3.2 Apparent Diffusion Coefficients

From the diffusion weighted images the ADC's in four different regions of interest (ROIs) were obtained. The different ROIs chosen from 1mm thick mid slice of the tumor are shown in Figure 5. The signal intensities were extracted for each ROI and ADCs measured using the Bruker Paravision software for diffusion analysis. The standard deviations were

recorded for the selected regions of interest shown in Figure5. The ADC values measured before therapy were in the expected range for the tumor type studied here.

The control ADC values were measured before the induction of PDT in 4 different regions in a 1mm axial image that corresponds to the central slice of the tumor. The volumes of the regions of interest were typically of the order of 6-7 mm^3. Significant changes in the ADC values for both Photofrin® and DOD-6 sensitizers were observed in the first two hours post PDT. These changes were more concentrated in region 4 (see figure 5). An increase in ADC was more evident with DOD-6 than with Photofrin®. In some regions a decrease in ADC was also observed. The four regions of interest in a given slice that were chosen for ADC measurements along the x, y, and z directions led to a total of twelve measurements of ADCs per slice. From the set of 12 measured values, we observed increases in 7 values and decreases in 5 for the case of Photofrin® and 10 increases and 2 decreases for the case of DOD-6. The maximum increase in ADC was ~54% with Photofrin® and 165% with DoD-6. Together our studies demonstrate that in the time frame where ^{31}P studies indicate build up of inorganic phosphate, the different regions of the tumor also undergo changes in the diffusion values which are indicative of a substantial increase in water diffusivity that may be attributable to major cell loss, reduced cell density, and widening of extracellular space leading to high water mobility (13). A decrease in ADCs has been attributed to possible cell membrane break down that block active ion and water transport that lead to decline in ADC.

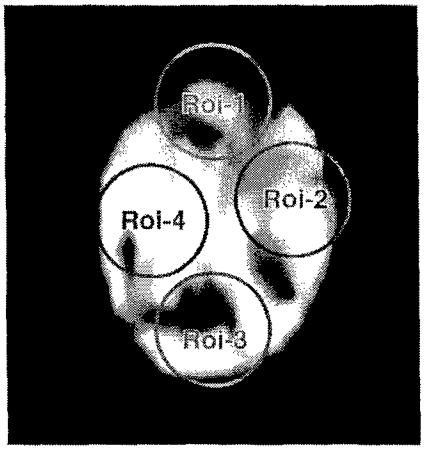

Figure 5: A diffusion weighted axial image from a central slice of the tumor recorded immediately following PDT. The four regions of interest that were considered in the study are also shown.

4. CONCLUSIONS

MR spectroscopic studies of tumors before and after photodynamic therapy may provide valuable insight into tissue response to different photosenitizers at different times post therapy. The results from different MR techniques have a significant potential in evaluating cellular and molecular events that follow photodynamic therapy involving different photosenitizers and their mode of action.

5. ACKNOWLEDGEMENTS

This research was funded by the Department of Defense (DAMD 17-99-1-9065).

6. REFERENCES

B.W. Henderson, S.M. Waldow, T.S. Mang, W.R. Potter, P.B. Malone, T.J. Dougherty, "Tumor destruction and kinetics of tumor cell death in two experimental tumors following photodynamic therapy," *Cancer Res*, 45, pp. 572-576, 1985.

2. T.L. Ceckler, R.G. Bryant, D. P. Penney, S. L. Gibson, R. Hilf , "^{31}P NMR spectroscopy demonstrates decreased ATP levels in vivo as an early response to photodynamic therapy," *Biochem.Biophys Res Commun*, 140, 273-279, 1986.

3. S. Naruse, Y. Horikawa, C. Tanaka, T. Higuchi, H. Sekimoto, S. Ueda, and K. Hirakawa, "Evaluation of the effects of photoradiation therapy on brain tumors with in vivo ^{31}P MR spectroscopy," *Radiology*, 160, pp. 827-830, 1986.

4. M. Chopp, H. Farmer, F.Hetzel and A.P. Schaap, "In vivo ^{31}P NMR spectroscopy of mammary carcinoma subjected to subcurative photodynamic therapy," *Photochem Photobiol* 46, pp. 819- 822, 1987.

5. R Hilf, S.L Gibson, D.P Penney, T.L. Ceckler, R.G. Bryant, "Early biochemical responses to photodynamic therapy monitored by NMR spectroscopy," *Photochem Photobiol,* 46, pp. 809-817, 1987.

6. S Ramaprasad, R K Pandey, R.M. Hawk, Y.H. Liu, "Responses to Photodynamic therapy in a murine tumor model-- ^{31}P NMR and water proton relaxation studies," *Environ Sci Health.* A28, pp. 2345-2357, 1993.

7. J.C. Bremner, J.K. Bradley, I.J. Stratford, G.E. Adams, "Magnetic resonance spectroscopic studies on real time changes in RIF-1 tumor metabolism and blood flow during and after photodynamic therapy," *B J Cancer,* 69, pp. 1083-1087, 1994.

8. S.K .Pandey , A.L Gryshuk, A Graham, K Ohkubo, S. Fukuzumi, M.P Dobhal, G. Zheng, Z. Ou, R, Zahn, K.M. Kadish, A. Oseroff, S. Ramaprasad, R.K. Pandey, "Fluorinated photosensitizers: Synthesis, Photophysical, Electrochemical, Intracellular Localization, In vitro photosensitizing efficacy and determination of tumor-uptake by ^{19}F in-vivo MR spectroscopy," *Tetrahedron,* in press

9. J. Denekamp, "The choice of experimental models in cancer research: The key to ultimate success or failure? ," *NMR Biomed,* 5, pp. 234-237, 1992.

10. P.R. Twentyman, J.M. Brown, J.W. Gray, A.J. Franko, M.A. Scoles, and R.F. Kallman, "A New mouse tumor model system (RIF-1) for comparison of end point studies," *J Nat Cancer Inst* 64, pp. 595-604, 1980.

11 A. Naressi, C.Couturier, J.M. Devos, M. Janssen, C. Mangeat, R. deBeer, D. Graveron-Demilly, "Java-based graphical user interface for the MRUI quantitation package," *MAGMA,* 12, pp. 141-152, 2001.

12. Y.H. Liu, R.M. Hawk, S. Ramaprasad, "In vivo relaxation time measurements on a murine tumor model-Prolongation of T_1 after photodynamic therapy," *Magn Reson Imaging,* 13, pp. 251-258, 1995

13. R.A. Kauppinen, "Monitoring cytotoxic tumor treatment response by diffusion magnetic resonance imaging and proton spectroscopy," *NMR Biomed,* 15, pp. 6-17, 2002.

PROGRESS IN BIOMEDICAL OPTICS AND IMAGING

Vol. 6, No. 23
ISSN 1605-7422

In vivo magnetic resonance measures of dark cytotoxicity of photosensitizers in a Murine tumor model

S. Ramaprasad, E. Ripp, J. Pi, S. S. Joshi,
S. K. Pandey, J. Missert, R. K. Pandey

Reprinted from

Medical Imaging 2005
Physiology, Function, and Structure from Medical Images

13–15 February 2005
San Diego, California, USA

Proceedings of SPIE
Volume 5746

SPIE paper # 5746-3

In Vivo Magnetic Resonance Measures of Dark Cytotoxicity of Photosensitizers in a Murine Tumor Model.

S. Ramaprasad[a*], E. Ripp[a], J. Pi[a], SS. Joshi[b], SK. Pandey[c], J. Missert[c], RK. Pandey[c]
[a]Department of Radiology, University of Nebraska Medical Center, Omaha, NE, 68198-1045, USA; [b]Department of Genetics and Cell Biology, University of Nebraska Medical Center, Omaha, NE, 68198-6395, USA; [c]PDT Center, Roswell Park Cancer Institute, Buffalo, NY, 14263, USA

SUMMARY

Photodynamic therapy (PDT) is a novel cancer treatment modality where the therapeutic action is controlled by light and the potency of the photosensitizer used. Development of new potent photosensitizers (PS) for clinical applications requires that the PDT effects are maximized while minimizing dark cytotoxicity. The dark toxicity of photosensitizers is generally confirmed using cell lines. Photososensitizers that appear promising from in vitro assays need further investigations under in vivo conditions. As in vivo MR methods have the potential to provide information on the tumor status, they can be very effective tools to study dark toxicity of tumors.

The tumor produced on the mouse foot dorsum was tested on two newly synthesized photosensitizers along with Photofrin as a control. The MR studies consisted of serial ^{31}P spectral measurements both before and after PS injection. The results show significant changes in the tumor metabolism with increased inorganic phosphate while using new photosensitizers. However these changes slowly approached control levels several hours later. The studies performed while using Photofrin did not show any significant changes indicating minimal or no dark cytotoxicity. Similar studies performed on normal tissue such as the muscle indicated that the energy metabolism was minimally compromised.

Our studies demonstrate that the effects of dark cytotoxicity can be observed by ^{31}P MR. The growth profiles of tumors treated with PS alone indicate that the metabolic changes are temporary and do not interfere with the tumor growth. The studies suggest that MR is a new method of monitoring the effect of PS administered toxicity in an in vivo model.

KEY WORDS: RIF tumor, Tumor Growth Profiles, Dark cytotoxicity, Photodynamic therapy, Magnetic Resonance Spectroscopy, ^{31}P MR, RF coils.

1. INTRODUCTION

Photodynamic therapy (PDT) is a novel cancer treatment modality in which the drug action is locally controlled by light (1). Development of new photosensitizers (PS) for clinical applications needs to minimize dark cytotoxicity while maximizing the PDT effects in the tumor. Photofrin with a long incubation time in human ovarian carcinoma cells has shown dark toxicity effects (2). Other photosensitizers such as Nile Blue A (NBA) have shown dark toxicity on human tumor cells in vitro (3). The dark toxicity of NBA was not due to apoptosis. The cytotoxicity of photosensitizers in an in vitro situation is often measured using a suitable cell system. For example the cytotoxicity in dark or in the presence of laser light is generally monitored by counting the number of cells in the untreated and PS treated cultures (4). Other methods such as MTT cell proliferation assay (5) is based on the ability of mitochondrial dehydrogenase enzyme from viable cells to cleave the tetrazolium rings of MTT and form a dark blue formazan crystal which is largely impermeable to cell membranes. The number of surviving cells is directly proportional of the formazan product created. The latter method has been used to detect a portion of dark toxicity manifested by Photofrin II (6).

Correspondence: Email:SRamaprsad@unmc.edu; Phone 402-559-6990; Fax 402-559-1011

Medical Imaging 2005: Physiology, Function, and Structure from Medical Images, edited by Amir A. Amini, Armando Manduca, Proceedings of SPIE Vol. 5746 (SPIE, Bellingham, WA, 2005) · 1605-7422/05/$15 · doi: 10.1117/12.593798

In the above in vitro models the effect is only seen in the number of cells that die and the number of healthy cells that remain after a treatment. The results depend upon the concentration of PS which remain constant during the time of incubation. However,in practice, build up of the PS in the tumor and its subsequent cytotoxicity is a dynamic process involving different absorption and elimination rates. Thus, a true and realistic model when used to determine the cytotoxicity should take into account the dynamics of PS in the model. Additionally, the presence of vasculature in tumors is not represented in cellular systems thereby making it a less effective representation of a tumors present in humans. Thus, a tumor model in a mammalian system should be of great preclinical value in obtaining more information on the effects of PS on the tumor either in the dark or in the presence of laser light. For these studies we use the murine tumor model where the tumor is grown on the foot dorsum.

We also monitored the murine tumor model with and without the administered PS by the noninvasive magnetic resonance technique. Two new water soluble photosensitizers (7) were tested for dark toxicity and tumor growth monitored over 4-6 weeks. Of the two photosensitizers used in this study, one was a chlorin derivative (DOD-6) and the other was a porphyrin derivative (DOD-2). The structures of these photosensitizers are shown n Figure 1 as compounds 1 and 2 respectively. The PS administered was in the dose range of 2.5-10μM/kg. Here we report the results of our studies on dark toxicity of two PS by in vivo ^{31}P MR and discuss their utility in the development of new photosensitizers

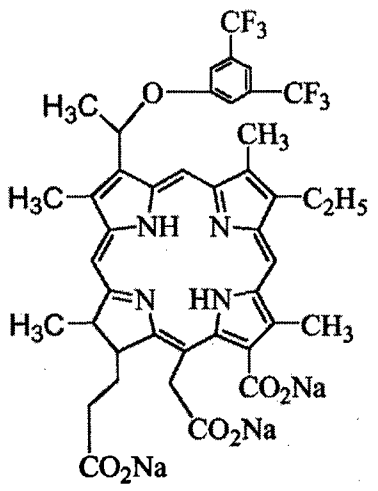

1

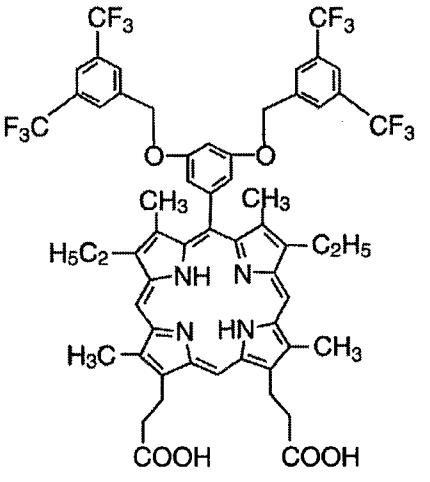

2

Figure 1: The structures of two water soluble photosensitizers used in these studies. The compounds **1** and **2** are chlorin and porphyrin based photosensitizers.

2. METHODS

2.1Animal and tumor model

Male C3H/HeJ mice, three to four weeks of age, were used in our studies. The mice were housed at five per cage in humidity and temperature controlled animal facility with a 12 hour light/dark cycle. All mice were fed standard chow and provided with water ad libitum. Mice treated with photosensitizers were maintained in subdued light for the experiments.

2.2 Tumor production

Choice of tumor model: An ideal tumor size for the project is one which is not too large to be a physiological burden to

the animal but large enough to provide high quality signal from small tumor volumes. The tumor size is generally kept between 1-10% of the body weight (8) and do not exceed 10%. The tumors grown on the foot dorsum to a volume of 300-400 µl were found to be appropriate for our studies. The tumor size we used in these studies were in the neighborhood of 1-2% of the body weight

Methods: Frozen RIF cells originally obtained from Roswell Park Cancer institute (Buffalo, New York) were maintained according to the general protocols of Twentyman et al (9) with appropriate changes of the growth media at least twice a week. Tumors on the foot dorsum were produced by inoculating subcutaneously with $2x10^5$ fresh RIF cells on three week old male C3H/HeJ mice (Jackson laboratories, Bar harbor, ME). The inoculation sites were observed two or three times a week for tumor growth until a tumor size of sufficient volume for NMR (200-300µl) and in vivo experiments was reached and used in this study. All MRI studies performed on foot tumors while the animal remained steady under 1% isoflurane anesthesia.

2.3 PDT

All PDT measurements were performed at 630nm using an Argon ion (Spectra physics model 2045) pumped dye laser (Spectra Physics, 375B). A fractionated laser irradiation scheme was employed that consisted of two laser irradiations, separated by a dark interval of 2 hours. Laser irradiation was done for ten minutes each along each one of the three tumor directions leading to 30 minutes of laser irradiation and a light dose of 270 J cm^{-2}. This method provides nearly uniform light delivery to the entire tumor mass.

The photosensitizers were administered IP at a dose of ~2-10µM/kg. PDT studies were performed on foot tumors while the animal remained steady under 1% isoflurane mixed with N_2O, and O_2. The photosensitizers considered in the study are: 1) Fluorinated chlorin photosensitizer (DOD-6) 2) Fluorinated porphyrin photosensitizer (DOD-2) and 3) Photofrin®. After 2-24 hours post drug administration, the tumors were illuminated with laser light at the required wavelength.

2.4 In vivo MR studies

The ^{31}P MR spectra were collected from the foot tumor both before and after administering the PS. The studies were performed using DOD-6, DOD-2 and photofrin the only FDA approved photosensitizer used in PDT treatment of patients. A Bruker 7T instrument and a home built saddle coil were used for these studies. The MR spectral parameters included a RF pulse of pulse of 20µs, a spectral width of 20 KHz, 8K data points and a 2s repetition time for a total accumulation time of 30 minutes. ^{31}P spectra were collected prior to injecting the drug, before and up to 6 hrs post PS administration. The percent inorganic phosphate (Pi) and the high energy phosphate (ATP) resonances were estimated using the AMARES algorithm as indicated in jMRUI software package (10).

2.5 Tumor growth before and after PS administration

Tumor measurements were done every day both before and after the treatment. The tumor volumes were estimated using the formula $V= \pi (a*b*c) /6$ where a, b and c are the tumor dimensions in three directions measured using a caliper. Tumor bearing animals were divided into treated and control groups. The control study groups were those that remained untreated throughout the experiment. The three tumor dimensions and the total tumor volume were recorded. The tumor volumes post PS administration were used to measure the tumor regression and were used to evaluate the effects of dark toxicity of different photosensitizers on mice tumor volumes and growth profiles. Growth profiles were produced for both the controls and treated tumors.

3. RESULTS

The photosensitizer DOD-6 showed significant increase in inorganic phosphate (Pi) resonance in the first 30 minutes post drug administration. Representative ^{31}P spectra when DOD-6 was administered at 10 and 2.5 µM/kg are shown in displays A and B in Figure 2. This increase in Pi persisted for 3-4 hours. Similar results were seen while using DOD-2 (See display C in Figure 2). Studies performed between 5-24 hours showed characteristics of control spectra recorded before drug injection. When photofrin was used at doses similar to those used above, no significant changes were seen in ^{31}P MR spectra indicating minimal dark toxicity for Photofrin (see display D in figure 2).

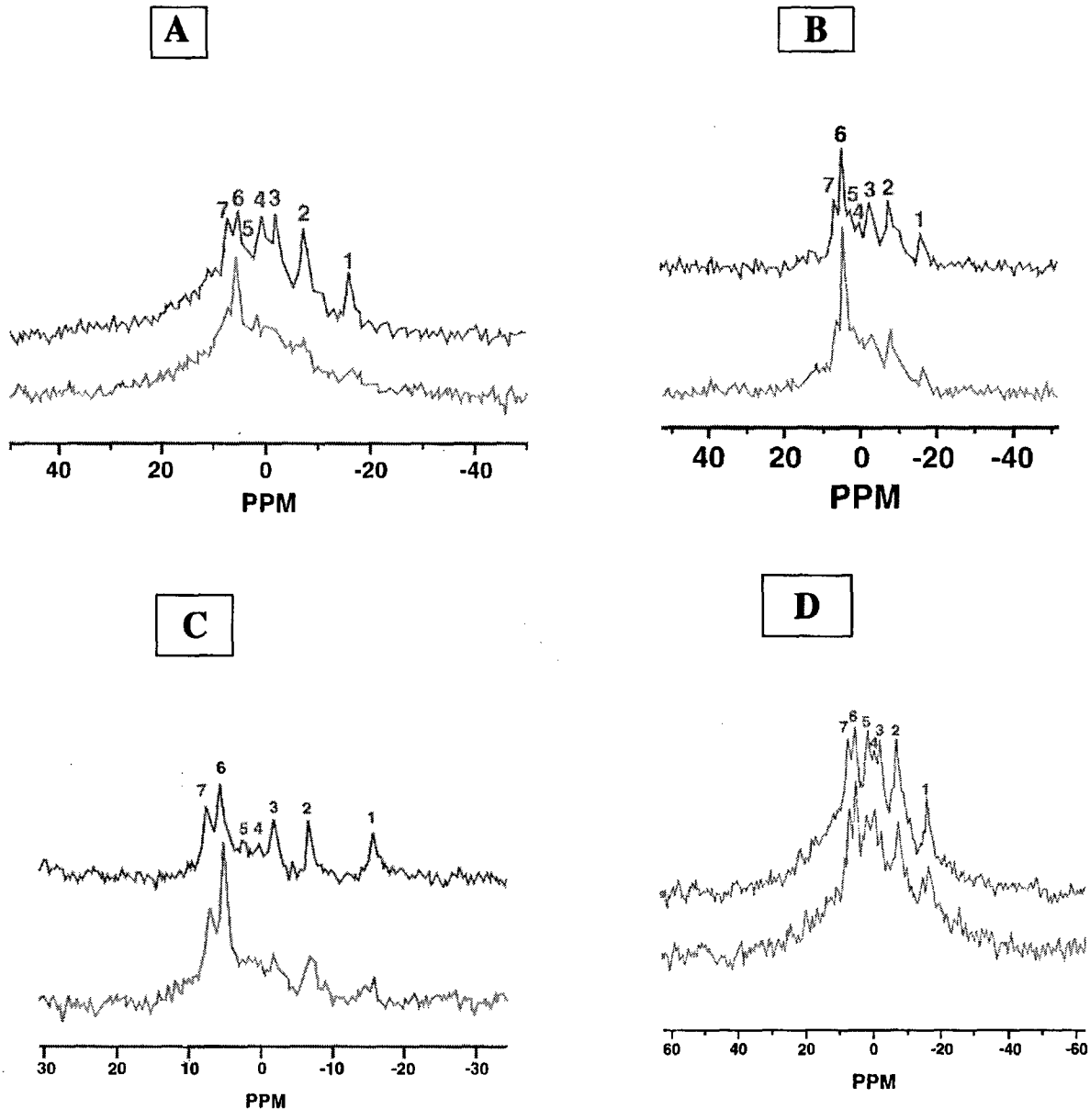

Figure 2: ^{31}P spectra of mouse foot tumor recorded before (upper trace) and after (lower trace) administration of Photosensitizers : A) DOD-6 administered at a dose of 10 μM/kg B) DOD-6 administered at a dose of 2.5 μM/kg C) DOD-2 administered at a dose of 10 μM/kg and D) Photofrin administered at a dose of 10 μM/kg respectively. The various peak assignments are: 1) β-ATP 2) α–ATP 3) γ- ATP 4) PCr 5) PDE 6) Pi and 7) PME.

A graphical representation of the changes involved in Pi and α-ATP peak intensities following the administration of 5 μM of DOD-6 is shown in Figure 3. The changes indicate an increase in Pi and a decrease in α-ATP peak post PS administration.

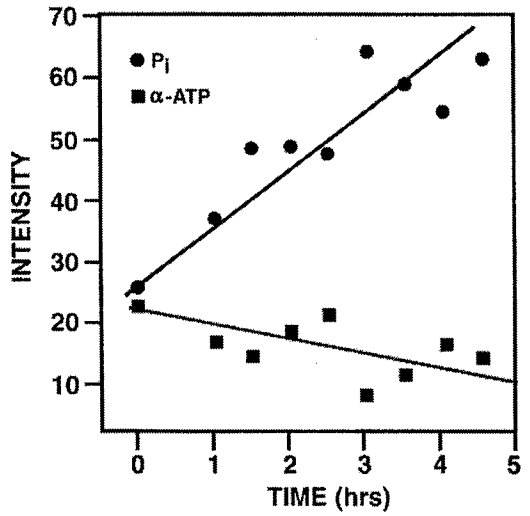

Figure 3: The changes observed over time in Pi and α-ATP peak intensities following the administration of 5μM/kg of DOD-6. The solid lines represent the increase in Pi and a corresponding decrease in α-ATP peaks.

4. Discussion

Dark toxicity was observed when the new photosensitizer (DOD-6) was administered at drug concentration of 2.5-10 μM/kg. A significant increase in inorganic phosphate (Pi) and a decrease in high energy phosphates were observed at 10 and 5μM/kg doses. However the magnitude of changes were significantly lower when the administered dose was 2.5μM/kg. Continuous monitoring of the tumor by ^{31}P MR over a period of 4.5 hrs showed an increase in Pi of approximately 146% and the decrease in α-ATP of ~38%. For PDT treated tumors an increase in Pi by as much as 280% and a decrease in α-ATP by 62% were observed. The tumor volume measurements were made for 4-6 weeks following the administration of single dose of the PS. The growth profile did not differ from the untreated ones. The cytotoxicity that results from the interaction of PS with laser light was in accordance with our earlier results (11). PDT studies performed post drug administration (usually 24 hrs after drug administration) showed significant tumor regression and the rate of regression was greater at 10μM/kg than at 5 μM/kg. Tumor volumes measured following PDT at 2.5 μM/kg dose did not show tumor regression.

While the changes in tumor metabolism upon administration of DOD-6 or DOD-2 are significant and clearly measurable by in vivo MR studies, dark toxicity alone does not appear to be sufficient to produce tumor regression. This is borne out by the fact that the PDT treated tumors showed significant tumor regression while PS treated tumors did not show significant deviations from untreated tumor growth profiles. Representative growth profiles of both PS treated and untreated tumors are shown in Figure 4. The growth profiles show that indeed the PS treated tumors are similar to the untreated control tumors.

The studies on tumors using the new Photosensitizers demonstrate that dark toxicity can be observed by ^{31}P MR. The tumor volumes monitored over several days did not show any tumor shrinkage as observed in PDT induced cytotoxicity. Although dark toxicity was shown by the two new PS, it was not strong enough to interfere with the normal tumor growth. Our study provides information on dark toxicity of a PS in an in vivo model and hence provides a more complete picture than those on cell lines. In vivo ^{31}P studies can be a valuable tool in selecting appropriate dose of the sensitizer which minimizes dark toxicity on normal cells and exerts maximum beneficial effects on the tumors. Because of its noninvasive nature theses studies should be translatable to patients under therapy.

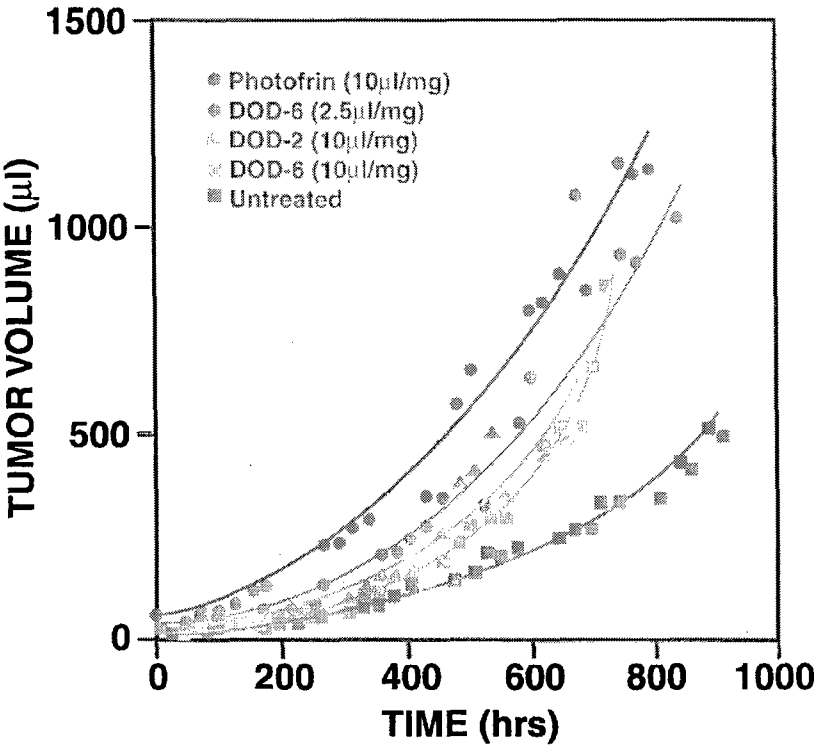

Figure 4: Growth profiles of control and photosensitizer treated tumors studied here.

5. CONCLUSIONS

MR spectroscopic studies of tumors before and after PS administration may provide valuable insight into tissue response to different photosenitizers at different times post therapy. The results from MR technique have a significant potential in evaluating cellular and molecular events that follow PS administration and after photodynamic therapy involving their mode of action. Application of in vivo MR studies to smaller tumor volumes using localized spectroscopic imaging technique may provide valuable information about cytotoxicity of PS in tumor models.

6. ACKNOWLEDGEMENTS

This research was funded by the Department of Defense (DAMD 17-99-1-9065).

7. REFERENCES

T.J. Dougherty, C.J. Gomer CJ, B.W.Henderson , G. Jori , D. Kessel , M. Korbelik , J. Moan and Q. Peng Photodynamic therapy, J.Natl. Cancer. Inst. 90:889-905, 1998.

2. J. Morgan , W.R. Potter , A.R.Oseroff . Comparison of photodynamic targets in a carcinoma cell line and its mitochondrial DNA-deficient derivative. Photochem. Photobiol. 71: 747-757, 2000

3 Z. Tong , G. Singh, A.J. Rainbow . Extreme dark cytotoxicity of Nile Blue A in normal human fibroblasts Photochem. Photobiol. 74:707-711, 2001.

4. K. Urbanska , B. Romankowa-Dixon , Z. Matuszak , J. Oszajca , P.Nowak-Sliwinska , G. Stochel. Indocyanine green as a prospective sensitizer for photodynamic therapy of melanomas. Acta Biochimica Polonica. 49, 387-391, 2002.

5 T. Mosmann . Rapid colorimetric assay for cellular growth and survival: application to proliferation and cytotoxicity assays. J. Immunol Methods. 16:55-63,1983.

6. D.A. Musser, A.R. Oseroff. The use of tetrazolium salts to determine sites of damage to the mitochondroial electron transport chain in intact cells following in vitro photodynamic therapy with Photofrin II. Photochem. Photobiol. 59:621-626,1994.

7. S.K .Pandey , A.L Gryshuk, A Graham, K Ohkubo, S. Fukuzumi, M.P Dobhal, G. Zheng, Z. Ou, R, Zahn, K.M. Kadish, A. Oseroff, S. Ramaprasad, R.K. Pandey, "Fluorinated photosensitizers: Synthesis, Photophysical, Electrochemical, Intracellular Localization, In vitro photosensitizing efficacy and determination of tumor-uptake by ^{19}F in-vivo MR spectroscopy," *Tetrahedron*, 59:10059-10073, 2003.

8. J. Denekamp. The choice of experimental models in cancer research: The key to ultimate success or failure? *NMR Biomed,* 5, 234-237,1992.

9. P.R. Twentyman, J.M. Brown, J.W. Gray, A.J. Franko, M.A. Scoles, and R.F. Kallman, "A New mouse tumor model system (RIF-1) for comparison of end point studies," *J Nat Cancer Inst* 64, pp. 595-604, 1980.

10. A. Naressi, C. Couturier, J.M. Devos, M. Janssen, C. Mangeat, R. deBeer, D. Graveron-Demilly, "Java-based graphical user interface for the MRUI quantitation package," *MAGMA*, 12, pp. 141-152, 2001.

11. S. Ramaprasad, E. Rzepka, J. Pi, SS. Joshi, M. Dobhal, J. Missert, R.K. Pandey (2004). Monitoring PDT Effects in Murine Tumors by spectroscopic and Imaging Techniques. Proceedings of SPIE (Medical Imaging). 5369:380-386.

Appendix-C

Curriculum vitae of participants who were trained during the grant period (2001-2004)

A. Elzbieta Rzepka -- Undergraduate level
B. Sangya Singh ---- Undergraduate level
C. Jiaxiong Pi —-- Graduate level
D. Mahabir Dobhal— Postdoctoral level
E. Suresh K. Pandey-- Postdoctoral level

ELZBIETA RIPP
4657 Mayberry St.
Omaha, NE 68106
(402) 934-4356

EDUCATION

University of Nebraska at Omaha, Omaha, NE
Bachelor of Science – Biology Major
Graduating class of 2003

Relevant Courses include:

Biology I & II	Genetics
Microbial Physiology	General Chemistry I & II
Molecular Biology of the Cell	Developmental Biology
Organic Chemistry	Endocrinology

Westside High School, Omaha, NE
Graduating class of 1998

Relevant Courses include:

Biology	Chemistry
Physics	

WORK EXPERIENCE

July 1998 - November 2001 — **The Sitar Restaurant**
Waitress

November 2001- Present — **University of Nebraska Medical Center**
Lab Technician

References

A. Thomas Weber
Department of Biology
University of Nebraska at Omaha
6001 Dodge St.
Omaha, NE 68182-0040
tweber@unomaha.edu
Phone: (402) 554-2619
Fax: (402) 554-3532

Dan M. Sullivan, Ph.D.
Department of Chemistry
University of Nebraska at Omaha
6001 Dodge St.
Omaha, NE 68182-0109
sully@unomaha.edu
Phone: (402) 554-3646
Fax: (402) 554-3888

ACTIVITIES

Nebraska Humane Society volunteer

Saint Margaret Mary's Church volunteer

Salvation Army volunteer

Presentations

Research Colloquium Poster Session on
1."In Vivo Magnetic Resonance Measurements of Lithium in Rat Hind Limb"
2. "MR Determination of Lithium in Plasma and RBC of Small Blood samples."
3."The Effects of Fluoxetine on Lithium Blood Levels in Rats."
Presented at the University of Nebraska Medical Center, Durham Outpatient West Atrium August 2002.

Pharmacokinetics and relaxivity of Lithium in Rat Thigh Muscle by MR Studies, E. Rzepka[1], S. Ramaprasad[1] Presented at the ISMRM Scientific Meeting, Toronto, Canada, 2003

Codrug Effects on Lithium in an Animal Model by ^{7}Li MR. K. Luterbach[1], E. Pierson[1], E. Rzepka[1], S. Ramaprasad[1]
[1]University of Nebraska Medical Center, Omaha, Nebraska, United States. Presented at the ISMRM Scientific Meeting, Toronto, Canada, 2003

In Vivo ^{19}F MR Studies of Fluorine Labeled Photosensitizer in Murine Tumor Model. S. Ramaprasad[1], E. Rzepka[1], S.S. Joshi[2], M.P. Dobhal[3], J. Missert[3], R.K. Pandey[3], Presented at the ESMRMB Scientific Meeting, at De Doelen Congress Center, Rotterdam, September 2003.

^{19}F MR Quantitation of Fluorine Labeled Photosensitizers in Tumors and Normal Tissue. S. Ramaprasad[1], E. Ripp[1], J. Pi[1,2], S. Joshi[3], J. Missert[4], M. P. Dobhal[4], R. K. Pandey[4] Presented at the ISMRM Scientific Meeting, Tokyo, Japan, 2004.

Quantative Mapping of Lithium in Rat Brain at Therapeutic Doses by Spectroscopic Imaging. S. Ramaprasad[1], J. Pi[1,2], E. Ripp[1] Presented at the ISMRM Scientific Meeting, Tokyo, Japan, 2004.

^{7}Li MR Studies of Codrug Effects on Plasma and RBC Lithium of Rats Under Li prophylaxis. S. Ramaprasad[1], E. Ripp[1], Presented at the ISMRM Scientific Meeting, Tokyo, Japan, 2004.

Publications:

1. **7Li MR Measures of Blood lithium-Correlation with Chemical Analysis Data.** Emily Pierson, Katie Luterbach, Elzbieta Rzepka, Subbaraya Ramaprasad , Magn. Reson. Imaging. 22, 123-126, 2004.

2. **Monitoring PDT Effects in Murine Tumors by Spectroscopic and Imaging Techniques.** S. Ramaprasad, E. Rzepka, J. Pi, SS. Joshi, M. Dobhal, J. Missert, RK. Pandey SPIE Proceedings vol 5369, 380-386. 2004.

3. In vivo magnetic resonance measures of dark cytoxicity of photosensitizers ina murine tumormodel. SPIE proceedings, vol5746, 16-22, 2005.

4. Pharmacokinetics of lithium in rat brain regions by spectroscopic imaging. S. Ramaprasad, E. Ripp, J. Pi, M. Lyon. Magn reson. Imaging. In press.

Objective: To become familiarized and to gain experience in the research field especially pertaining to cancer studies.

Employment Background:
At University Medical Center at Omaha

Cell Culture

Maintained four different lines of cells. SKBR 3, MRA 231, and MRA453 all breast cancer cells. The three lines of breast cancer cells were maintained from November of 2001 the end of the year. Currently maintaining RIF-1 cells received from Roswell Park Cancer Inst. The RIF-1 cells are being maintained since Feb. 2002.

Doubling time

Finding out the doubling time of RIF-1 cells was accomplished with the use of the fisher scientific hemacytometer.

Freezing and thawing of cells

I am experienced in freezing all four lines of cells listed above. Method: mix a fifty to fifty solution containing media and cryoprotectant media then dilute cells in this and put one ml in each container. I have also started culturing RIF-1 cells from a frozen sample that was brought in from Roswell Park Cancer Institute.

Growing and maintaining RIF-1 tumors

I have injected RIF-1 cells into C3h/Hej mice both on the flank and also on the dorsal side of the foot. Once tumors were visible I kept track of the tumor volumes and made sure tumors stayed within a specific growth window. If the volume got too extensive I put the animal down.

Numbering of mice

I have weighed and numbered over one hundred mice. Procedure: by piercing their ears using a ear piercing code; five mice were kept per cage in special micro isolators.

Numbering of rats

I have weighed and numbered over two hundred rats. Procedure: writing the number on the rats tail with a magic marker. This process worked well as long as the animal only needed to be kept track of for a couple of weeks.

Drawing blood from rats and mice

I have drawn blood from around thirty rats. Method used was to anesthetize them, make sure animal was sedated by lightly pinching their foot. Once this was accomplished the blood was drawn from the heart. .8-1.4 ml of blood was extracted from the animals. To keep the blood from clotting one ml of an anticoagulant solution was added.
Recently just started extracting blood from mice. I have drawn blood from a couple mice. Generally around one ml of blood can be drawn from a mouse. Same method followed as in the rat procedure.

Anesthetizing of small animals

I am in the process of using two methods of anesthetics. The first is generally used before the blood drawing. This method is a cocktail of Ketamine and Xylasine that is injected into the thigh region of a rat or mouse.

The second method is by using an anesthetizing machine containing isoflurane of 1.5, N20 at 600 cc/min., and O2 at 200 cc/min. The animals are anesthetized in two to five minutes. This method of anesthetizing is generally used before and during MRI studies and also when the cocktail of Ketamine and Xylasine is not available.

Extraction of Neural Tissue

I have extracted neural tissue from over two hundred rats. Method used : The animal is laid on its back and with a pair of dull tipped scissors you make an incision through the throat area and cut through the bone. Then pull back the skin till the skull is exposed you then make to incisions on both sides and cut along the sides of the skull. Once the neural tissue is exposed you lightly go around with a spatula to loosen and release the neural tissue from its cavity.

Extraction of Thigh Tissue

I have recently extracted thigh tissue from eight rats. Method used: The animal's fur and skin around the thigh region are removed using a scalpel. The muscle of the thigh is then cut around the thigh and pulled back to releases it from the bone.

Tail Vein Injections

I have practiced Tail vein injections on around ten mice and feel fairly confident with this procedure. Method used: the mouse is first set under a heat lamp for a minute or so to allow for the tail veins to become more visible. The mouse is then taken and restricted in a flat bottomed restrainer. The solution being used is then injected into one of the four mice veins' making sure the needle does not go in to deep. If procedure is successful then the solution is visible going through the vein into the body.

Spectroscopy

I am experienced in the use of a Bio Spec 1601 to find different wavelengths of photofrin solutions, which are currently being used on RIF-1 tumor cells.

MRI Studies

I have run many rat blood studies relating to Li levels in RBC and plasma I have also helped out with different MRI studies relating with lithium distribution in a rats thigh and proton and phosphorus studies pertaining to mice studies. The three types of image sequences that I am familiar with are: one pulse sequence, 60 spec 1d T2 sequence, and 1m spec 1d T2 although I have helped out with many others. I also integrated some of the data that was attained through image sequences and am involved in various data processing.

I have analyzed the levels of lithium in the brains of a few rats using paravision software and have also participated on a few image pharmakinetic studies that have been done recently.

I also supervised the animals breathing rate and their levels of anesthetic during the experiments.

Using a laser

I have participated in many experiments using a laser machine on C3h/Hej mice containing tumors on both the flank and the dorsal side of the hind foot using photodynamic therapy.

PDT studies

I have participated in multiple PDT studies. These PDT studies on mice have been done using photosensitive drugs such as photofrin, DOD1, DOD2, DOD6, and DOD_JM_4. During these PDT sessions the drug is first injected two to twenty four hours prior to the laser treatments. The animals are then anesthetized and are treated with the laser on three sides (the top and two sides of the tumor) for uniform penetration.

I have also participated in some preliminary tumor imaging studies, and some T1and T2 measurements that were taken before and after the PDT was done.

CD Backup

I am Currently in the process of transferring and backing up data from MRI studies using the Unix C Shell operating system.

Shipment of Hazardous Goods

I have recently been certified to ship Infectious substances with or without dry ice, and diagnostic specimen. I have prepared and shipped samples of neural and thigh tissue recently.

Sangya Singh
7116 Jones Circle #8
Omaha, NE, 68106
(402) 990- 7165
singhsangya@hotmail.com

Objective: To acquire a challenging position in biological research utilizing analytical and investigative skills while building on previous lab experience.

Education: University of Nebraska at Omaha; NE
Bachelor of Science in Biotechnology (in December 2005).

Honors: Dean's list.

Relevant Experience

7/2004 - present **University of Nebraska Medical Center Omaha, NE**
Research Technician

- Design and carry out a wide range of PDT (Photodynamic Therapy) experiments on small rodent tumor models and monitor PDT effects as well as the effects of photosensitizers alone in murine tumors by spectroscopic technique.
- Collect, organize and analyze the MR data using the Bruker Paravision software.
- Experience handling and anaesthetizing small animals.
- Perform cell culture, harvest tumor cells and freeze cells.
- Perform literature searches of relevant topics and obtain articles to the project.
- Maintain daily lab records and order lab supplies.

8/2005 - 12/2005 **University of Nebraska Medical Center Omaha, NE**
Intern

- Compose and present a written report on Magnetic Resonance Spectroscopic Quantitation and PDT effects of Fluorine labeled Photosensitizers.
- Investigate MR spectroscopic studies of tumors before and after photodynamic therapy.
- Compare the tumor response to PDT therapy using photosensitizers before and after the therapy.
- Measure and calculate the tumor volume and conduct the laser irradiation on tumors.

07/2002 - 08/2004 **University of Nebraska at Omaha, NE**
Undergraduate research assistant

- Performed cellular and molecular experiments, including plasmid extraction, DNA digestion with restriction enzymes, PCR, IPTG tests, vector expressions, Agarose gel electrophoresis and the

preparation of competent bacteria.
- Maintained good lab report summarizing the findings of biological analysis.
- Conducted routine lab duties including autoclaving glass wares and pipettes, making solutions and media; checking and ordering supplies.

Publication:

Reiling, S. A., J. A. Jansen, B. J. Hanley, **S. Singh**, C. Chattin, M. Chandler and D.W. Rowen. 2005. Prc Protease Promote Mucoidy in MucA mutants of *Pseudomonas aeruginosa*. Microbiology, 151, 2251-2261.

S. Ramaprasad, E. Ripp, J. Pi , S. Singh ,M. Lyon(2005) Region Specific Pharmacokinetics of Lithium in a Mammalian Brain by MRSI technique. Proceedings of the Symposium on Trace elements in humans: Satellite Symposium on Lithium, Athens, Greece.

Presentation

Presented Magnetic Resonance Spectroscopic Quantitation and PDT effects of Fluorine Labeled Photosensitizers at "Era of Hope": Breast Cancer Research Program Meeting; June 8-11, 2005.

Abstract:

Magnetic Resonance Spectroscopic Quantitation and PDT effects of fluorine labeled photosensitizers. S. Ramaprasad, J. Pi, **S Singh**, S. S. Joshi, M. Dobhal, J. Missert, R.K. Pandey

References:

Available upon request.

Jiaxiong Pi

Address:
7070 Capitol Court, #678
Omaha NE, 68132
Tel: (402)203-9736(C) , (402)559-3865 (O)
E-mail: jpi_2003@yahoo.com Homepage: http://www.geocities.com/pijx/

Summary:
Highly motivated, creative and knowledgeable computer science graduate student with four years of experience in programming, database manipulation and ten years of experience in data processing and analysis

Qualifications:

- Good programming skill in Java, Fortran, C, C++, IDL, VB, SQL, HTML, ASP and Shell Script
- Good knowledge of TCP/IP protocols (TCP, UDP, IP, ICMP and ARP), AutoCad and Oracle DBA
- Familiar with Unix, Window 2000/NT/XP and Linux
- Strong background in mathematics and physics
- Responsible, efficient, cooperative and eager to learn new technology

Education:

University of Nebraska at Omaha — January 2002-August 2005
M.S. Computer Science — GPA: 3.7/4.0
Degree Date: August 2005

Dalhousie University (Canada) — September 1999-August 2001
M.S. Atmospheric Science — GPA: 4.0/4.0
Degree Date: August 2001

Lanzhou University (China) — September 1990-June 1994
B.S. Atmospheric Physics & Atmospheric Environment — GPA: 3.8/4.0
Degree Date: June 1994

Work Experience:

Valmont Industries, Inc
Valley, Nebraska
IT Intern — February 2005-current

- Analyze and implement systems for automation of drafting process

University of Nebraska Medical Center — May 2003-August 2005
Graduate Assistant

- Create and modify MRI pulse program
- MRI data acquisition, spectrum and image processing and Analysis

University of Nebraska at Omaha May-August 2003
Department of Computer Science

- Developed a matching tool for components reuse (matching and adaptation)

University of Nebraska at Omaha August-December 2003
College of Information Science and Technology

- Developed a web front-end accessed Equipment, Maintenance, User Tracking (EMU) System (ASP and MS Access)

University of Nebraska-Lincoln August-October 2002
Department of Architectural Engineering – Dr. Lily Wang
Part-time programmer

- Developed audio play & evaluation system (Java)

Dalhousie University September 1999-August 2001
Physics Department
Teaching Assistant/Research Assistant

- Simulated Arctic cloud with GESIMA model for international project-FIRE.ACE/SHEBA

Chinese Academy of Meteorological Science June 1994-August 1999
Beijing, China
Assistant Researcher
Processed and analyzed PMS data on PC
Studied the variation of IN concentration in Beijing and its effect on climate

Honors:

- Awarded Lanzhou University scholarship for four consecutive years
- Won second Prize in General Physics contest held at Lanzhou University, 1990
- Won third Prize in Mathematics contest held at Lanzhou University, 1991
- Ranked No. 2 in the final evaluation for 4 academic years in Lanzhou University.
- Received Regent Tuition Waver (RTW) Scholarship at the University of Nebraska at Omaha, August, 2002- May, 2003
- Appointed Research Assistant position at Dalhousie University (1991-2001) and University of Nebraska Medical Center (2003-2005)
- Awarded the Travel stipend to attend the ISMRM meeting at Miami, Florida, May, 2005.

Publications:

- Pharmacokinetics of lithium in rat brain regions by spectroscopic imaging. S. Ramaprasad, E. Ripp, J. Pi, M. Lyon. Magn. Reson. Imaging. In press.

- S. Ramaprasad, E. Ripp, **J. Pi,** SS. Joshi, J. Missert, M. Dobhal and R. Pandey, "In-vivo magnetic resonance measures of dark cytotoxicity of photosensitizers in a Murine tumor model", Proceedings of *SPIE,vol 5746, 16-22, 2005.*

- S. Ramaprasad, E. Rzepka, **J. Pi**, SS. Joshi, M. Dobhal, J. Missert, RK. Pandey, "Monitoring PDT Effects in Murine Tumors by Spectroscopic and Imaging Techniques", Proceedings of *SPIE USA*, V.5369, 380-386, 2004.
- U. Lohmann, J. Zhang and **J. Pi**, "Sensitivity studies of the effect of increased aerosol concentrations and snow crystal shape on the snowfall rate in the Arctic", *J. Geophys. Res.*, 108(D11), 4341, doi:10.1029/2003JD003377, 2003.

Abstracts:

- **J. Pi**, Y. Shi and Z. Chen, "Similarity and cluster analysis algorithm for Microarrays using R* Tree", accepted by *2005 IEEE computational Systems Bioinformatics Conference*, August 8 -11, 2005, Stanford University, California.
- S Ramaprasad, **J. Pi** and E. Ripp, S. S. Joshi, J. Missert, M. P. Dobhal. R. K. Pandey, "Dark cytotoxicity measures of photosensitizers in a murine tumor model by 31P MR Studies", 21st Annual Meeting, European Society for Magnetic Resonance in Medicine and Biology, September 9-12, 2004, Copenhagen, Denmark.
- S. Ramaprasad, **J. Pi** and E. Ripp, "Quantative Mapping of Lithium in Rat Brain at Therapeutic Doses by Spectroscopic Imaging", *Proceeding of 12th International Society for Magnetic Resonance in Medicine,* May 15-21, 2004, Tokyo, Japan.
- S. Ramaprasad, E. Ripp, **J. Pi**, S. S. Joshi, J. Missert, M. P. Dobhal, and R. K. Pandey, "^{19}F MR Quantitation of Fluorine Labeled Photosensitizers in Tumors and Normal Tissue" *Proceeding of 12th International Society for Magnetic Resonance in Medicine,* May 15-21, 2004, Tokyo, Japan.
- **J. Pi** and U. Lohmann, "Anthropogenic Aerosol Effect On Arctic Precipitation-A Case Study With GESIMA Model" *Proceedings of 35th Canadian Meteorological and Oceanographic Society (CMOS) Conference*, Page 99, 26-30 May, 2001
- L. You, S. Yang, X. Wang and **J. Pi**, "A study of Variation Characteristic of Ice Nuclei Concentration in Thirty Years at Beijing?', *Processing of 14th International Conference on Nucleation and Atmospheric Aerosols*, 26-30 August, 1996, Helsinki, Finland, p330~333.

References:

Available upon request

Curriculum -vitae

Name *Dr. Mahabeer Prasad Dobhal*

Date of Birth April 14, 1956

Postal Address 01,Teachers Residence
University Campus
University of Rajasthan
Jaipur- 302004
India

Educational Qualification

B.Sc , from Agra University, Agra (1973)

B.Ed., from Agra University, Agra (1974)

M.Sc., from Garhwal University,Srinagar (1976)

Ph.D.from University of Rajasthan , Jaipur(1982)

Research Experiences

1. ▶August 1976 to February 1982 worked for Ph.D. degree on the project entitled Chemical Investigation of Medicinal Plants of Garhwal Region under the supervision of Prof.B.C.Joshi .
2. ▶December 1982 to April 1983 worked as Post – Doctoral fellow with Prof. B.C.Joshi.
3. ▶In May 1983 UGC Research Associateship was awarded ,during this period,(May 1983 to August 1984) chemical investigation of some medicinal plants was carried and a few anti-epileptic agents were isolated.

Work Experiences

1. Worked as a Production Chemist in Navin Chemicals Ltd. NOIDA (India)
2. From September 1984 I have been working as an Assistant Professor in the Department of Chemistry ,University of Rajasthan, Jaipur .

List of Publications

1.	Chemical investigation of *Roylea elegans* **part-I**	**M.P. Dobhal** B.C. Joshi	Herba Polon, **25**, 95	1979
2.	Chemical investigation and biological screening of the stems of *Rhododendron anthopogon*	**M.P. Dobhal** Y.C. Joshi B.C. Joshi	Die Pharmazie **36**, 381	1981
3.	Studies of Potential heterocyclic sulphones as antimicrobial agents. Synthesis & antimicrobial activitity of some novel substituted arylsulphonyl benzo (f) quinoline	R.P. Bahuguna, Y.C. Joshi, **M.P. Dobhal**, B.C. Joshi, H.N. Mangal	Heterocycles, 16, 1955	1981

4.	Spectral studies of some substituted arylthiobenzo (f) quinolines	R.P. Bahuguna, Y.C. Joshi, **M.P. Dobhal**, R.K. Pande, B.C. Joshi	J. Heterocyclic Chem. 5495, 66	1982
5.	Chemical constituents of the stems of *Roylea elegans*	S. Ansari Y.C. Joshi, **M.P. Dobhal**, B.C. Joshi	Die Pharmazie 37, 72	1982
6.	Phytochemical investigation of the roots of *Colebrookia oppositifolia*	S. Ansari **M.P. Dobhal** R.P. Tyagi B.C. Joshi F.S.K. Barar	Die Pharmazie 37, 72	1982
7.	Chemical investigation and Pharmacological screening of *Roylea elegans* Part-II	S. Kumar, **M.P. Dobhal**, B.C. Joshi, F.S.K. Barar	Herba Polon 27, 99	1982
8.	Chemical investigation of the roots of *Anisomeles indica*	S. Ansari, **M.P. Dobhal**	Die Pharmazie 37, 453	1982
9.	A review on genus *Rhododendron*	**M.P. Dobhal**, Y.C. Joshi B.C. Joshi	Herba Polon 29, 65	1983
10.	Spectral and antimicrobial studies of some substituted arylthibenzo (h) quinolines	R.P. Bahuguna, Y.C. Joshi, **M.P. Dobhal**, B.C. Joshi, H.N. Mangal	J. Inst. of Chemists (India) **56**, 185.	1984
11.	Chemical investigation of various species of the plants belonging to *Berberdiaceae*	**M.P. Dobhal** B.C. Joshi	Rasayan Samiksha **2**, 26	1986
12.	Chemical investigation of aerial parts of *Portulacca sufructicosa*	Y.P. Agrawal **M. P. Dobhal**	Herba Polon **33**, 71	1987
13.	Chemical investigation of *Euonymus Pendulus* Characterization of a new isoflavone (Garhwalin)	**M.P. Dobhal** Y.P. Agrawal B.C. Joshi	Die Pharmazie 42, 558	1987

14.	Chemical investigation of the seed coats of *Prunus amygdalus*. Isolation and characterization of a new biflavone	B.C. Joshi A.K. Chauhan, **M.P. Dobhal**, V.P. Agrawal	Herba Polon 33, 163	1987
15.	A review on medicinal plants, showing anticonvulsant activity	A.K. Chauhan **M.P. Dobhal**,	J. Ethnopharmacology **22**, 11	1988
16.	Phytochemical studies of stems of *Anisomeles indica*	**M.P. Dobhal**, A.K. Chauhan, S. Ansari, B.C. Joshi	Fitoterpia **59**, 155	1988
17.	Chemical investigation of *Catalpa longissima* Part-I	A.K. Chauhan **M.P. Dobhal**, P.N. Uniyal	Herba Polon **34**, 4	1988
18.	Chemical investigation of *Berberis chitria* 'Ham' - Isolation and characterization of isoquinoline alkaloids	**M.P. Dobhal**, V.K. Goel, B.C. Joshi	Die Pharmazie **43**, 659	1988
19.	Chemical investigation and biological activity of *Berberis chitria*	**M.P. Dobhal** G.S. Negi	Himalayan Chem. Pharma, Bull **5**, 41	1988
20.	Characterization of a new alkaloids from the roots of *Berberis chitria*	A.K. Chauhan **M.P. Dobhal**	Die-Pharmazie **44**,	1989
21.	Structure and activity relationship of isoquinoline alkaloids.	R.S. Gupta V.P. Dixit, **M.P. Dobhal**	Fitoterapia **61**, 67	1990
22.	Chemical constituents of the bark of *Euonymus echinatus*	A.K. Chauhan, **M.P. Dobhal**, Diwakar Sharma	Himalayan Chem. & Pharm.Bull. **6**, 21	1989
23.	A review on genus *Rhododendron* - Part II	**M.P. Dobhal**	Herba Polon **37**, 89	1991
24.	*In Vitro* antimicrobial efficacy of *Berberis chitaria* extracts	**M.P. Dobhal** Y.C. Joshi	Fitoterapia **63**, 69	1992
25.	A new isoquinoline alkaloid from *Berberis chitria*	**M.P. Dobhal**, A.K. Chauhan,	Indian Science Congress Assoc.	1993

26. A Review on genus *Euonymus*	A.M. Hassan, C. Kaushik **M.P. Dobhal**	Herba Polon **41**,	1995
27. A Review on genus *Eupatorium* Part-I	A.M. Hassan, **M.P. Dobhal** B.C. Joshi, G.S. Negi	Him.Chem. & Pharma Bull. **12**, 1-10	1995
28. Synthesis of some new sulphide sulphone and triazolo derivatives of pyridobenzodiazepines	B.C. Joshi R.P. Tyagi Madhu Chauhan, **M.P. Dobhal**	Indian J. of Heterocyclic Chem. **5**, 277-80	1996
29. A Review of the Chemical Constituents in the genus *Eupatorium* Part-II	A.M. Hassan, **M.P. Dobhal** G.S. Negi B.C. Joshi	Himalayan Chem. & Pharm. Bulletin **12**	1996
30. Morphometric and biochemical changes in tests of *Presbytis entellas* (Langur) Followed by aristolochic acid administration	R.S. Gupta **M.P. Dobhal**, V.P. Dixit	Annals of Biology **12**, 328-34.	1996
31. A review on the chemical constituents in the genus *Eupatorium* - Part-III	A.M. Hassan, **M.P. Dobhal** G.S. Negi B.C. Joshi	Himalayan Chem. & Pharm. Bulletin **14**,	1997
32. A brief review on chemical constituents of some medicinally important species of Genus *Plumeria*	A.M. Hassan B.C. Joshi **M.P. Dobhal**	Asian J. of Chemistry **9**, 571-78.	1997
33. A review on cyclopeptide alkaloids	Chetan Kaushik **M.P. Dobhal**	Himalyan Chem. & Pharm. Bulletin **15**, 22-32	1998
34. Ferulic acid aster from *Plumeria* bicolor	**M.P. Dobhal** A.M. Hasan M.C. Sharma B.C. Joshi	Phytochemistry **51**, 319-21	1999
35. Effects of coumarin derivatives on testicular population in Langur monkeys.	R.S. Gupta, V.P. Dixit **M.P. Dobhal**	Himalayan Chem. & Pharm. Bulletin.	1999

36. Antifertility studies and Chemical investigation of *Colebrookia oppositifolia* leaf extract in male albino rats.	R.S. Gupta R.K. Yadav, V.P. Dixit, **M.P. Dobhal**	Fitoterapia	1999
37. Antifertility studies of the root extract of the *Barlaria prionitis* in male albino rats with special reference to testicular cell population dynamics.	R.S. Gupta P. Kumar, V.P. Dixit, **M.P. Dobhal**	J. Ethnopharmacology **70**, 111-17	2000
38. Effect of Organoantimony Compounds sterically hindered bifunction legands on the reproductive systems.	R.K. Sharma **M.P. Dobhal**, Y.P. Singh, R.S. Gupta	Metal Based Drugs 7, 271-74	2000
39. Hypocholeserolemic effect of the oleoresin (*Capsicum annum*) in gerbils.	R.S. Gupta V.P. Dixit, **M.P. Dobhal**	Phytotherapy Research 15, 1-3,	2001
40 Effect of Alstonia scholaris bark extract on testicular function of Wistar rats	R.S. Gupta **M.P. Dobhal**	Asian J. Andrology 4, 175 – 78	2002
41 Antispermatogenic effect and chemical investigation of Opuntia dillenii	R.S.Gupta A.Sharma **M.P. Dobhal**	Pharmaceutical Biol. 40 , 411-415	2002
42 A review on potentiality of medicinal plants as the source of new contraceptive principles.	R.Unny **M.P. Dobhal** R.S.Gupta	Phytomedicine 10 ,233 – 260	2003
43. "Fluorinated Photosensitizers: Synthesis, Photophysical, Electrochemical and *In-Vitro* Photosensitizing Efficacy"	**Pandey, S.K** Gryshuk, A.L Graham, A Ohkubo, K Fukuzumi, S Dobhal, M.P Zheng, G Zhan, R Kadish, K.M Ramaprasad, S Oseroff, A Dougherty, T.J Pandey, R.K	Tetrahedron, 59, 10059-10073	2003
44. Monitoring PDT Effects in Murine Tumors by Spectroscopic and Imaging Techniques.	S. Ramaprasad E. Rzepka J. Pi, SS. Joshi **M. Dobhal** J. Missert R.K. Pandey	*SPIE USA*, 6 5369-44	2004

References

1. **Prof B.C.Joshi**, Ph.D., D.Sc.
   5 / 74, SFS, Agrawal Farms
   Mansarovar, Jaipur- 302020 (India)

2. **Dr. Mahendra Kumar**, Ph.D.
   Department of Chemistry
   University of Rajasthan
   Jaipur –302004 (India)

Suresh K. Pandey, Ph.D.

Work:
Photodynamic Therapy Center
Roswell Park Cancer Institute
Elm and Carlton Streets
Buffalo, NY 14263, USA
Phone: 716-845-3377; Fax: 716-845-8920

Home:
182 Kenville Road, Apt. A
Buffalo, NY 14215
Phone: 716-836-1934
Email:sureshkpandey@yahoo.com
suresh.pandey@roswellpark.org

Educational Qualification

- Ph. D. Medicinal Chemistry; **2000**; Banaras Hindu University, Varanasi, India & Central Drug Research Institute, Lucknow, India.
- M. Sc. Organic Chemistry; **1995**; Banaras Hindu University, Varanasi, India.
- B. Sc. (Honors) Chemistry; **1993**; Banaras Hindu University, Varanasi, India.

Research Interest

- Design, synthesis and structure activity relationship (SAR) studies of novel biologically active compounds.
- Synthesis and practical utility of multimodality photosensitizers.
- Synthesis of target specific phtotosensitizers and imaging agents.

Research Experience

- **2001-current**: Post Doctoral Fellow
  Photodynamic Therapy Center, Medical Research Complex, Roswell Park Cancer Institute, Elm & Carlton Streets, Buffalo, NY 14263, USA. (***Mentor: Prof. R.K. Pandey***)
  - Synthesized fluorinated and non-fluorinated porphyrins to harness imaging requirement for the tumor tissues. It was found that in addition to have symmetric fluorinated substituents for sharp intense signal by *in vivo* fluorine NMR, overall ampiphilicity of the compound also plays a crucial role.
  - In another project chlorins, and their carbohydrates conjugates (mainly β-galactose analogs) are being synthesized for their targeted anticancer activity. The structure of the conjugates was confirmed by ^{1}H-^{1}H COSY, TOCSY and ROESY NMR experiments, while their purity was checked by HPLC. Galectin (a β-galatcoside glycoproteins overexpressed in tumor cells) binding assays have been carried out in addition to *in vitro* and *in vivo* studies for above conjugates to elucidate their efficacy & mechanism of action. The molecular modeling of these conjugates is also in progress.
  - Synthesis of iodinated chlorins and bacteriochlorins are under progress. These compounds are converted to the corresponding radioactive analog of Iodine (^{124}I) for the purpose of positron imaging tomography (PET) and therapy. In some cases these compounds are found to be better than FDG (a standard PET tracer) for distinguishing boundaries between normal and tumor tissues. An application for the **US patent has been filed** for these compounds and quantification studies are underway. In addition, attempts to make these compounds target specific is in progress.
  - Published 4 papers, 2 in press, filed 1 patent and presented 4 papers in the national /international conferences.

- **1995-2001**: Graduate Fellow
  Medicinal Chemistry Division, Central Drug Research Institute, Lucknow, India. ***Mentors: 1. Dr. A.K. Saxena***, Scientist "F" & Deputy Director, Medicinal Chemistry Division, Central Drug Research Institute, Lucknow, India. 2. ***Prof. (Late) A.K. Mukerjee***, Department of Chemistry, Banaras Hindu University, Varanasi, India.
  Thesis entitled **"Design and Syntheses of Cholecystokinin(CCK) Antagonists and Antithrombotic Agents"**
  - Synthesized racemic and chiral isomers (R/S) of pyrido(3,4-b)indoles (known as β-carbolines) by rigidification of respective racemic and chiral (R/S) tryptophan and tryptamine for their antiulcer and antinociception activity which is mediated by cholecystokinin (CCK) receptor antagonism. Quantitative structure activity relationship (QSAR) and molecular modeling were also carried out to determine the pharmacophore responsible for the activity.
  - Synthesized tetracyclic lactams and nitrogen, sulphur containing heterocycles (viz. thiazolines, pyrrolidines, piperidines, piperazines) for antithrombotic and antiischemic activities. QSAR studies were then performed to assess the impact of physicochemical parameters on the biological activity.
  - Published 6 papers, filed 3 patents and presented 5 papers in conferences.

Technical Experience

Sound knowledge of chemistry including bioorganic chemistry; Column Chromatography; Chromatotron; IR; UV-Visible; HPLC; NMR(^{1}H, ^{13}C and COSY, TOCSY, ROESY) spectroscopy; Mass spectroscopy (Interpretation), 2D/3D-QSAR and small molecule molecular modeling; Fluorescence Imaging; Nuclear Imaging (Positron Emission Tomography); ELISA; etc.

Supervisory Experience

Planned and successfully supervised high school and undergraduate students towards their their poster and oral presentations.

Awards

- **Qualified Graduate Aptitude Test for Engineering (GATE) 1995; conducted jointly by Indian Institute of Technology and Institute of Science, India.**
- Qualified National Eligibility Test (NET) for Junior Research Fellowship and Lecturer ship 1995, jointly conducted by Council of Scientific and Industrial Research (CSIR) and University Grant Commission (UGC), India.

Fellowships

- 1995-1996: Research Assistantship, Ministry of Health & Family Welfare, Government of India, New Delhi, India.
- **Recipient of prestigious national fellowship towards graduate studies for 5 years period from1996-2001 as below.**
  - **1996-1998**: Junior Research Fellowship, Council of Scientific and Industrial Research (CSIR), Government of India, New Delhi, India.
  - **1998-2001**: Senior Research Fellowship, Council of Scientific and Industrial Research (CSIR), Government of India, New Delhi, India.

Publications

- **Papers**

1. Tripathi, R.C.; **Pandey, S.K.**; Kar, K.; Dikshit, M. and Saxena, A.K. "Synthesis and SAR studies of 1-substituted-n-(4-alkoxycarbonypiperidin-1-yl)alkanes as potent Antiarrhythmic Agents" Bioorganic and Medicinal Chemistry Letters, **1999**, *9*, 2693-2698.
2. Pandya, T.; **Pandey, S.K.**; Tiwari, M.; Chaturvedi, S.C. and Saxena, A.K. "3D-QSAR studies of Triazolinone based Balanced AT_1/AT_2 Receptor Antagonists" Bioorganic and Medicinal Chemistry, **2001**, *9*, 291-300.
3. Saxena, A.K.; **Pandey, S.K.**; Tripathi, R.C. and Raghubir, R. "Synthesis, Molecular Modeling and QSAR studies in chiral 2,3-disubstituted-1,2,3,4-tetrahydro-9H-pyrido[3,4-b]indoles as potential modulators of opioid antinociception" Bioorganic and Medicinal Chemistry, **2001**, *9*, 1559-1570.
4. **Pandey, S.K.**; Awasthi, K.K. and Saxena, A.K. "Microwave assisted Stereospecific synthesis of (*S*)-3-substituted 2,3,6,7,12,12a-hexahydropyrazino[1',2': 1,6] pyrido [3,4-b]indole-1,4-diones" Tetrahedron, **2001**, *57*, 4437-4442.
5. Saxena, A.K.; **Pandey, S.K.**; Seth, P.K.; Singh, M.P.; Dikshit, M. and Carpy, A. "Synthesis and QSAR studies in 2-(N-aryl-N-aroyl)amino-4,5-dihydrothiazole derivatives as potential Antithrombotic Agents" Bioorganic and Medicinal Chemistry, **2001**, *9*, 2025-2034.
6. **Pandey, S.K.**; Naware, N.B.; Trivedi, P. and Saxena, A.K. "Molecular Modeling and 3D-QSAR studies in 2-aziridinyl- and 2,3-bis(aziridinyl)-1,4-naphthoquinonyl sulfonate and acylate derivatives as potential antimalarial agents" SAR and QSAR in Enviornmental Research, **2001**, *12*, 547-564.
7. Gryshuk, A.L.; Graham, A.; **Pandey, S.K.**; Potter, W.R.; Missert, J.R.; Oseroff, A.; Dougherty, T.J. and Pandey, R.K. "A First Comparative Study of Purpurininide-Based Fluorinated vs. Non-Fluorinated Photosensitizers for Photodynamic Therapy" Photochemistry and Photobiology, **2002**, *76*, 555-559.
8. **Pandey, S.K.**; Gryshuk, A.L.; Graham, A.; Ohkubo, K.; Fukuzumi, S.; Dobhal, M.P.; Zheng, G.; Zhan, R.; Kadish, K.M.; Ramaprasad, S.; Oseroff, A.; Dougherty, T.J. and Pandey, R.K. "Fluorinated Photosensitizers: Synthesis, Photophysical, Electrochemical and *In-Vitro* Photosensitizing Efficacy" Tetrahedron, **2003**, 59, 10059-10073.
9. Li, G.; **Pandey, S.K.**; Dobhal, M.P.; Mehta, R.; Chen, Y.; Gryshuk, A.L.; Olson, K. R-.; Oseroff, A. and Pandey, R.K. "Functionalization of OEP-Based benzochlorins to Develop Carbohydrate Conjugated Photosensitizers. Attempt to Target β-Galactoside Recognized Proteins" Journal of Organic Chemistry, **2004**, 69, 158-172.
10. Ramaprasad, S.; Ripp, E.; Pi, J.; Joshi, S.S.; **Pandey, S.K.**; Missert, J. and Pandey, R.K."*In Vivo* Magnetic Resonance Measures of Dark Cytotoxicity of Photosensitizers in a Murine Tumor Model" Proceedings of SPIE (Medical Imaging), **2005**, *5746*, 16-22.
11. **Pandey, S.K.**; Gryshuk, A.L; Sajjad, M.; Zheng, X.; Chen, Y.; , Abouzeid, M.M; Morgan, J.; Charamisinau, I.; Nabi, H.A.; Oseroff, A. and Pandey, R.K. "Multimodality Agents for Tumor Imaging (PET, Fluorescence) and Photodynamic Therapy. A Possible See and Treat Approach" accepted, Journal of Medicinal Chemistry **2005.**
12. Tamiaki, H.; Shimamura, Y.; Yoshimura, H.; **Pandey, S.K.** and Pandey, R.K. "Self-Aggregation of Synthetic Zinc 3-Hydroxymethyl-purpurin-18 and N-Hexylimide Methyl Esters in an Aqueous Solution as Models of Green Photosynthetic Bacterial Chlorosomes" accepeted, Chemistry Letters 2005.
13. Zheng, X.; **Pandey, S.K.**; Morgan, J.; Camacho, S.; Bellnier, D.A.; Pandey, R.K. "Examining Potential of Pyropheophorbide *a*-Carbohydrate Conjugates for Targeted Photodynamic Therapy" manuscript under preparation.

➢ **Patents**

1. **Pandey, S.K.**; Awasthi, K.K.; Tripathi, R.C.; Bhandari. K.; Thapaliyal, H. and Saxena, A.K.; Indian Patent 1446/DEL/**99**. "A new improved process for the synthesis of 1-oxo-1,2,3,4,6,7,12,12a-octahydropyrazino[2',1':6,1]pyrido[3,4-b] indole".
2. **Pandey, S.K.**; Srivastava, A.; Awasthi, K.K.; Tripathi, R.C.; Srivastava, S.; Arun. J.; Saxena, R.M.; Ray, M.; Shukla, R.; Dubey, M.P. and Saxena, A.K.; Indian Patent 1451/DEL/**99**. "Novel 1-(4-aryl/heteroarylpiperazin/pieradin-1-yl)-n-(quinoloxy-6/7/8-yl/(un)substitutedpyrrolidin-2-oxo-1-yl) alkanes/alkanones and their salts as potential therapeutic agents".
3. **Pandey, S.K.**; Srivastava, A.; Awasthi, K.K.; Tripathi, R.C.; Srivastava, S.; Arun. J.; Saxena, R.M.; Ray, M.; Shukla, R.; Dubey, M.P. and Saxena, A.K.; Indian Patent 1452/DEL/**99**. "Novel 1-(4-aryl/heteroarylpiperazin/pieradin-1-yl)-n-(quinoloxy-6/7/8-yl/(un)substitutedpyrrolidin-2-oxo-1-yl) alkanes/alkanones and their salts as potential therapeutic agents and a process for synthesis thereof".
4. Pandey, R.K.; Sajjad, M.; Oseroff, A.; **Pandey, S.K.** and Gryshuk, A.L. Filed for US patent **2005**. "Porphyrin based compounds for PET Imaging and PDT".

➢ **Presentations**

1. Tripathi, R.C.; **Pandey, S.K.**; Raghubir, R. and Saxena, A.K. "Synthesis and SAR studies in chiral 2,3-disubstituted-1,2,3,4-tetrahydro-9H-pyrido(3,4-b)indoles as potential CCK-A and CCK-B antagonists" International Symposium on Perspectives in Biomolecular Research, CDRI, Lucknow, India, Jan.12-13, **1998**.
2. Raghubir, R.; **Pandey, S.K.**; Tripathi, R.C. and Saxena, A.K. "Modulation of Opioid analgesia by CCK-antagonists" 31st Annual Conference of Indian Pharmacological Society, CDRI, Lucknow, India, Dec.18-20, **1998**.
3. Saxena, A.K.; **Pandey, S.K.**; Tripathi, R.C. and Raghubir, R. " Synthesis and 3D-QSAR studies in chiral 2,3-disubstituted-1,2,3,4-tetrahydro-9H-pyrido[3,4-b]indoles as potential modulators of opioid antinociception" 5th IUPAC International Symposium on Bio-organic Chemistry (ISBOC-5), NCL, Pune, India, Jan.30-Feb.4, **2000**.
4. **Pandey, S.K.**; Dikshit, M. and Saxena, A.K. "Synthesis and QSAR studies in 2-(N-aryl-N-alkyl/arylcarbonyl)amino-4,5-dihydrothiazole derivatives as potential Antithrombotic Agents" 5th IUPAC International Symposium on Bio-organic Chemistry (ISBOC-5), NCL, Pune, India, Jan.30-Feb.4, **2000**.
5. **Pandey, S.K.**; Naware, N.B.; Trivedi, P. and Saxena, A.K. "Molecular Modeling and 3D-QSAR studies in 2-aziridinyl- and 2,3-bis(aziridinyl)-1,4-naphthoquinonyl sulfonate and acylate derivatives" Current Trends in Drug Design and Discovery (CTDDR-2001), CDRI, Lucknow, India, Feb. 11-15, **2001**.
6. **Pandey, S.K.**; Zheng, X.; Graham, A.; Dobhal, M.P.; Missert, J.R.; Camacho, S.; Olson, K. R.-; Shibata, M.; Bellnier, D.A.; Oseroff, A.R. and Pandey, R.K. "Purpurin-Lactose Conjugates as Target-Specific Photosensitizers for PDT". 227th American Chemical Society National meeting, Anaheim, CA, USA, March 27-April 01, **2004**.
7. Zheng, X.; **Pandey, S.K.**; Camacho, S.; Morgan, J.; Bellnier, D.A. and Pandey, R.K. "Pyropheophorbide-carbohydrate conjugates as galectin-specific photosensitizers for photodynamic therapy". 3rd International conference on Porphyrins and Phthalocyanines (ICCP-3), New Orleans, USA, July 11-16, **2004**.
8. Tamiaki, H.; Shimamura, Y.; **Pandey, S.K.** and Pandey, R.K. "Self-aggregation of synthetic self-aggregative chlorophylls possessing an anhydride or N-hexylimide moiety". 85th Annual Meeting of Chemical Society of Japan, 3G7-39, Yokohama, Japan, March 28, **2005**.

Affiliations

- Member of the American Chemical Society; 2001-current.

Languages & Computer Competency

Fluent in English and Hindi. Well versed in use of computers and scientific software's related to research and education. Proficient in- Word, Excel, Power Point, Sigma plot, Origin, Prizm, Chemdraw, Nuts, MestReC.